In Situ Copolymerization of Ethylene & Propylene In The presence of Titania Nanofillers

BY

Omer Yahya Bakather

A Dissertation Presented to the
DEANSHIP OF GRADUATE STUDIES

KING FAHD UNIVERSITY OF PETROLEUM & MINERALS

DHAHRAN, SAUDI ARABIA

In Partial Fulfillment of the
Requirements for the Degree of

DOCTOR OF PHILOSOPHY

In

CHEMCAL ENGINEERING

APRIL 2014

KING FAHD UNIVERSITY OF PETROLEUM & MINERALS

DHAHRAN- 31261, SAUDI ARABIA

DEANSHIP OF GRADUATE STUDIES

This thesis, written by **Omer Yahya Bakather** under the direction his thesis advisor and approved by his thesis committee, has been presented and accepted by the Dean of Graduate Studies, in partial fulfillment of the requirements for the degree of **DOCTOR OF PHILOSOPHY IN CHEMICAL ENGINEERING.**

Dr. Mamdouh Al-Harthi
(Advisor)

Dr. Ibnelwaleed Ali Hussein
(Member)

Dr. Muataz Ali Atieh
(Member)

Dr. Housam Binous
(Member)

Dr. Mohammed Ba-Shammakh
(Member)

for Dr. Usamah Al-Mubaiyedh
Department Chairman

Dr. Salam A. Zummo
Dean of Graduate Studies

19/6/14
Date

DEDICATION

To my beloved parents, my wife, my brothers, my sister and my children: Mohammad, Elaf, Yahya and Baraa.

ACKNOWLEDGMENTS

I am very grateful to my advisor, **Dr. Mamdouh Al-Harthi** for his confidence, supervision and support throughout the development of this study. I also want to thank my other committee members **Prof. Ibnelwaleed Ali Hussein, Dr. Muataz Ali Atieh**, **Dr. Housam Binous** and **Dr. Mohammed Ba-Shammakh** for their guidance, and cooperation. I really want to thank King Fahd University of Petroleum & Minerals (KFUPM) and I would like to thank all the KFUPM members and graduate students for the friendship they showed during the time of this study. I would like to thank all my family their encouragement, love, prayers and patience.

Finally, I wish to acknowledge the assistance of Deanship of Scientific Research, King Fahd University of Petroleum and Minerals for their support for providing adequate funds and infrastructure under Project no. IN101018.

TABLE OF CONTENTS

LIST OF FIGURES

LIST OF TABLES

LIST OF ABBREVIATIONS

MAO	Methyaluminoxane
MADC	methylaluminum dichloride
TCB	1,2,4-Trichlorobenzene
$(\eta\text{-}C_5H_5)_2M$	Symmetrical, classical, “sandwich” metallocene structure
Crystaf	Crystallization analysis and fractionation
GPC	Gel permeation chromatography
^{13}C NMR	Carbon 13 Nuclear magnetic resonance
DSC	Differential scanning calorimetry
XRD	X-ray Diffraction
SEM	Scanning Electron Microscopy
TGA	Thermal Gravimetric Analysis

ABSTRACT (ENGLISH)

Full Name: Omer Yahya Bakather

PhD Thesis Title: In Situ Copolymerization of Ethylene & Propylene In The presence of Titania Nanofillers

Major Field: Chemical Engineering

Date of Degree: April 2014

Polymer industry in Saudi Arabia is a fast growing segment of the industry because of the availability of the raw materials and low cost production. In this study, different catalysts were synthesized and used in ethylene and ethylene/propylene polymerization. A vanadium (III) complex bearing a salicylaldiminato ligand of the general formula $[RN=CH(2,4\text{-}^{t}Bu_2C_6H_2O)]VCl_2(THF)_2$, where R = 2,6-$^{i}Pr_2C_6H_3$, was used as a catalyst. Titanium dioxide doped with iron nanofillers were synthesized by a sol-gel process and was used to investigate the effect of nanofillers on the ethylene homopolymer and ethylene/ propylene copolymer properties. Polyethylene and polyethylene/polypropylene nanocomposites were synthesized using vanadium (III) complex bearing salicylaldiminato ligands in the presence of TiO_2/Fe nanofiller. The molecular weight (M_w) was found to increase on adding TiO_2/Fe nanofiller in both polyethylene and polyethylene/polypropylene nanocomposites. The maximum catalyst activity was obtained by using 15 mg of the TiO_2/Fe nanofiller. The degradation temperature of polyethylene nanocomposites was increased by increasing the TiO_2/Fe nanofiller.

However, the opposite trend was observed in polyethylene/polypropylene nanocomposites due to the increasing of the polypropylene content. Crystallization analysis fractionation (Crystaf) and ^{13}C NMR showed that the polypropylene content was increased as the TiO_2/Fe nanofiller amount increased.

Titanium dioxide doped with tungsten (TiO_2/W) nanofillers are used to study the effect of nanofillers on the polyethylene nanocomposites properties in the presence of the vanadium (III) catalyst. Using titanium dioxide doped with tungsten (TiO_2/W) resulted in increasing the molecular weight (M_w) of polyethylene nanocpomposites up to five times compared to the neat polyethylene. The optimum dosage of the TiO_2/W nanofiller was 10 mg which molecular weight (M_w) was 1.2×10^{6} ($g.mol^{-1}$). The catalyst activity was increased up to 60 % by using the same amount of the TiO_2/W nanofiller.

Polyethylene and ethylene/propylene copolymer nanocomposites were synthesized by using Bis(cyclopentadienyl)zirconium (IV) dichloride in the presence of TiO_2/Fe nanofiller. The molecular weight (M_w) was found to be increased by adding the TiO_2/Fe nanofiller in polyethylene nanocomposites. The maximum catalyst activity was achieved by using 10 mg of TiO_2/Fe nanofiller in all polyethylene and polyethylene/polypropylene nanocomposites. The melting temperature (T_m) and crystallinity of polyethylene nanocomposites were increased by using TiO_2/Fe nanofiller. However, the opposite trend was observed in polyethylene/polypropylene nano-composites due to the increasing of the polypropylene content. Polypropylene content was increased when the TiO_2/Fe nanofiller amount increases.

Non-isothermal crystallization kinetics of polyethylene and polyethylene/polypropylene nano-composites were well fitted with Avrami-Erofeev

model. The crystallization behavior of ethylene/propylene copolymers nanocompopsites was influenced by the comonomer distribution.

For the first time, pressure sensitive adhesives (PSAs) were produced by copolymerization of ethylene and propylene copolymerization using a special catalyst with methyl aluminoxane (MAO) as a cocatalyst. Three different molar feed ratios (50:50, 60:40 and 40:60) of ethylene/propylene (E/P) respectively, were used to investigate the adhesion properties of produced copolymer and the results showed the molar feed ratio (50:50) of (E/P) resulted in producing the highest adhesion properties.

ABSTRACT (ARABIC)

ملخص الرسالة

الاسم الكامل : عمر يحيى باكثير

عنوان الرسالة : كوبلمرة الإيثيلين و البروبيلين بوجود المالئات النانومترية للتيتانيا

التخصص: الهندسة الكيميائية

تاريخ الدرجة : ابريل ٢٠١٤

تعتبر صناعة البوليمرات في المملكة العربية السعودية قطاع سريع النمو بسبب توفر المواد الخام والإنتاج بتكلفة منخفضة. في هذه الدراسة ، فقد تم تصنيع المحفزات المختلفة و المستخدمة في بلمرة الاثيلين و الاثيلين / البروبيلين . لقد استخدم حفاز الفاناديوم (III) المعقدة ذو الصيغة العامة $[RN=CH(2,4\text{-}{}^{t}Bu_2C_6H_2O)]VCl_2(THF)_2$ حيث ان (R) يمثل مجموعة فنيل(Ph).

لقد تم تصنيع مالئات (nanofillers) لاكسيد التيتانيوم النانومترية غير مطعمة والمطعمة بالحديد (TiO_2/Fe) باستخدام تقنية الصل-جل (sol-gel) وذلك لاستخدامها لاول مره في دراسة تاثيرها على خواص بوليمر الاثيلين وكوبوليمر الاثيلين والبروبيلين باستخدام حفازات الفانديوم المعقده والمساعد المحفز (methylaluminum dichloride).

لقد بينت النتائج ان الوزن الجزيئي (M_w) زاد نتيجة إضافة (TiO_2/Fe) في المركبات النانومتريه (nanocomposites) لكل من البولي اثيلين و كوبوليمر الاثيلين والبروبيلين. تم الحصول على أقصى قدر من نشاط الحفاز باستخدام ١٥ ملجم من (TiO_2/Fe) النانومترية. وقد ارتفعت درجة الحرارة تدهور في المركبات النانومتريه للبولي ايثلين (nanocomposites) عن طريق زيادة المالئة(TiO_2/Fe) . ومع ذلك ، لوحظ الاتجاه المعاكس في المركبات النانومتريه (nanocomposites) لكل البولي ايثيلين / البولي بروبلين ويرجع ذلك إلى زيادة المحتوى البولي بروبلين . وأظهر تحليل التبلور بالتجزئة (Crystaf) و الفحص بالرنين المغناطيسي

(C^{13}NMR) أن محتوى مادة البولي بروبيلين زادت مع زيادة كمية (TiO_2/Fe).

ولقد تم استخدام المالئة النانومترية لثاني أكسيد التيتانيوم مطعم بالتنغستن (TiO_2/W) لدراسة تأثير المالئة النانومترية على خصائص المركبات النانومتريه (nanocomposites) لبولي الايثيلين في وجود حفار الفاناديوم (III) . ان استخدام ثاني أكسيد التيتانيوم المطعم بالتنغستن (TiO_2 / W) أدى إلى زيادة الوزن الجزيئي (M_w) لمركبات (nanocpomposites) البولي إثيلين تصل إلى خمسة أضعاف مقارنة مع البولي اثيلين غير المركب (neat). كانت الجرعة المثلى من TiO_2 / W هي 10 ملغ جيث كان الوزن الجزيئي (M_w) ١,٢ x ١٠^{٦} ($g.mol^{-1}$). و تم ايضا زيادة نشاط الحفاز إلى ٦٠٪ باستخدام نفس الكمية من المالئة الناومترية TiO_2/W .

لقد تم انتاج البولي ايثيلين والايثيلين / البروبيلين باستخدام حفاز الزركونيوم (IV) كلوريد باستخدام المالئة النانومتريه ل (TiO_2/Fe) . ولقد اثبتت النتائج زيادة الوزن الجزيئي (M_w) بإضافة TiO_2/Fe للبولي اثيلين. وقد تحقق اعلى نشاط للحفاز باستخدام ١٠ ملجم من TiO_2/Fe في جميع انواع البولي ايثيلين ومركبات البولي ايثيلين / البولي بروبلين النانومترية. وزادت درجة حرارة انصهار (T_m) و التبلور لمركبات البولي ايثلين النانومترية باستخدام المالئة النانومترية TiO_2/Fe nanofiller . وقد لوحظ الاتجاه المعاكس في البولي ايثيلين / البولي بروبلين للمركبات النانومترية ويرجع ذلك إلى زيادة محتوى البولي بروبلين . تم زيادة المحتوى البولي بروبلين بزيادة كمية المالئة النانومترية TiO_2/Fe .

لقد تم دراسة حركية تبلور كلا من البولي ايثلين و البولي ايثيلين / البولي بروبلين للمركبات النانومترية باستخدام معادلة Avrami - Erofeev.

للمرة الأولى، تم إنتاج مواد لاصقة من خلال البلمرة من الاثيلين و البروبيلين ة باستخدام حفاز خاص بوجود المركب المحفز methylaluminoxan (MAO). واستخدمت ثلاث نسب مولية مختلفة (٥٠:٥٠ ، ٦٠:٤٠ و ٤٠:٦٠) من الاثيلين / البروبيلين (E / P) على التوالي لدراسة خصائص التصاق البوليمرات المنتجة وقد اعطت نسبة (٥٠ : ٥٠) من (E / P) أعلى خصائص للالتصاق.

Chapter 1

INTRODUCTION

1.1 General Background

Polyolefins are a rapid growing sector of the polymer industry with the maximum production of nearly 120 million tons a year because of their low cost production, reduced environmental effect and variety of applications. Among these polyolefins, polypropylene and polyethylene are considered the most vital commercial thermoplastic polymers that account about two thirds of consumed plastic materials. Polypropylene and polyethylene are normally used in many applications such as toys, packaging, constructions, etc. [1].

Polyethylene with low density and high branching degree was produced initially by radical polymerization at high temperature and pressure. Polypropylene with low molecular weight was in the beginning produced by many cationic initiators. Ethylene is usually copolymerized with propylene to improve final product properties such as toughness, clarity and flexibility. The invention of Ziegler-Natta catalysts enabled to produce a lot of polymers such as high density polyethylene and polypropylene and their copolymers at low pressure and temperature. The discovery of metallocene catalysts has enabled to control the stereoregularity and the molecular weight distribution [2, 3].

Recently, new early-transition metal complexes (FI catalysts) were developed by change of ligand design which contains a pair of nonsymmetric phenoxyimine ligands. These complex catalysts are very active catalysts for α-polyolefins. Ligand design plays a vital role in the catalyst activity and polymer properties such as morphology and molecular weight [4].

Polyolefins composites have recently paid a great attention because of their exceptional mechanical properties, flammability and gas barrier properties and thermal stability depending on the shape, loading, particle size, dispersion of the fillers and bonding [5-15].

1.2 Scope of the Study

The polymer industry in Saudi Arabia is one of the biggest industries in the world and it is expanding very fast. Nanotechnology is one of the promising and attractive areas that significantly influence our daily life. Application of nanotechnology to polymer research is very interesting. This study aims to study the new catalytic processes in the copolymerization of ethylene with propylene in presence nanofillers such as: nanotitana, titania deped with iron (Fe) and tungesten (W) and develop new materials for usage in automobile, petroleum, construction industries, etc.

1.3 Objectives

This study focuses on the homo and copolymerization studies of ethylene with propylene using different metallocene complex catalysts to develop polyolefins nanocomposites with advanced properties for various applications. The main objectives of the present study could be summarized as follows:

1- To synthesize early transition metal catalysts for the homo and copolymerization of ethylene and propylene.

2- To study the polymerization activity of newly synthesized catalysts using methylaluminum dichloride (MADC) and methylaluminoxane (MAO) as cocatalysts.

3- Homo and copolymerization studies will be carried out by varying parameters like temperature, monomers concentration and nanofillers dosage.

4- To synthesize polyolefin nanocomposites by the addition of nanofillers like (eg. nano titania, Fe-doped titania, W- doped titania) during the polymerization.

5- To study the microstructure of polymers obtained using NMR, XRD, SEM, etc.

6- To study the polymer properties by DSC, TGA, CRYSTAF and GPC.

This thesis consists of seven chapters. Chapter 1, the present one, is this introduction. The descriptions of the other following chapters are as follows:

Chapter 2 presents a literature review on polymer synthesis, especially polyethylene, polypropylene and their copolymerzaion Chapter 3 provides a full description of the experimental setup, instrumentation used and analysis procedures. The rest chapters (4-7) were formatted as journal papers which are proposed to be submitted in the soon future. Therefore, Each chapter of the four chapters starts with an introduction to give background and literature review related to present work done in the current chapter. After that, the experimental method, results and their discussion were presented. Finally, each chapter was concluded with main conclusions.

Chapter 2

LITERATURE REVIEW

2.1 Polymer Structure & Terminology

The word "polymer" was derived from from Greek word πολύς (polus, meaning "many, much") and μέρος (meros, meaning "parts, units"), therefore polymer means many parts or units. A polymer is a big molecule made from a lot of repeated subunits, called monomers (a monomer drives from Greek mono meaning "one" and meros "part"). The repeating units are typically based on a carbon backbone (known as organic polymers). In some cases, they are based in a non-carbon backbone (known as inorganic polymers). Polymers exist in either natural (as silk, proteins), or synthesized (as polypropylene, polyethylene, nylon).

The polymer is called a homopolymer if it is made up from only one kind of monomer and a copolymer if it is made up of two or more kinds of chemically different monomers [16, 17].

2.2 Classification of Polymers

The polymers are classified in different ways based on [16, 17]:

2.2.1 Thermal Behavior

The polymers are classified based on thermal behavior into:

- **Thermoplastics:** These polymers have very long molecules chains connected to each other by weak Van der Waals forces. They melt and flow when they are heated and become flexible and soft and they become solid when they are cooled. Therefore, they are easily reshaped and recycled. Examples of these polymers are polypropylene (PP), nylon (polyamide), polystyrene, polyethylene, etc.
- **Elastomers:** The polymer chains exist in above their glass transition state at room temperature and they are rubbery. The polymer chains can be crosslinked, or connected by covalent bonds at high temperatures. Crosslinking in elastomers is known vulcanization such as natural rubber (polyisoprene), polyisobutylene, polybutadiene, styrene butadiene rubber (SBR), etc.
- **Thermosets:** They have extensive crosslinks between their chains and therefore they decompose when are heated and cannot be reshaped or recycled. Examples of these polymers are unsaturated polyesters, vulcanized rubber, epoxy, etc.

2.2.2 Source the polymers

- **Natural polymers:** Polymers are found in nature, such as starch, natural rubber, DNA, proteins, etc.
- **Synthetic polymers:** Polymers are made by human such as polyethylene, polypropylene, Teflon, polyvinylchloride (PVC), etc.

2.2.3 Polymer Structure

- **Linear:** The polymer chains are connected to each other by linear chains such as nylon, polyethylene, etc.
- **Branched:** The polymer chains are connected to each other by linear chains with branches or chains such as low density polyethylene (LDPE), starch, etc.
- **Crosslinked:** The polymer chains are connected to each other by a three dimensional network (cross linked) such as melamine/formaldehyde resins, polystyrene/butadiene, etc.

2.2.4 Polymerization mechanism

- **Chain growth polymerization or addition polymerization:** In this method, the polymers are made by adding monomers to the polymer chain without elimination of any molecules. Chain growth polymerization is divided into ionic polymerization and free radical polymerization.

- **Step growth polymerization or condensation polymerization:** In this method, the polymers are made by adding monomers to the polymer chain with losing some molecules such as water.

2.2.5 Polymerization processes

- **Bulk polymerization:** No solvents are used in this method and reactants are the monomer and the initiator. This method produces higher pure polymers and more products. However, it is difficult to control temperature rising and producing broad molecular weight distribution polymers.
- **Solution polymerization:** In this method, a miscible solvent is used to reduce the viscosity and thus reducing heat rising. This method is easier to control the temperature, but it gives lower yield.
- **Suspension polymerization:** In this method, the polymer and monomer have to be insoluble in the suspension media such as water. The Initiator is soluble in the monomer and insoluble in water.
- **Emulsion polymerization:** This method is similar to suspension method, but the initiator is insoluble in the monomer and soluble in suspension media (water). The obtained polymer by this method is colloidal and has a narrow molecular weight distribution. However, the yield and purity is low.
- **Precipitation (slurry) polymerization:** In this method, the polymer is insoluble in monomer and solvent but monomer is soluble in the solvent.

- **Interfacial polymerization:** In this method, the polymerization reaction takes place at the interface of two immiscible solvents, typically water and an organic solvent. One reactant should be miscible in the water phase and the other is miscible in the organic phase.

2.3 Polyethylene

Polyethylene (PE) is the most popular plastic polymer with an annual production around 80 million tonnes due to the lots of applications in everyday life and industry and particularly in coatings, packaging, house wares [18]. Polyethylene is classified due to its density, molecular weight and the degree of branching to: high-density polyethylene (HDPE), low-density polyethylene (LDPE), ultra high molecular weight of polyethylene (UHMWPE) and linear low-density polyethylene LLDPE. Low density of polyethylene (LDPE) is a branched homopolymer and contains chemical groups such as methyl, ethyl, etc. It was synthesized initially in 1933 by using a free-radical polymerization at high temperature and pressure. It has a density range of 0.910–0.940 g/cm^3. LLDPE is synthesized by copolymerization of ethylene with α-olefins such as 1-hexene and 1-octene in the presence of metallocene and Ziegler-Natta via coordination techniques. It has a density range of 0.915–0.925 g/cm^3. HDPE is a highly crystalline polymer with few or without branches. It has a density greater than 0.94 g/cm^3. HDPE is usually synthesized by Ziegler-Natta catalysts, metallocene catalysts or chromium/silica catalysts [18, 19]. Ultra-high molecular weight polyethylene (UHMWPE) is an exceptional polymer with unique mechanical and

physical properties such as chemical resistance, thermal stability, impact resistance, abrasion resistance and lubricity as a result of their supermolecular structure and the high molecular weight [20, 21]. Ultra-high molecular weight polyethylene (UHMWPE) can be used in medical fields as joint replacements and joint arthroplasty or in the military as personal armor and vehicle armor and in various industry applications [22, 23]. Ultra-high molecular weight polyethylene is obtained by polymerization of ethylene at low pressure using Zeigler-Natta catalyst supported by fixing $TiCl_4$ or $VOCl_3$ onto amorphous SiO_2 [20, 24].

Table 2-1: Summary of the common applications of polyethylene types.

Polyethylene	Applications
HDPE	Milk jugs, crates, boxes, bottles, water pipes, houseware, toys, petrol tanks, industrial wrapping and film.
LDPE	Agricultural film, milk carton coatings, laboratory dispensing and wash bottles.
LLDPE	Packaging films, thin walled containers, stretch and cling wraps, toys, cable covering, and lids.
UHMWPE	Personal armor and vehicle armor, gears, bearings, joint replacements, artificial joints and machine parts.

2.4 Polypropylene

Polypropylene (PP) is a semi crystalline thermoplastic polymer consisting of a carbon chain with a methyl group which is connected to each second carbon of the chain. Polypropylene (PP) with a crystalline isotactic structure was first produced by Giulio Natta and Karl Rehn in March 1954 [25]. Polypropylene is used in many applications such as packaging, laboratory equipment, textiles, and automotive. Propylene is copolymerized with ethylene to improve its mechanical and thermal properties [26, 27].

2.5 Catalysts Types for Polymerization of Alkenes

The alkenes (olefins) are defined as unsaturated chemical compounds consisting of at least one carbon–carbon double bond with general formula C_nH_{2n} [1].

2.5.1 Ziegler–Natta catalysts

These catalysts were discovered by Karl Ziegler (Germany) and Giulio Natta (Italy) in 1953 for alkenes polymerization [25]. They were prized the Nobel Prize in Chemistry in 1963. These catalysts have been used widely in polymer synthesis due to their ability to prepare stereoregular polymers. Ziegler–Natta catalysts can be classified due to their solubility into: heterogeneous supported catalysts based on titanium compounds and homogeneous catalysts typically based on complexes of Zr, Hf and Ti [28].

2.5.2 Phillips/Chrome catalysts

The Phillips/Chrome catalysts were discovered by Hogan and Banks at Phillips Petroleum Co. in 1958. These catalysts are made from chromium oxides which are impregnated with silica [29]. About more than 30% of the world polyethylene production is produced by theses catalysts. These catalysts do not need any activator (cocatalyst) to be active and they must be used at high temperatures ($T > 130\ ^{o}C$) [30].

2.5.3 Metallocene catalysts

Metallocene catalysts are considered the most recent adding to the olefin polymerization catalysts chapter. They have a general formula $(C_5H_5)_2MX_2$ and consist of two cyclopentadienyl anions Cp ($C_5H_5^-$) bonded to a transition metal (M) (titanium, zirconium, and hafnium) are halogen atoms (X) (mostly chlorine, Cl) as shown in Figure 2.1. Metallocenes by themselves are not active for polymerization. They usually are activated by using methylaluminoxane (MAO) or borate compounds. The polymer produced using metallocene catalysts has a narrow molecular weight distribution, lower polydispersity [3, 31].

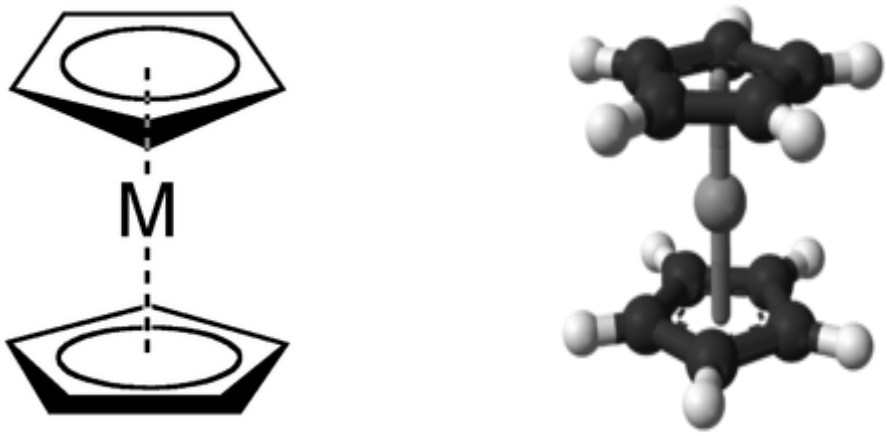

(a) (b)

Figure 2-1: (a) General structure of metallocene (b) Ball and stick structure

2.5.4 Post-metallocene catalysts

Post-metallocene catalysts are a new class of homogeneous catalysts for olefin polymerization. They are made of late transition metal complexes bearing bulky, neutral, α-diimine ligands as shown in Figure 2.2. These catalysts have been used to produce a high density of polyethylene [32].

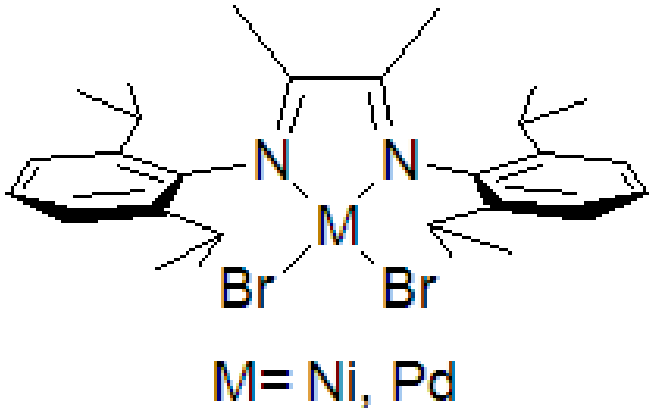

Figure 2-2: General structure of post-metallocene catalysts.

2.6 Cocatalysts used in the Activation of Metallocenes

Metallocenes by themselves are not active for polymerization. They typically are activated by using methylaluminoxane (MAO) or borate compounds. The invention of methylaluminoxane (MAO) was the initiate for researches and novelty of new categories of extremely active olefins polymerization catalysts. Using MAO compounded with different transition metals as cocatalyst allows synthesizing polymers with a well known microstructure, stereoregularity and tacticity with exceptional properties. Methylaluminoxanes have a general structure formula $(Al(CH_3)O)_n$ [3, 33].

2.7 Mechanism of Metallocene Catalysis

The mechanism of polymerization of olefins by using metallocene catalysts can be explained by choosing zirconium and MAO as an example [34-38].

2.7.1 Chain initiation

The metallocene reacts with the MAO, the chlorine atoms are replaced by methyl groups on the metallocene. MAO then work as a Lewis acid (an electron-pair acceptor) and the positive ion is created by sharing electrons from C-H bonds. Zirconium (Zr) becomes positively charged, resulting in opening a coordination site on the Zr center to coordinate ethylene via its π-electrons and attracts the double bond electrons. Then, the alkyl group (R) (e.g. CH_3) migrates from the Zr atom to a carbon atom of the ethylene as shown in Figure 2.3

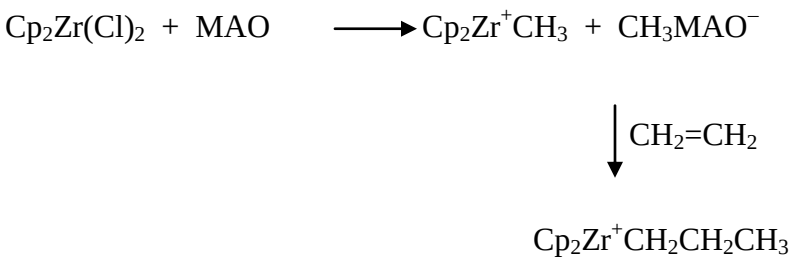

Figure 2-3: Chain initiation scheme.

2.7.2 Propagation

Propagation continues with addition of monomers to the active species, i.e. the carbenium ion. In this step, the alkyl group (R) (e.g. CH_3) moves to allow an additional ethylene molecule to coordinate to zirconium and the process is repeated in the same manner and the polymer chain becomes longer and longer.

2.7.3 Termination

The termination step is occurred by the movement of a hydrogen atom on the β-carbon of the alkyl of the growing polymer chain back to the metal center, resulting in the dissociation of the polymer and the metal center. The polymerization can be stopped by adding of hydrogen gas (H_2) to the reaction system.

2.8 Polymer Nanocomposites

Nanocomposites are new materials synthesized by using fillers which at least one of their dimensions has a range 1 to 100 nm. Polymer nanocomposites are made by adding small amounts (less than 5% by weight) of nano-sized particles [39].

2.8.1 Preparation methods

There are many methods to prepare nanocomposites and all of these methods aim to provide strong physical interactions between the polymer and nanofillers because the weak interactions between them result in poor thermal and mechanical properties and the contrast is correct. To achieve these strong interactions, the

nanofillers should be well dispersed inside the polymer matrix [40]. The methods are [40]:

2.8.1.1 Chemical vapor deposition

In this method, a volatile solid is deposited on a substrate to produce the desired materials with very high purity and very small particle size. This method is usually used for coatings and to produce very fine powders. The main disadvantage of this method is the low yield.

2.8.1.2 Polymerized complex

This method is based on Pechini process and using polymeric precursor. It is usually used to make a broad variety of ceramic oxides. The main advantages of this process are the accurate control of stoichiometry and homogeneity of mixing of multi components on a molecular level.

2.8.1.3 High-energy ball milling process

High-energy ball milling method is used in different industries to make a size reduction for a lengthy time. This method is suitable for producing large amounts of nanomaterials due to their flexibility, cost-effectiveness and scalability.

2.8.1.4 Hydrothermal synthesis

In this method, the reactants are either suspended or dissolved in water and then moved to acid digestion closed reactors.

2.8.1.5 Microwave synthesis

In this method, the microwaves are used for generating a chemical deposition on solid surfaces such as the fabrication of carbon nanotubes and coils.

2.8.1.6 Sol–gel synthesis

Sol–gel synthesis is a promising and efficient method due to its simplicity because it can be used at normal pressures and temperatures. It is cheaper compared to other methods and it allows controlling properties of the final product by changing the process parameters such as solution temperature, the ratio of precursor to acid and solvent and sonication time. For these advantages, the Sol – gel method was selected to produce all the nanofillers which were used in this study.

2.9 Titania Nanocomposites

Different inorganic nanoparticles were used such as titanium dioxide (TiO_2) [41-44], silicon dioxide (SiO_2) [45-48], Aluminium trioxide (Al_2O_3) [49, 50] and zirconium dioxide (ZrO_2) [51, 52] have been employed to develop polymer properties.

Polymer-based TiO_2 composites have been studied in the literature, like high impact polystyrene (HIPS)/nano-TiO_2 [53] and polyamide/nano-TiO_2 composite [54]. However, titania filled polyolefins will be the focus of our discussion.

TiO_2 filled polyethylene composites were prepared by Wang et al [55] in 2005 by using a two-step melt compounding using an extruder. The results showed that

strength and tensile strength were improved by about 45% and 50%, respectively compared with neat.

Supaphol et al., [56] in 2007 blended polypropylene (PP) with TiO_2 using an extruder for melt blending. They found that crystallization exotherm for each sample was bigger and moved towards a lower temperature when the cooling rates were increased. However the melt blending technique is not the best since it typically results in nanoparticle aggregation and phase separation, low mechanical properties and weak interfacial adhesion between the filler and the polymer matrix [57-59]. These drawbacks can be overcome by using in situ polymerization method. Kaminsky et al., showed the handling of filler surfaces with metallocene-based catalysts could be utilized in the synthesis of polyolefin nanocomposites [3, 60].

Ethylene was polymerized at 5 bar in a stirred powder bed reactor with silica supported rac-$Me_2Si[Ind]_2ZrCl_2$/methylaluminoxane (MAO) temperatures between 40°C and 80°C using NaCl as support bed and triethylaluminium (TEA) as a scavenger for impurities. The results showed that polymerization rate and the rate of deactivation increase by increasing the temperature [61]. Gas-phase polymerization of ethylene was studied using a zirconocene catalyst supported on mesoporous molecular sieves impregnated with methylaluminoxane and bis(butylcyclopentadienyl)zirconium dichloride [62].

Tannous and Soares investigated the influence of polymerization conditions on the gas-phase polymerization of ethylene with a supported metallocene catalyst (Cp_2ZrCl_2/SiO_2) using a semi-batch autoclave reactor [63]. Guoet al., synthesized

metal oxide-isotactic polypropylene nanocomposites using C_2-symmetric metallocene catalyst dichloro[rac-ethylenebisindenyl]zirconium(IV) ($EBIZrCl_2$) immobilized on methylaluminoxane (MAO)-treated barium titanate ($BaTiO_3$) or titanium dioxide (TiO_2) nanoparticles to enhance the polymer strength [64].

Owpradit et al., impregnated TiO_2 nanofillers with dMMAO to get dMMAO/TiO_2 and study the effect of crystalline phases of titania on the intrinsic activity to synthesize LLDPE/TiO_2 nanocomposites by in situ polymerization in the presence of the zirconocene/dMMAO catalyst. Ethylene/1-hexene were copolymerized by using zirconocene catalyst and in the presence of dMMAO/TiO_2. The catalytic activity was increased about four times by using the anatase TiO_2 compared to the rutile TiO_2 [65]. Polypyrrole (PPy) and Titanium (IV)-doped synthetic nanostructured iron(III) oxide (NITO) nanocomposites were produced by in situ polymerization by using $FeCl_3$ as initiator. The experiments showed that the polymer nanocomposites have higher thermal stability than pure polymer [66].

Chapter 3

METHODOLOGY

All materials were analytical grade reagents and used without further purification. Dionized water was obtained by the deionization of distilled water by using a Milli-Q water purification system (Millipore). All used glasswares were Pyrex and cleaned with soap and washed with deionized water and dried in an oven at 160 ^{O}C. More details of these materials are shown in Table 3.1.

Table 3-1: List of main chemicals and providers.

Material	Material purity	Material provider
Hydrochloric acid	10 % (V/V)	Sigma-Aldrich
Titanium (IV) isopropoxide	99.99%	Fisher Scientific
Iron (III) nitrate nonahydrate $Fe(NO_3)_3 \cdot 9H_2O$	99.9 %	Sigma Aldrich
Methanol	99.9%	Fisher Scientific
Tungsten (VI) oxide	99.995%	Sigma-Aldrich
Ethanol	99.5	Fisher Scientific
Bis(cyclopentadienyl) zirconium (IV) dichloride($C_{10}H_{10}Cl_2Zr$)	98%	Sigma-Aldrich
Ethylene, ethylene and propylene gas mixtures	99.95%	SIGAS
VCl_3 $(THF)_3$	97%	Sigma-Aldrich
Tetrahydrofuran	99.9%	Sigma-Aldrich
Toluene	99.8%	Sigma-Aldrich
1,2,4-Trichlorobenzene HPLC	99.5%	Sigma-Aldrich
Methylaluminoxane solution (MAO)	10 wt. % in toluene	Sigma-Aldrich
Methylaluminum dichloride (MADC)	1.0 M in hexanes	Sigma-Aldrich

3.1 Catalysts Synthesis

In our study, the ligands and complexes were synthesized according to Figure 3-1. Substituted salysilaldehyde and aniline when reacted in the presence of formic acid undergo imine reaction to form the ligand **B**. The ligand **B** on treating with a corresponding metallating agent like $VCl_3(THF)_3$, $CrCl_3(THF)_3$ complexes of Cr and V were formed and used for polymerization reactions in combination with various cocatalysts. Legends and complexes were purified by standard techniques like column chromatography, crystallization, etc. Ligands and complexes were characterized by NMR, IR, MS, and elemental analysis. However, chromium complex was eliminated from this study due to its very sensitivity to the oxygen (O_2) and therefore the activity of the catalyst was very low.

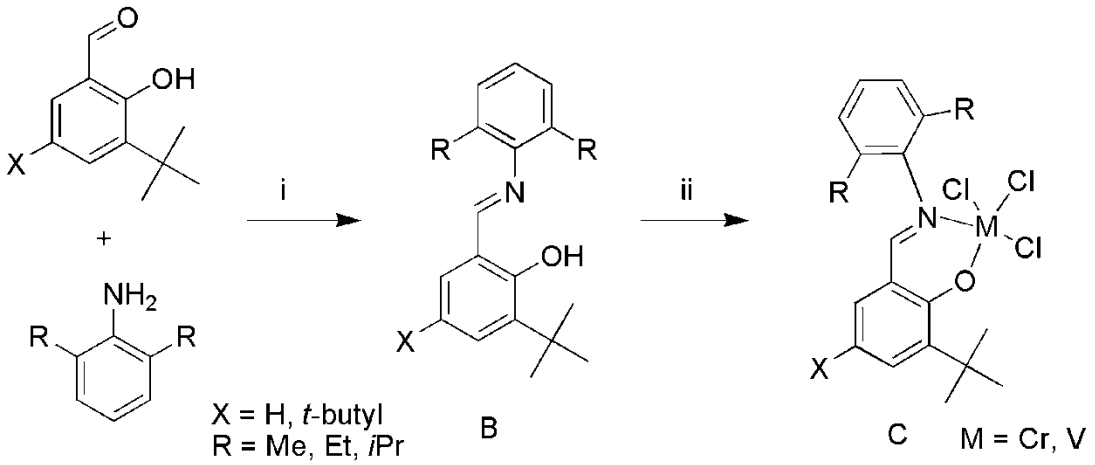

Figure 3-1: Synthesis of early transition metal complexes. i) H+/MeOH, ii) $VCl_3(THF)_3$, $CrCl_3(THF)_3$

3.2 Synthesis of Undoped and Doped Titania Nanofillers

Undoped titania nanofillers were synthesized by a sol-gel process under constant sonication as following: 500 μL of titanium (IV) alkoxide precursor in ١٥ mL ethanol was hydrolyzed in the presence of 1 mL of water at room temperature to form white solution of hydrolyzed titania particles. For iron doped titania nanofillers, an inorganic precursor $Fe(NO_3)_3{\cdot}9H_2O$ (١% solution) was dissolved in 5 mL of ethanol solution and added to the hydrolyzed titania solution under constant sonication (500 rpm) for 30 minutes. After that, the precipitate was washed with ethanol many times to remove excess NO_3^-, Fe^{3+}. The precipitate was dried overnight at 100 ^{0}C and then heated for 5 hours to convert the amorphous titania into the crystalline anatase form. Finally, the product was ground into a fine powder [67]. The samples were denoted as Ti for undoped titania and TiO_2/Fe for iron doped titania. The same procedure was followed to prepare titania doped with tungsten (TiO_2/W) by using 1.2 grams of tungsten (VI) oxide which were dissolved in 25 ml of ethanol.

3.3 Polymerization

Polymerization reaction was taken place in a 250 mL round-bottom flask provided with a magnetic stirrer. The catalyst and various amounts of the nanofiller were added to the flask and filled with 80 mL of toluene. Then, the flask was put in an oil bath at equilibrated temperature (30 °C) and nitrogen gas was removed by a vacuum pump. Then ethylene was supplied into the reactor. After 10 minutes of the saturation of ethylene in toluene, The cocatalyst was charged into the flask and polymerization reaction was

started. After 10 minutes, polymerization reaction was quenched by adding 250 mL of methanol containing HCl (5 vol. %). Finally, the polymer was put in an oven at 50 °C for 24 hours for drying. The same procedure was followed for ethylene/propylene copolymerization.

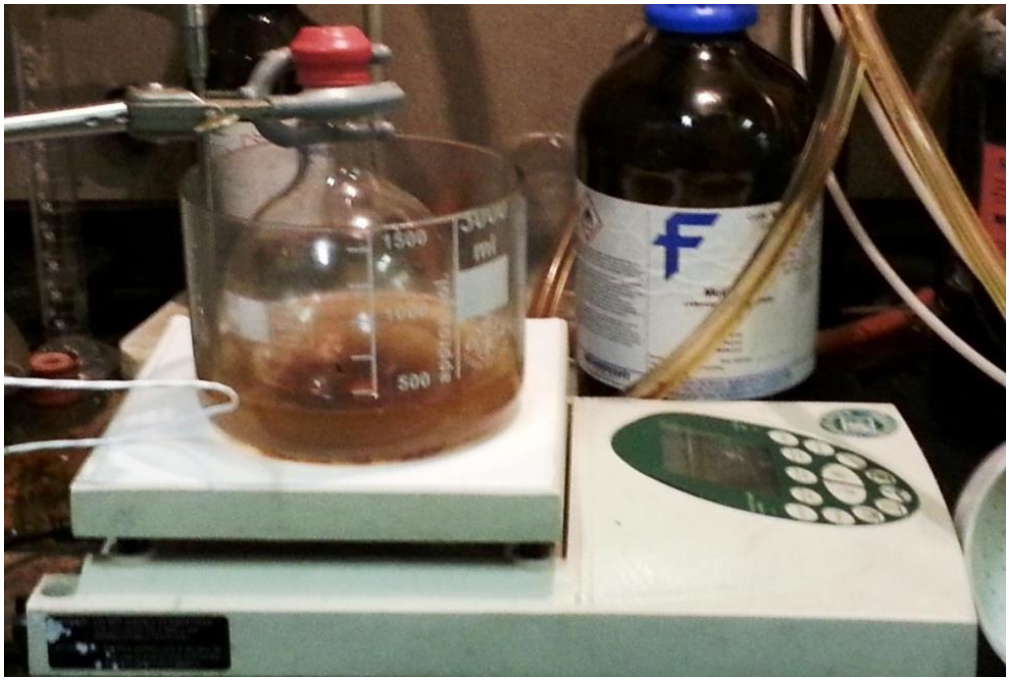

Figure 3-2: A photo of the polymerization system.

3.4 Characterization of polymer nanocomposites

The following techniques have been employed to characterize the produced polymer nanocomposites:

- Differential Scanning Calorimetry (**DSC**).
- X-ray Diffraction (**XRD**).
- Scanning Electron Microscopy (**SEM**).
- Crystallization Analysis Fractionation (**CRYSTAF**).
- Nuclear Magnetic Resonance Analysis (**NMR)**.
- Thermal Gravimetric Analysis (**TGA**).
- Gel permeation chromatography **(GPC).**

3.4.1 Differential Scanning Calorimetry (DSC)

Differential Scanning Calorimetry (DSC) is a well known thermal analysis technique that measures the difference in heat flow rate (endothermic and exothermic transitions) between a sample and inert reference as a function of temperature and time. It is used to characterize foods, organic or inorganic materials, polymers, pharmaceuticals. This technique provides some information, such as: melting temperature (T_m), glass transition temperature (T_g), degree of crystallinity (X_c), crystallization time and temperature, heat of fusion, specific heat, etc [68, 69].

In this study, the differential scanning calorimetry (DSC) was performed by using a TA Q1000 instrument as shown in Figure 3-3. The Crystallinity of ethylene and ethylene/propylene copolymer nanocomposites (X_c %) and melting temperature (T_m) were

measured by using 5-7 mg of the produced polymer. Cooling and heating cycles were performed in a nitrogen environment at the rate of 10°C min^{-1} from a temperature of 30 °C to 160 °C.

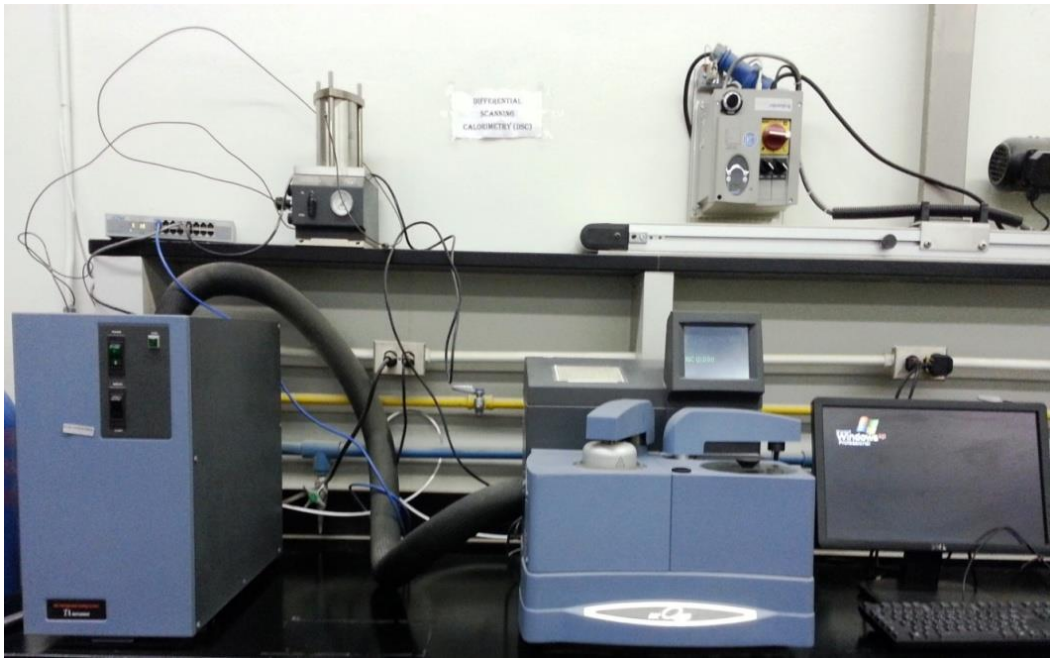

Figure 3-3: Differential scanning calorimetry (DSC).

3.4.2 X-ray Diffraction (XRD)

X-ray diffraction is a non-destructive and qualitative analysis, which is used to investigate the crystal structure, physical properties and chemical composition [68]. In this research, the crystallinity measurements were carried out by using a LABX XRD-6000, Shimadzu Diffractometer operating at 40 kV, 40 mA. X-rays of 1.541 A° wavelength generated by Cu Kα source as shown in Figure 3-4. The angle of

diffraction 2θ was varied from 2° to 70°.

Figure 3-4: An x-ray diffraction system.

3.4.3 Scanning Electron Microscopy (SEM)

Scanning electron microscopy is a microscope produces images of objects by using the electrons instead of light. It is widely used in industry, medical, scientific researches, etc. to investigate the morphology of the objects such as metals, catalyst, polymers, composites, etc. Scanning electron microscopy (SEM) is consisting of an electron gun, magnetic lenses, detectors, deflection coils and the display units as shown in Figure 3-5. The principle is the electron gun produces a high energy of electrons beam

that pass through lenses and hit the sample. Once the electrons beam strike the sample, the variety of signals are collected by the detectors. To get clear images by using the SEM, specimens have to be electrically conductive at the surface to avoid the accumulation of electrostatic charge on the surface. For non conductive specimens, they must be coated by electrically conducting material such as gold, gold/palladium alloy, copper, platinum, etc. by using low-vacuum sputter coating [70, 71].

Figure 3-5: Scanning Electron Microscope (SEM) system.

Morphology of polyethylene / polyethylene nanocomposites was studied using scanning electron microscopy (SEM) using the polymer films prepared as follows: First, aluminum substrates with 10 mm x 15 mm x 2 mm dimensions were heated up to 160 °C. Then, polyethylene / polyethylene nanocomposites powders were put inside the hot

substrates and compressed by using Carver 25-ton press (Figure 3-5) by applying 4000 pounds load for 5 minutes. After that, the substrates were cooled to get uniform polymer films. Finally, the films were put in liquid nitrogen and quickly cracked.

Figure 3-6: A Hydraulic Carver press.

3.4.4 Crystallization Analysis Fractionation (CRYSTAF)

Crystallization analysis fractionation (CRYSTAF) is an analytical technique which is used to determine the distribution of chain of semicrystalline polymers. CRYSTAF is considered a vital characterization technique in polymer characterization because it gives essential information the structure and the mechanism of the polymerization.

CRYSTAF instrument (Figure 3-7) is a completely automated instrument which is used for the quick measurement of the Chemical Composition Distribution (CCD) in Polyolefins. During crystallization analysis fractionation technique, the polymer is separated to its comonomer content. The main advantages of CRYSTAF instrument are [72]:

- The process is fully automated and only one temperature ramp is required to achieve the process.
- Up to five samples can be loaded and the end of the process, the lines and vessels are cleaned automatically.
- The time required for analysis by using CRYSTAF instrument is less compared to the TREF instrument.
- CRYSTAF instrument can be connected to the TREF to give more information about chemical composition distribution (CCD) in some complex resins.

Figure 3-7: CRYSTAF instrument system.

3.4.5 Nuclear Magnetic Resonance Analysis (NMR)

Nuclear magnetic resonance (NMR) is a powerful analytical analysis, which is widely used in many scientific researches to investigate molecular physics, crystals structures, polymer structures, etc. The principle is the nuclei in a magnetic field absorb and reemit electromagnetic radiation [73, 74]. In our research, ^{13}C NMR and ^{1}H were used to determine the composition of ethylene/propylene (E/P) copolymer and catalyst composition using a Bruker AVANCE III-600 NMR spectrometer (Figure 3-8) and 1, 2, 4-trichlorobenzene as a solvent.

Figure 3-8: A 600 NMR spectrometer.

3.4.6 Thermal Gravimetric Analysis (TGA)

Thermal gravimetric analysis (TGA) or thermogravimetric analysis is used to measure either mass loss or gain of a material as a function of temperature or time in a controlled atmosphere. TGA provides information about chemical and physical phenomenon such as decomposition, solid-gas reactions (e.g., reduction an oxidation) and chemisorptions, phase transitions [75]. SDT Q600 (TA instruments, USA) was employed to study the thermal gravimetric analysis as shown in Figure 3-9. The samples were heated in nitrogen atmosphere from 30° to 650 °C at a heating rate of 10 °C per minute.

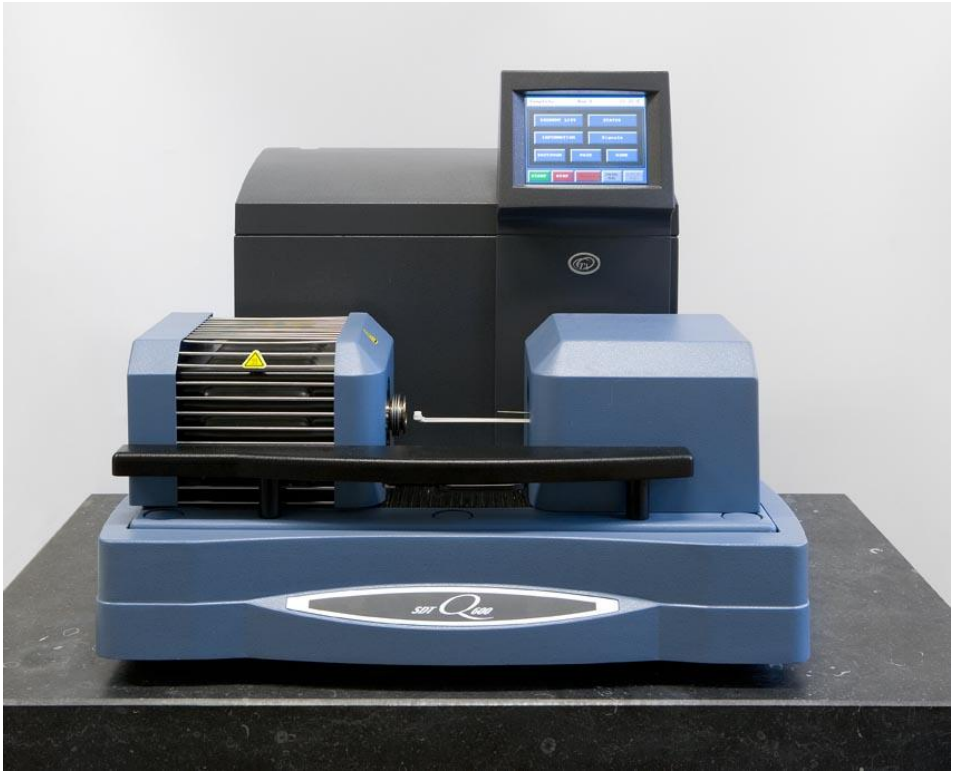

Figure 3-9: SDT Q600 system.

3.4.7 Gel permeation chromatography (GPC).

Gel permeation chromatography (GPC) or size exclusion chromatography (SEC) is a chromatographic technique which is used to separate molecules in solution based on their size or molecular weights by passing them through columns including a microporous packing material. GPC is widely used to characterize proteins, polymers, nanoparticles, etc. [76]. In this study, the molecular weights of polyethylene and polyethylene/polypropylene nanocomposites were determined by triple detection-high temperature gel permeation chromatography (GPC) (model: HT-GPC 350, Malvern, Figure 3-10) and using 1, 2, 4-trichlorobenzene as a solvent. Twenty-five mg of the material was placed into a 40 mL glass vial and accurately weighed and 10 mL of the solvent was added using a clean 10 mL glass pipette. The vial was capped with a Teflon coated cap and the samples were placed into the Vortex Auto Sampler and left to dissolve for 3 hrs at 160 °C while stirring gently. The calibration curves were obtained from polystyrene standards.

Figure 3-10: Gel permeation chromatography (GPC) system.

3.5 Crystallization Kinetics Model

In this study, the effects of nanofiller on the crystallization kinetics of homo polyethylene and ethylene /propylene copolymer were investigated using nonisothermal Avrami-Erofeev crystallization model by following the same procedure as reported by Atiqullah et al., by using cooling rate of 10°C/min [77].

The nonisothermal Avrami-Erofeev crystallization rate equation is given by:

$$\frac{d\alpha(T)}{dT} = \frac{k_0}{\beta} \times exp\left[-\frac{E_a^A}{R}\left(\frac{1}{T} - \frac{1}{T_0}\right)\right] \times n(1-\alpha(T))[-ln(1-\alpha(T))]^{\frac{n-1}{n}} \qquad (3\text{-}1)$$

Where:

$$f(\alpha(T)) = n(1-\alpha(T))[-ln(1-\alpha(T))]^{\frac{n-1}{n}} \quad (3\text{-}2)$$

$$k'(T) = k_0 \times exp\left[-\frac{E_a^A}{R}\left(\frac{1}{T}-\frac{1}{T_0}\right)\right] \quad (3\text{-}3)$$

$$E_a^A(\text{apparent crystallization energy}) = E_{grow} - E_{nucl} \quad (3\text{-}4)$$

$$k_0 = \left(\frac{K_s N_0}{V_0}\right)\frac{k_{grow,0}}{k_{nucl,0}} \quad (3\text{-}5)$$

$$k_{grow}(T) = k_{grow,0} \times exp\left[-\frac{E_{grow}}{R}\left(\frac{1}{T}-\frac{1}{T_0}\right)\right] \quad (3\text{-}6)$$

$$k_{nucl}(T) = k_{nucl,0} \times exp\left[-\frac{E_{nucl}}{R}\left(\frac{1}{T}-\frac{1}{T_0}\right)\right] \quad (3\text{-}7)$$

$$\alpha(T) = \frac{\alpha_w(T)}{\alpha_w(T)+{\rho_c}/{\rho_a}[1-\alpha_w(T)]} \quad (3\text{-}8)$$

E_{grow} and E_{nucl} are the corresponding activation energies and $f(\alpha(T))$ is Avrami-Erofeev nonisothermal crystallization function. n is the dimension of the growing crystal. V_0 represents the initial volume of the molten polymer. N_0 represents the number of germ nuclei. K_s is the shape factor for the growing nuclei. $k_{grow,0}$ and $k_{nucl,0}$ represent the frequency factors for crystal growth and nucleation respectively. $k_{grow}(T)$ and $k_{nucl}(T)$ follow the Arrhenius form [78, 79]. T_0 is the reference temperature. ρ_c and ρ_a are the densities of the crystalline and amorphous phases, respectively. The values reported for polyethylene are ρ_c = 1.004 g/mL and ρ_a = 0.853 g/mL (Atiqullah et al. 2012).

$\alpha_w(T)$ can be found from the data of a constant cooling rate (second cycle) of nonisothermal DSC experiment.

$$\alpha_w(T) = \frac{\Delta H(T)}{\Delta H_{total}} = \frac{\int_{T_0}^{T}\left(\frac{dH}{dT}\right)dT}{\int_{T_0}^{T_\infty}\left(\frac{dH}{dT}\right)dT} \quad (3\text{-}9)$$

Where $\Delta H(T)$ is the enthalpy corresponding to temperature T of crystallization. ΔH_{total} represents the maximum enthalpy obtained at the end of the nonisothermal crystallization process. T_0 and T_∞ represent the initial and the final temperatures of crystallization, respectively.

3.5.1 Numerical solution of the crystallization kinetics

The non-linear model system was solved using NonLinearModelFit of MATHEMATICA. The performance of the crystallization kinetics model was evaluated based on the coefficient of determination (R^2), 95% confidence interval, standard error and the variance.

References

1. Pistikopoulos, E.N., M.C. Georgiadis, and A.C. Kokossis, *21st European Symposium on Computer Aided Process Engineering*. 1st ed. 2011: Elsevier.
2. Busico, V. and R. Cipullo, *Microstructure of polypropylene.* Progress in Polymer Science, 2001. 26(3): p. 443-533.
3. Kaminsky, W., *New polymers by metallocene catalysis.* Macromolecular Chemistry and Physics, 1996. 197(12): p. 3907-3945.
4. Houghton, J., et al., *Transition-metal complexes of phenoxy-imine ligands modified with pendant imidazolium salts: Synthesis, characterisation and testing as ethylene polymerisation catalysts.* Journal of Organometallic Chemistry, 2008. 693(4): p. 717-724.
5. Jeon, H.G., et al., *Morphology of polymer/silicate nanocomposites High density polyethylene and a nitrile copolymer.* Polymer Bulletin, 1998. 41(1): p. 107-113.
6. Zhao, C., et al., *Mechanical, thermal and flammability properties of polyethylene/clay nanocomposites.* Polymer Degradation and Stability, 2005. 87(1): p. 183-189.
7. Gopakumar, T.G., et al., *Influence of clay exfoliation on the physical properties of montmorillonite/polyethylene composites.* Polymer, 2002. 43(20): p. 5483-5491.
8. Zanetti, M., P. Bracco, and L. Costa, *Thermal degradation behaviour of PE/clay nanocomposites.* Polymer Degradation and Stability, 2004. 85(1): p. 657-665.
9. Shin, S.-Y.A., et al., *Polyethylene–clay hybrid nanocomposites: in situ polymerization using bifunctional organic modifiers.* Polymer, 2003. 44(18): p. 5317-5321.

10. Wang, J., et al., *Preparation of a PE/MT Composite by Copolymerization of Ethylene with In-Situ Produced Ethylene Oligomers under a Dual Functional Catalyst System Intercalated into MT Layer.* Macromolecular Rapid Communications, 2001. 22(17): p. 1422-1426.

11. Alexandre, M., et al., *Polyethylene-layered silicate nanocomposites prepared by the polymerization-filling technique: synthesis and mechanical properties.* Polymer, 2002. 43(8): p. 2123-2132.

12. Yang, F., et al., *Preparation and properties of polyethylene/montmorillonite nanocomposites by in situ polymerization.* Journal of Applied Polymer Science, 2003. 89(13): p. 3680-3684.

13. Jin, Y.-H., et al., *Polyethylene/Clay Nanocomposite by In-Situ Exfoliation of Montmorillonite During Ziegler-Natta Polymerization of Ethylene.* Macromolecular Rapid Communications, 2002. 23(2): p. 135-140.

14. Wei, L., T. Tang, and B. Huang, *Synthesis and characterization of polyethylene/clay–silica nanocomposites: A montmorillonite/silica-hybrid-supported catalyst and in situ polymerization.* Journal of Polymer Science Part A: Polymer Chemistry, 2004. 42(4): p. 941-949.

15. Kuo, S.-W., et al., *Syntheses and characterizations of in situ blended metallocence polyethylene/clay nanocomposites.* Polymer, 2003. 44(25): p. 7709-7719.

16. Fried, J., *Polymer Science and Technology* 2nd ed. 2003: Prentice Hall.

17. Rodriguez, F., *Principles of Polymer Systems, .* 4th ed. 1996: Taylor & Francis.

18. Piringer, O.G. and A.L. Baner, *Plastic packaging: interactions with food and pharmaceuticals*. 2nd ed. 2008: Wiley.

19. Saini, D.R. and A.V. Shenoy, *Viscoelastic properties of linear low density polyethylene melts.* European Polymer Journal, 1983. 19(9): p. 811-816.

20. Velikova, M., *Study of the effect of the nature of catalyst systems on the molecular structure and properties of ultra-high molecular weight polyethylene.* European Polymer Journal, 2001. 37(6): p. 1255-1262.

21. Li, S.B., Albert H, *Current concepts review Ultra-high molecular weight polyethylene The material and its use in total joint implants.* Journal Of Bone & Joint Surgery American Volume, 1994. 76((7)): p. 1080-1090.

22. Kurtz, S.M., et al., *Advances in the processing, sterilization, and crosslinking of ultra-high molecular weight polyethylene for total joint arthroplasty.* Biomaterials, 1999. 20(18): p. 1659-1688.

23. Simis, K.S., et al., *The combined effects of crosslinking and high crystallinity on the microstructural and mechanical properties of ultra high molecular weight polyethylene.* Biomaterials, 2006. 27(9): p. 1688-1694.

24. Minkova, L., M. Velikova, and D. Damyanov, *Structural investigations of nascent polyethylenes obtained on supported titanium and vanadium catalyst systems.* European Polymer Journal, 1988. 24(7): p. 661-665.

25. Natta, G. and P. Corradini, *Structure and properties of isotactic polypropylene.* Il Nuovo Cimento Series 10, 1960. 15(1): p. 40-51.

26. KARIAN, *Handbook of Polypropylene and Polypropylene Composites*. 2nd ed. 2003: Marcel Dekker

27. Akay, M., *Introduction to Polymer Science and Technology*. 1st ed. 2012: bookboon.

28. Ray Hoff and R.T. Mathers, *Handbook of Transition Metal Polymerization Catalysts*. 1st ed. 2010: John Wiley & Sons.

29. Groppo, E., et al., *The Structure of Active Centers and the Ethylene Polymerization Mechanism on the Cr/SiO_2 Catalyst: A Frontier for the Characterization Methods.* Chemical Reviews, 2005. 105(1): p. 115-184.

30. Theopold, K.H., *Homogeneous Chromium Catalysts for Olefin Polymerization.* European Journal of Inorganic Chemistry, 1998. 1998(1): p. 15-24.

31. Hlatky, G.G., *Metallocene catalysts for olefin polymerization: Annual review for 1996.* Coordination Chemistry Reviews, 1999. 181(1): p. 243-296.

32. Domski, G.J., et al., *Living alkene polymerization: New methods for the precision synthesis of polyolefins.* Progress in Polymer Science, 2007. 32(1): p. 30-92.

33. Kaminsky, W., *Discovery of Methylaluminoxane as Cocatalyst for Olefin Polymerization.* Macromolecules, 2012. 45(8): p. 3289-3297.

34. Siedle, A.R., et al., *Mechanism of olefin polymerization by a soluble zirconium catalyst.* Journal of Molecular Catalysis A: Chemical, 1998. 128(1–3): p. 257-271.

35. Lohrenz, J.C.W., et al., *A density functional study on the insertion mechanism and chain termination in Kaminsky-type catalysts; comparison of frontside and backside attack.* Journal of Organometallic Chemistry, 1995. 497(1-2): p. 91-104.

36. Woo, T.K., L. Fan, and T. Ziegler, *A density functional study of chain growing and chain terminating steps in olefin polymerization by metallocene and constrained geometry catalysts.* Organometallics, 1994. 13(6): p. 2252-2261.

37. Ustynyuk, L.Y., et al., *Zirconocene catalysts for olefin polymerization: A comparative DFT study of systems with Al- and B-containing activators.* Journal of Organometallic Chemistry, 2012. 700(0): p. 166-179.

38. Kaminsky, W., *Olefin polymerization catalyzed by metallocenes*, in *Advances in Catalysis*. 2001, Academic Press. p. 89-159.

39. Gacitua, W.E., A.A. Ballerini, and a.J. Zhang, *Polymer nanocomposites: synthetic and natural fillers—a review.* Maderas Cienciay Tecnología, 2005. 7(3): p. 159–178.

40. Biswas, M. and S. Ray, *Recent Progress in Synthesis and Evaluation of Polymer-Montmorillonite Nanocomposites*, in *New Polymerization Techniques and Synthetic Methodologies*. 2001, Springer Berlin Heidelberg. p. 167-221.

41. Nussbaumer, R.J., et al., *Polymer-TiO_2 Nanocomposites: A Route Towards Visually Transparent Broadband UV Filters and High Refractive Index Materials.* Macromolecular Materials and Engineering, 2003. 288(1): p. 44-49.

42. Wang, Z., et al., *Dispersion Behavior of TiO_2 Nanoparticles in LLDPE/LDPE/TiO_2 Nanocomposites.* Macromolecular Chemistry and Physics, 2005. 206(2): p. 258-262.

43. Chen, X.D., et al., *Roles of anatase and rutile TiO_2 nanoparticles in photooxidation of polyurethane.* Polymer Testing, 2007. 26(2): p. 202-208.

44. Owpradit, W. and B. Jongsomjit, *A comparative study on synthesis of LLDPE/TiO2 nanocomposites using different TiO_2 by in situ polymerization with zirconocene/dMMAO catalyst.* Materials Chemistry and Physics, 2008. 112(3): p. 954-961.

45. Jongsomjit, B., E. Chaichana, and P. Praserthdam, *LLDPE/nano-silica composites synthesized via in situ polymerization of ethylene/1-hexene with MAO/metallocene catalyst.* Journal of Materials Science, 2005. 40(8): p. 2043-2045.

46. Kontou, E. and M. Niaounakis, *Thermo-mechanical properties of LLDPE/SiO_2 nanocomposites.* Polymer, 2006. 47(4): p. 1267-1280.

47. Chaichana, E., B. Jongsomjit, and P. Praserthdam, *Effect of nano-SiO_2 particle size on the formation of LLDPE/SiO_2 nanocomposite synthesized via the in situ polymerization with metallocene catalyst.* Chemical Engineering Science, 2007. 62(3): p. 899-905.

48. Li, K.-T., C.-L. Dai, and C.-W. Kuo, *Ethylene polymerization over a nano-sized silica supported Cp^2ZrCl_2/MAO catalyst.* Catalysis Communications, 2007. 8(8): p. 1209-1213.

49. KUO, et al., *PEEK composites reinforced by nano-sized SiO_2 and Al_2O_3 particulates*. Vol. 90. 2005, Lausanne, SUISSE: Elsevier. 11.

50. Desharun, C., B. Jongsomjit, and P. Praserthdam, *Study of LLDPE/alumina nanocomposites synthesized by in situ polymerization with zirconocene/d-MMAO catalyst.* Catalysis Communications, 2008. 9(4): p. 522-528.

51. Jongsomjit, B., et al., *Characteristics of LLDPE/ZrO_2 nanocomposite synthesized by in-situ polymerization using a zirconocene/MAO catalyst.* Iranian Polymer Journal (English Edition), 2006. 15(5): p. 433-439.

52. Jongsomjit, B., J. Panpranot, and P. Praserthdam, *Effect of nanoscale SiO_2 and ZrO_2 as the fillers on the microstructure of LLDPE nanocomposites synthesized via in situ polymerization with zirconocene.* Materials Letters, 2007. 61(6): p. 1376-1379.

53. Turton, T.J. and J.R. White, *Effect of stabilizer and pigment on photo-degradation depth profiles in polypropylene.* Polymer Degradation and Stability, 2001. 74(3): p. 559-568.

54. Titelman, G.I., et al., *Discolouration of polypropylene-based compounds containing magnesium hydroxide.* Polymer Degradation and Stability, 2002. 77(2): p. 345-352.

55. Wang, Z., et al., *Preparation and characterization of polyethylene/TiO_2 nanocomposites.* Composite Interfaces, 2006. 13(7): p. 623-632.

56. Supaphol, P., et al., *Non-isothermal melt-crystallization and mechanical properties of titanium(IV) oxide nanoparticle-filled isotactic polypropylene.* Polymer Testing, 2007. 26(1): p. 20-37.

57. Schroeder, R., L.A. Majewski, and M. Grell, *High-Performance Organic Transistors Using Solution-Processed Nanoparticle-Filled High-k Polymer Gate Insulators.* Advanced Materials, 2005. 17(12): p. 1535-1539.

58. Badheka, P., et al., *Effect of dehydroxylation of hydrothermal barium titanate on dielectric properties in polystyrene composite.* Journal of Applied Polymer Science, 2006. 99(5): p. 2815-2821.

59. Parvatikar, N. and M.V.N. Ambika Prasad, *Frequency-dependent conductivity and dielectric permittivity of polyaniline/CeO_2 composites.* Journal of Applied Polymer Science, 2006. 100(2): p. 1403-1405.

60. Kaminsky, W. and F. Renner, *High melting polypropenes by silica-supported zirconocene catalysts.* Die Makromolekulare Chemie, Rapid Communications, 1993. 14(4): p. 239-243.

61. Rossi, G.B., et al., *Bottom-Up Synthesis of Polymer Nanocomposites and Molecular Composites: Ionic Exchange with PMMA Latex.* Nano Letters, 2002. 2(4): p. 319-323.

62. Kumkaew, P., et al., *Gas-phase ethylene polymerization using zirconocene supported on mesoporous molecular sieves.* Journal of Applied Polymer Science, 2003. 87(7): p. 1161-1177.

63. Tannous, K. and J.B.P. Soares, *Gas-phase polymerization of ethylene using supported metallocene catalysts: Study of polymerization conditions.* Macromolecular Chemistry and Physics, 2002. 203(13): p. 1895-1905.

64. Guo, N., et al., *Supported metallocene catalysis for in situ synthesis of high energy density metal oxide nanocomposites.* Journal of the American Chemical Society, 2007. 129(4): p. 766-767.

65. Owpradit, W., et al., *Synthesis of LLDPE/TiO_2 nanocomposites by in situ polymerization with zirconocene/dMMAO catalyst: effect of [Al]/[Zr] ratios and TiO_2 phases.* Polymer Bulletin, 2011. 66(4): p. 479-490.

66. Nandi, D., et al., *Polypyrrole–titanium(IV) doped iron(III) oxide nanocomposites: Synthesis, characterization with tunable electrical and electrochemical properties.* Materials Research Bulletin, 2012. 47(8): p. 2095-2103.

67. Kumbhar, A. and G. Chumanov, *Synthesis of Iron(III)-Doped Titania Nanoparticles and its Application for Photodegradation of Sulforhodamine-B Pollutant.* Journal of Nanoparticle Research, 2005. 7(4): p. 489-498.

68. Groenewoud, W.M., *Chapter 1 - Differential scanning calorimetry*, in *Characterisation of Polymers by Thermal Analysis*, W.M. Groenewoud, Editor. 2001, Elsevier Science B.V.: Amsterdam. p. 10-60.

69. Haines, P.J., M. Reading, and F.W. Wilburn, *Chapter 5 Differential Thermal Analysis and Differential Scanning Calorimetry*, in *Handbook of Thermal Analysis and Calorimetry*, E.B. Michael, Editor. 1998, Elsevier Science B.V. p. 279-361.

70. McMullan, D., *Scanning electron microscopy 1928–1965.* Scanning, 1995. 17(3): p. 175-185.

71. Khursheed, A., *Recent developments in scanning electron microscope design*, in *Advances in Imaging and Electron Physics*, W.H. Peter, Editor. 2001, Elsevier. p. 197-285.

72. Soares, J.B.P. and S. Anantawaraskul, *Crystallization analysis fractionation.* Journal of Polymer Science Part B: Polymer Physics, 2005. 43(13): p. 1557-1570.

73. Cudby, M.E.A. and H.A. Willis, *The Nuclear Magnetic Resonance Spectra of Polymers*, in *Annual Reports on NMR Spectroscopy*, E.F. Mooney, Editor. 1972, Academic Press. p. 363-389.

74. Oliveira, I.S., et al., *2 - Basic concepts on nuclear magnetic resonance*, in *NMR Quantum Information Processing*, I.S. Oliveira, et al., Editors. 2007, Elsevier Science B.V.: Amsterdam. p. 33-91.

75. Cheremisinoff, N.P., *2 - Thermal analysis*, in *Polymer Characterization*, N.P. Cheremisinoff, Editor. 1996, William Andrew Publishing: Westwood, NJ. p. 17-24.

76. Sandler, S.R., et al., *Experiment 18 - Gel permeation chromatography*, in *Polymer Synthesis and Characterization*, S.R. Sandler, et al., Editors. 1998, Academic Press: San Diego. p. 140-151.

77. Atiqullah, M., et al., *Crystallization kinetics of PE-b-isotacticPMMA diblock copolymer synthesized using $SiMe_2(Ind)_2ZrMe_2$ and MAO cocatalyst.* AIChE Journal, 2013. 59(1): p. 200-214.

78. Routray, K. and G. Deo, *Kinetic parameter estimation for a multiresponse nonlinear reaction model*. AIChE Journal, 2005. 51(6): p. 1733-1746.

79. Hossain, M.M. and H.I. de Lasa, *Reactivity and stability of Co-Ni/Al_2O_3 oxygen carrier in multicycle CLC.* AIChE Journal, 2007. 53(7): p. 1817-1829.

Chapter 4

Novel Approach to Control the Properties of Polyethylene and Polyethylene/ Polypropylene Nanocomposites

Abstract

In this study, a vanadium (III) complex bearing a salicylaldiminato ligand of the general formula [RN=CH(2,4-^{t}Bu$_2$C$_6$H$_2$O)]VCl$_2$(THF)$_2$, where R = 2,6-^{i}Pr$_2$C$_6$H$_3$, was used as a catalyst. Titanium dioxide doped with iron nanofillers were synthesized by a sol-gel process and was used to investigate the effect of nanofillers on the ethylene homopolymer and ethylene/ propylene copolymer properties. To the best of our knowledge, this is the first time titanium dioxide doped with iron has been used as nanofillers in ethylene polymerization and ethylene/propylene copolymerization using a vanadium complex with methyl aluminum dichloride as a cocatalyst. Besides catalyst activity, the molecular weight (M_w) of the obtained polymer, molecular weight distribution, copolymer composition, crystallinity and thermal characteristics of polyethylene and polyethylene/polypropylene nanocomposites were investigated.

Keywords: ethylene/ propylene copolymer, nanocomposites, titanium dioxide doped with iron.

4.1 Introduction

Today, polyolefins are a rapid growing sector of the polymer industry with the highest amount of production at nearly 120 million tons a year. The copolymer of ethylene with propylene is a vital commercial product. The structure and copolymer composition theoretically depend on catalyst characteristics, like homogeneity and stereospecificity. The results reveal that the physical properties of ethylene-propylene (EP) copolymers depend on the number of chemically inverted propylene units and the monomer sequence distribution [1, 2]. Ethylene/propylene copolymerization was carried out by using different catalysts such as a Zeigler-Natta catalyst, postmetallocene and metallocene catalysts. It is imperative to mention that the invention of the metallocene catalysts has resulted in developing of polyolefins industry and become possible to get stereoregular polymers with a predetermined structure [3]. Recently, methylaluminum dichloride (MADC) was found to be a potential cocatalyst in polymerization/oligomerization [4].

Polyolefin nanocomposites have excellent thermal stability, mechanical properties and flammability and gas barrier properties depending on the particle size, shape, loading, bonding and dispersion of the fillers [5-7]. There are three important methods to make polymer composites: solution mixing [8], melt compounding [9] and in situ polymerization [10]. In-situ polymerization is a promising method because it provides a homogeneous dispersion of filler in the polymer matrix [11].

Different inorganic nanoparticles have been employed such as titanium dioxide (TiO_2) [12-15], silicon dioxide (SiO_2) [16, 17], aluminum trioxide (Al_2O_3) [18, 19] and zirconium dioxide (ZrO_2) [20, 21] to improve thermal and mechanical of the polymer

composites. TiO_2 polymer composites have been widely investigated in the literature to improve thermal and mechanical properties of the polymer [15].

The use of metallocene catalysts with titanium dioxide as nanofiller is an excellent combination to improve polymer properties [11]. In this study, we used titanium dioxide doped with iron (TiO_2/Fe) to investigate the effect of iron on the ethylene homopolymer and ethylene/ propylene copolymer properties. As we mentioned earlier, this is the first time titanium dioxide doped with iron has been used as a nanofiller in ethylene polymerization and ethylene propylene copolymerization using a vanadium complex with MADC as a cocatalyst. The molecular weight (M_w), molecular weight distribution (MWD), copolymer composition, crystallinity and thermal characteristics of polyethylene and polyethylene/polypropylene nanocomposites were investigated.

4.2 Experimental Methods

4.2.1 Materials

Ethylene, premixed ethylene, and propylene gas mixtures were purchased from SIGAS with two different molar ratios (50:50) and (60:40) of ethylene and propylene respectively. Titanium (IV) n-butoxide, iron (III) nitrate nonahydrate $Fe(NO_3)_3{\cdot}9H_2O$, methanol and ethanol were purchased from Fisher Scientific. VCl_3 (THF) $_3$, and tetrahydrofuran were obtained from Sigma Aldrich. Solvents were purified by standard techniques. All manipulations were performed under N_2 environment using standard schlenk and glove box techniques.

4.2.2 Catalyst synthesis

A vanadium(III) complex bearing salicylaldiminato ligand, [RN=CH(2,4-$^{t}Bu_2C_6H_2O$)] $VCl_2(THF)_2$, where R = 2,6-$^{i}Pr_2C_6H_3$, was synthesized according to the reported procedure [22], where $VCl_3(THF)_3$ (0.75 g) was dissolved in dried tetrahydrofuran (20 mL) and added slowly to a solution of salicylaldiminato ligand (0.40 g) in tetrahydrofuran (20 mL) to form a red mixture. Then, the mixture was stirred for 10 minutes, and Et_3N (0.3 mL, 0.216 g) was added and stirred for 4 hours at room temperature. The solution was then concentrated to 10 mL, and the mixture was filtered to remove NH_4Cl. Red-black crystals were formed by diffusion of *n*-hexane (20 mL) into the solution with a yield of 60%.

4.2.3 Synthesis of doped titania nanofillers

Undoped titania nanofillers were synthesized by a sol-gel process under constant sonication as following: 500 μL of titanium (IV) alkoxide precursor in ١٥ mL ethanol was hydrolyzed in the presence of 1 mL of water at room temperature to form white solution of hydrolyzed titania particles. For iron doped titania nanofillers, an inorganic precursor $Fe(NO_3)_3{\cdot}9H_2O$ (١% solution) was dissolved in 5 mL of ethanol solution and added to the hydrolyzed titania solution under constant sonication (500 rpm) for 30 minutes. After that, the precipitate was washed with ethanol many times to remove excess NO_3^-, Fe^{3+}. The precipitate was dried overnight at 100 ^{0}C and then heated for 5 hours to convert the amorphous titania into the crystalline anatase form. Finally, the product was ground into a fine powder [23]. The samples were denoted as TiO_2/Fe for iron doped titania.

4.3 Polymerization

Polymerization reaction was taken place in a 250 mL round-bottom flask provided with a magnetic stirrer. 1.8 mg of the catalyst and various amounts of the Fe/TiO_2 nanofiller (5, 10 and 15) mg were added to the flask and filled with 80 mL of toluene. Then, the flask was put in an oil bath at equilibrated temperature (30 °C) and nitrogen gas was removed by a vacuum pump. Then ethylene was supplied into the reactor. After 10 minutes of the saturation of ethylene in toluene, 1 mL of the cocatalyst (MADC) was charged into the flask and polymerization reaction was started. After 10 minutes, polymerization reaction was quenched by adding 250 mL of methanol containing HCl (5 vol. %). Finally, the polymer was put in an oven at 50 °C for 24 hours for drying.

4.4 Characterization

4.4.1 GPC Analysis

The Molecular weight of polyethylene and polyethylene/polypropylene nanocomposites was determined by triple detection-high temperature gel permeation chromatography (GPC) (model: HT-GPC 350, Malvern) using 1, 2, 4-trichlorobenzene as a solvent. Twenty-five mg of the material was placed into a 40 mL glass vial and accurately weighed and 10 mL of the solvent was added using a clean 10 mL glass pipette. The vial was capped with a Teflon coated cap and the samples were placed into the Vortex Auto Sampler and left to dissolve for 3hrs at 160 °C while stirring gently.

4.4.2 DSC Analysis

Crystallinity of ethylene and ethylene/propylene copolymer nanocomposites (X_c %) and melting temperature (T_m) were measured by differential scanning calorimetry (DSC) from TA instruments Q1000. Cooling and heating cycles were carried out in a nitrogen environment at the rate of 10 °C min^{-1} from a temperature of 30 °C to 160 °C.

4.4.3 Thermal Stability

Thermal degradation measurements were carried out by thermogravimetric measurements using an SDT Q600 (TA instruments). Samples weighing around 5 mg were heated in a nitrogen environment from 25 to 850 °C at a heating rate of 10 °C per minute.

4.4.4 Crystaf Analysis

Crystallization analysis fractionation (CRYSTAF) (Polymer Char, Spain) of the copolymers was performed using an IR detector in 1, 2, 4-trichlorobenzene in a 50-mL stainless-steel stirred vessel and the crystallization rate was 0.2 °C/min.

NMR Analysis: ^{13}C NMR was used to determine the composition of ethylene/propylene (E/P) copolymer using a Bruker AVANCE III-600 NMR spectrometer and 1, 2, 4-trichlorobenzene as a solvent.

4.5 Results and Discussion

4.5.1 Polyethylene nanocomposites

In this study, polyethylene nanocomposites were prepared by in-situ polymerization using TiO_2/Fe nanofillers. The activity of the catalyst increased when TiO_2/Fe nanofillers were added. It was found that the maximum activity of the catalyst was achieved using 15 mg of TiO_2/Fe nanofiller which equals 1446 kg PE/mol.V.h.bar (Table 4-1, entry 4) compared to the control (1135 kg PE/mol.V.h.bar, Table 4-1, entry 1). The increase in the activity of the catalyst could be due to the increase in the chain propagation rate [11]. The experiments were repeated several times and these results are reproducible with error less than 2%.

The molecular weight (M_w) was found to increase by adding the TiO_2/Fe filler with vanadium complex during polymerization. The optimum value for the filler was 5 mg (Entry 2, Table 4-1) which is 55.5×10^4 ($g.mol^{-1}$). An increase in the filler concentration to 10 and 15 mg resulted in a decrease in the molecular weight (M_w) when compared to the 5 mg of filler concentration but still showed a significant increase compared to the control. The increase in the molecular weight (M_w) could be contributed to the increase in the chain propagation rates. The polydispersity index (PDI) was decreased by adding the TiO_2/Fe nanofiller and decreased with an increasing the amount of the TiO_2/Fe nanofiller as shown in Table 4-1. This decrease in PDI improved the thermal properties of the polyethylene nanocomposites. For the sake of reproducibility, the molecular weight (M_w) analysis was repeated three times for each entry and the average values were tabulated with an error less than 3%, as shown in Table 4-1.

The thermal properties of the polyethylene nanocomposites were measured by differential scanning calorimetry. The melting temperatures of polyethylene and polyethylene nanocomposites samples were determined by DSC from the second heating cycle and the average values for three experiments were selected with error less than 2%. No significant changes were observed in the (T_m) values. Polyethylene nanocomposites showed a melting temperature (T_m) slightly higher (Entry 2, 3 and 4, Table 4-1) than that of the control (Entry 1, Table 4-1) due to both the presence of the filler and the increase in the crystallinity of the polyethylene nanocomposites. The percentage of crystallinity in the polyethylene nanocomposites samples was determined by using DSC analysis and showed that it increased when the amount of the filler was increased, as shown in Table 4-1. The highest percent crystallinity (60%) was obtained using 15 mg of the TiO_2/Fe filler (Entry 4, Table 4-1). Compare this to the control which is 50% (Entry 1, Table 4-1). The increase in the crystallinity could be contributed to the Fe/TiO_2 nanofillers which could play as nucleating agents [24]. The percentage of crystallinity was calculated using the following expression:

$$\% \text{ of crystallinity} = (\Delta H_{fus}/\Delta H^{o}_{fus}) \times 100 \qquad (4\text{-}1)$$

Where ΔH_{fus} is the enthalpy of fusion of the polyethylene composites, and ΔH^{o}_{fus} is the enthalpy of fusion of the 100% crystalline polyethylene. Table 4-1 summarizes the results of the polymerization and polymer nanocomposites characteristics.

Table 0-1: Experimental conditions and properties of polyethylene prepared by in situ polymerization using a vanadium complex catalyst and an MADC co-catalyst system at 1.3 bar [a]

Entry No.	Filler (mg)	Activity [b]	M_w [c] (× 10^{-4})	PDI (M_w/ M_n)	T_m [d] (^{O}C)	X_c [e] (%)
1.	0	1135	19.6	3.7	136	50
2.	5	1192	55.5	2.4	137	54
3.	10	1353	46.1	3.0	137	58
4.	15	1446	39.1	2.8	137	60

[a] polymerization conditions: toluene = 80 mL, Temp = 30 ^{o}C, Time = 10 min, catalyst amount = 1.8 mg, cocatalyst amount = 1 mL, filler is Fe (1%) doped TiO_2, [b] kg PE/mol.V.h.bar, [c] determined by GPC , [d, e] determined by DSC.

The degradation temperature of polyethylene nanocomposites increased when TiO_2/Fe filler was added to the polymerization reaction as shown in Figure 4-1 (a). The increase in degradation temperature is attributed to the higher molecular weight and filler content . About 16 wt.% of the control polyethylene (Entry 1, Table 4-1) started to degrade at 120 °C and the rest at 421 °C. This early degradation may be due to the presence of a low molecular weight portion which is verified by the higher PDI of control polyethylene (PDI = 3.7, Entry 1, Table 4-1) compared to polyethylene nanocomposites (PDI = 2.4, 3.0 and 2.8, Table 4-1) (Entry 2, 3 and 5) respectively. This higher PDI of control polyethylene suggests that it has a low molecular weight segment in addition to the majority high molecular weight segment. This result was confirmed by TGA derivative weight curves (Figure 4-1 (b)). As shown in Figure 4-1 (b), a small peak

appeared at 120 °C which refers to the degradation of the low molecular weight segment in the control polyethylene sample as shown in Figure 4-1 (b).

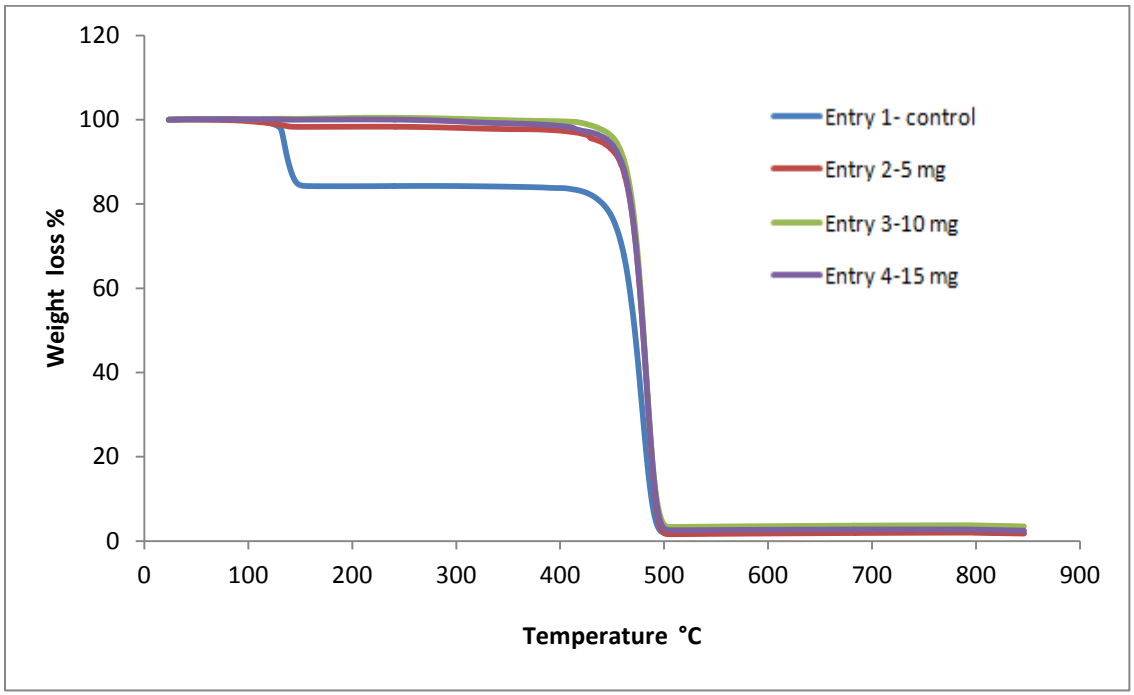

(a)

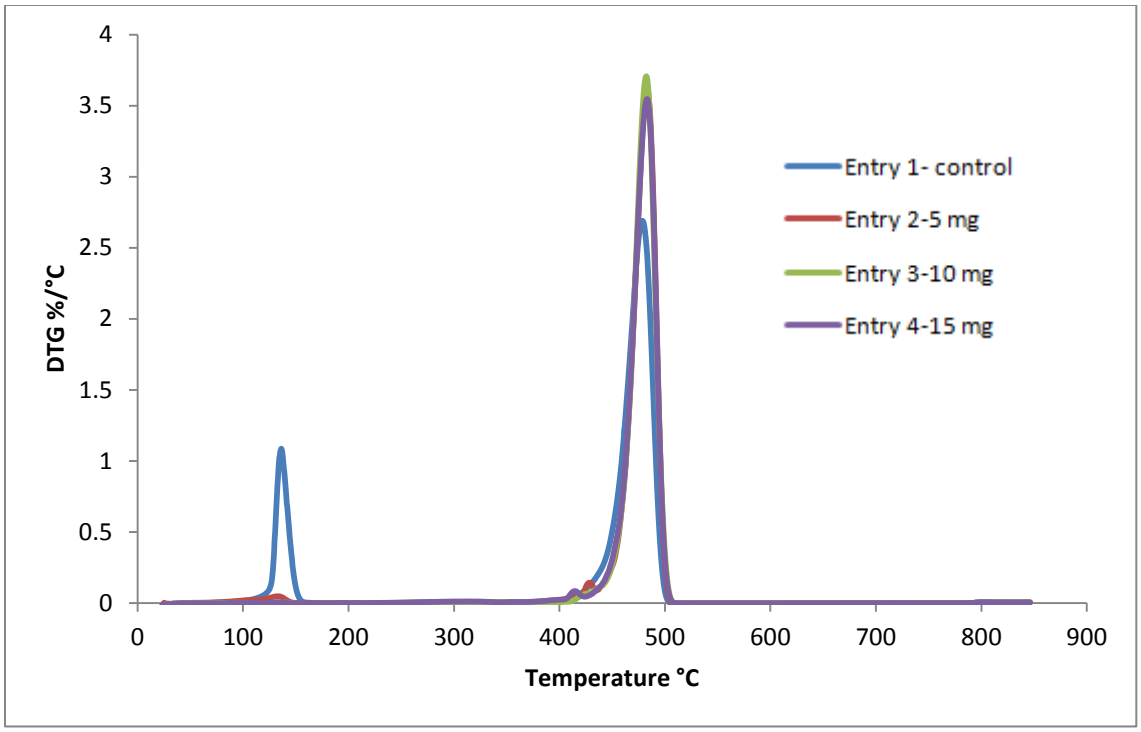

(b)

Figure 0-1: Temperature degradation of polyethylene and polyethylene nanocomposites determined by thermal gravimetric analysis (TGA): (a) weight curves (b) derivative weight curves.

4.5.2 Ethylene/propylene copolymer nanocomposites

Ethylene/propylene copolymer nanocomposites were prepared by in situ polymerization in the presence of nanofillers. The activity of the catalyst increased when TiO_2/Fe nanofillers were added. For 50:50 molar ratios of E/P, it was found that the maximum activity of the catalyst was achieved when 15 mg of the TiO_2/Fe nanofiller was used which equals 2595 kg (PE/PP)/mol.V.h.bar (Table 4-2, entry 2) compared to the control (1809 kg ((PE/PP)/mol.V.h.bar, Table 4-2, entry 1). The same phenomenon occurred in the (60/40) molar ratio of E/P, where the activity was increased from 1507 kg (PE/PP)/mol.V.h.bar (Table 4-2, entry 3) up to 1596 and 1622 kg (PE/PP)/mol.V.h.bar

by adding 5 and 15 mg of the TiO_2/Fe nanofiller respectively (Table 4-2, entry 4 and 5) . The increase in the activity of the catalyst could be due the increasing in the chain propagation rate [11].

Polypropylene fraction (PP %) in ethylene/propylene copolymer was calculated as published by Cheng [25] using ^{13}C NMR. The mole percent of polypropylene (mol %) was calculated by using the following formulas:

$$\text{mol \% of PP} = \frac{2t}{s+t} = \frac{2p}{s+p} \qquad (4\text{-}2)$$

Where:

$$s = \sum_{ij} S_{ij} \qquad (4\text{-}3)$$

$$t = \sum_{ij} T_{ij} \qquad (4\text{-}4)$$

$$p = \sum_{ij} P_{ij} \qquad (4\text{-}5)$$

S, T, and P represent to secondary (methylene), tertiary (methine), and primary (methyl) carbons respectively. More details are available in the previous reference [25].

It is important to recognize that polypropylene fraction in ethylene/propylene copolymer was found to be increased by adding TiO_2/Fe nanofiller with vanadium complex. When 15 mg of TiO_2/Fe nanofiller was added, the polypropylene fraction was increased to 25%. From ^{13}C NMR spectra of 50/50 molar ratio of ethylene/propylene, there was only homo polyethylene (Entry 1, Table 4-2). However, the polypropylene

fraction was increased to 4.1 using 15 mg of the TiO_2/Fe nanofiller (Entry 2, Table 4-2). The polypropylene fraction was increased from 3.7 to 9.1 and 25 by using 5 and 15 mg of TiO_2/Fe respectively for 60/40 molar ratio of E/P (Entry 3, 4 and 5, Table 4-2). It is worthy to mention that, the catalyst was used to polymerize propylene but no product was obtained.

The molecular weight (M_w) was found to increase by adding the TiO_2/Fe filler using the vanadium catalyst in polyethylene/polypropylene nanocomposites samples. The molecular weight (M_w) was found to increase on adding 15 mg of the TiO_2/Fe nanofiller up to 40.7×10^4 ($g.mol^{-1}$) (Entry 2, Table 4-2) compared to 32.4×10^4 ($g.mol^{-1}$) in the control sample (Entry 1, Table 4-2) for a 50/50 molar ratio of E/P. For a 60/40 molar ratio of E/P, the optimum value for the filler was 5 mg (Entry 4, Table 4-2) which was 33.6×10^4 ($g.mol^{-1}$). An increase in the filler concentration to 15 mg resulted in a decrease in the molecular weight (M_w) when compared to the 5 mg of filler concentration but still showed a significant increase compared to the control. Polydispersity index (PDI) was increased by adding the TiO_2/Fe nanofiller from 2.7 to 3.6 (Entry 1 and 2, Table 4-2) and from 1.9 to 3.9 and 3.3 (Entry 3,4 and 5 , Table 4-2) of a 50/50 and a 60/40 molar ratio of ethylene/propylene respectively. This increase in PDI resulted in lowering the thermal properties of polyethylene/polypropylene nanocomposites. It is worthy to mention, that these results are reproducible with an error of less than 4 %.

The percentages of crystallinity of polyethylene/polypropylene nanocomposites were determined by DSC analysis and the results showed that the percentage of crystallinity was decreased when the amount of the filler increased as shown in Table 2, where the

lowest % crystallinity was obtained by using 15 mg of the TiO_2/Fe filler. This was due to the increasing polypropylene percent when the amount of the TiO_2/Fe filler increases.

The melting temperature (T_m) of the polyethylene/polypropylene nanocomposites was reduced by adding the TiO_2/Fe nanofiller in both (50/50) and (60/40) molar ratios of E/P as shown in Table 4-2. This decrease in melting temperature may be due to the decrease in percentage of crystallinity because of the increasing polypropylene content [26]. These values are the averages of three experiments for each entry as shown in Table 4-2.

Table 0-2: Experimental conditions and properties of ethylene/propylene copolymer prepared by in situ copolymerization using a vanadium complex catalyst and an MADC co-catalyst system at 1.3 bar[a]

Entry No.	**E/P mol/mol**	**Filler (mg)**	**Activity** [b]	**PP** [c] **(%)**	M_w [d] **(× 10^{-4})**	**PDI**	T_m [e] **(^{O}C)**	X_C [f] **(%)**
1.	50/50	0	1809	0	32.5	2.7	138	52
2.	50/50	15	2595	4.1	40.7	3.6	135	45
3.	60/40	0	1507	3.7	17.3	1.9	121	40
4.	60/40	5	1596	9.1	33.6	3.9	124	38
5.	60/40	15	1622	25	21.5	3.3	116	31

[a] Copolymerization conditions: Toluene = 80 mL, Temp = 30 ^{o}C, Time = 10 min, Catalyst amount = 1.8 mg, cocatalyst amount= 1 mL, filler is Fe (1%) doped TiO_2, [b] kg(PE/PP)/mol h bar, [c] Determined by ^{13}C NMR, [d] determined by GPC, [e,f] determined by DSC.

Crystallization analysis fractionation (Crystaf) was used to confirm the results obtained by ^{13}C NMR and DSC. Crystaf results showed that, the crystallinity temperature decreases and Crystaf profiles become broader when TiO_2/Fe is added due to an increase in polypropylene content in the ethylene/propylene copolymer as shown in Figure 4-2 and Figure 4-3. Two peaks were observed when the TiO_2/Fe nanofillers were added which confirm the presence of polypropylene in obtained copolymer. The decrease in Crystaf peak temperature may be due to changing of the thermodynamic interaction parameter for the copolymer fraction [26].

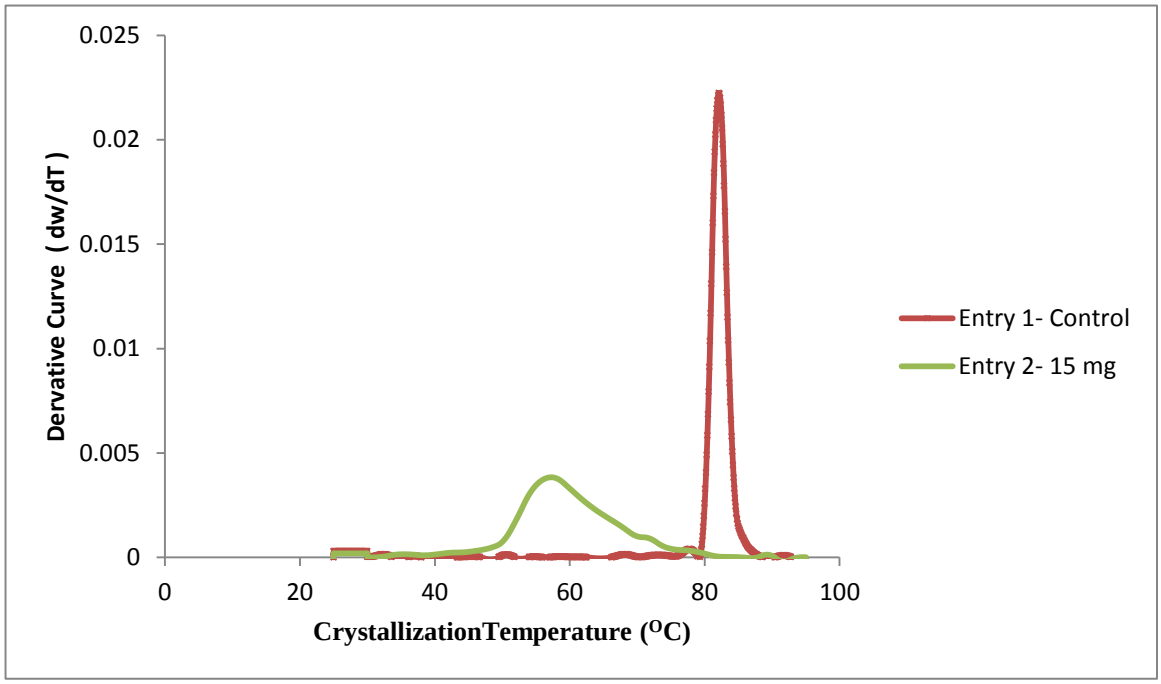

Figure 0-2: Differential crystallization analysis fractionation (Crystaf) profiles of 50/50 molar ratio of (E/P).

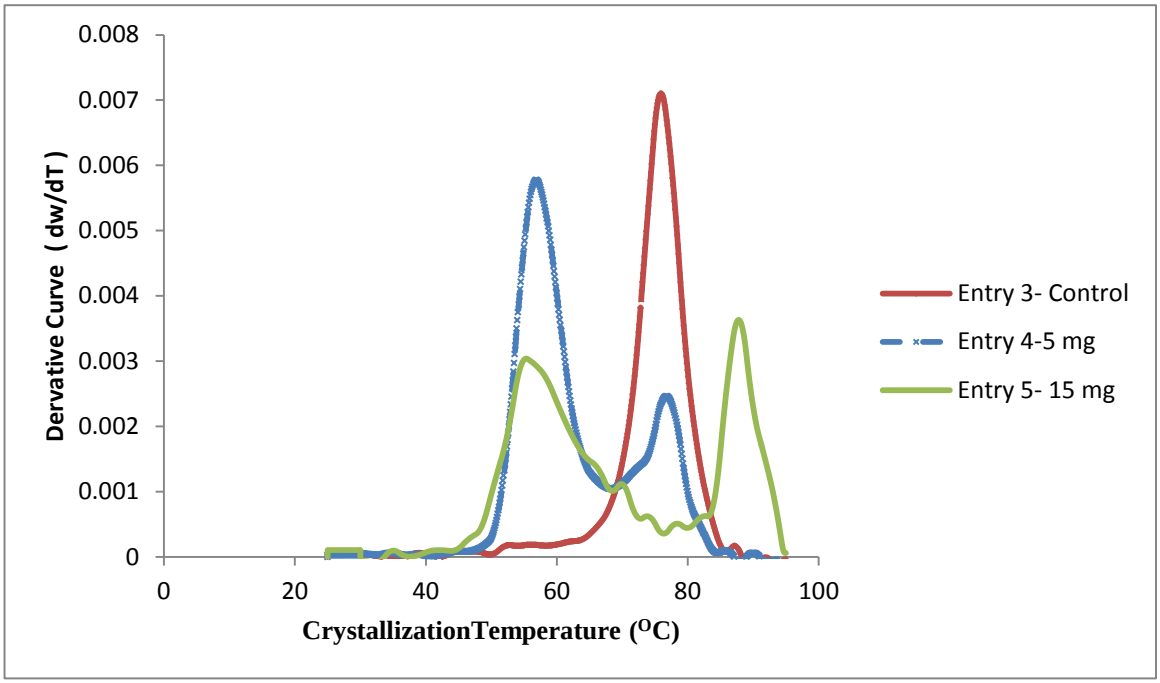

Figure 0-3: Differential crystallization analysis fractionation (Crystaf) profiles of 60/40 molar ratio of (E/P).

In general, degradation temperature of the ethylene/propylene copolymer nanocomposites decreased when the TiO_2/Fe filler was added to polymerization reactions in both (50/50) and (60/40) molar ratios of E/P as shown in Figure 4-4 (a and b) and Figure 4-5(a and b) respectively. The decrease in degradation temperature is attributed to the decrease in melting temperature (T_m) and percentage of crystallinity (X_c) because of the increase in polypropylene content. However, for entry 3 and 4 (Table 4-2), the temperature of the ethylene/propylene copolymer nanocomposites was almost the same since the molecular weight (M_w) of entry 4 was increased and crystallinity was 38 which is close to 40 for the control (Entry 3, Table 4-2). This equality in degradation temperature may be contributed to the increase in the molecular weight (M_w) and crystallinity (X_c %). About 6 wt.% of the ethylene/propylene copolymer nanocomposites

(Entry 2, Table 4-2) started to degrade at 100 °C and the rest at 420 °C as shown in Figure 4-4 (b). This early degradation may be due to the higher PDI of the ethylene/propylene copolymer nanocomposites (PDI = 3.6, Entry 2, Table 4-2) compared to control ethylene/propylene copolymer (PDI = 2.7, Entry 1, Table 4-2). This higher PDI of ethylene/propylene copolymer nanocomposites proposes a slow molecular weight segment in addition to the majority of the high molecular weight segment. This result was confirmed by TGA derivative weight curves (Figure 4-4(b)) which show that there were two peaks, the shorter one started at 120 °C, which refers to the degradation of the low molecular weight segment in the ethylene/propylene copolymer sample (Entry 1, Table 4-2), and the higher one stated at 138 °C, which refers to the degradation of the low molecular weight segment in the ethylene/propylene copolymer nanocomposite sample (Entry 2, Table 4-2) as shown in Figure 4-4(b). The same phenomenon was observed in the (60/40) feed molar ratio of E/P, there was a small peak that started at 120 °C when the PDI was increased (PDI = 3.9, Entry 4, Table 4-2) as shown in Figure 4-5(b). The experiments were repeated many times and the same phenomenon was obtained.

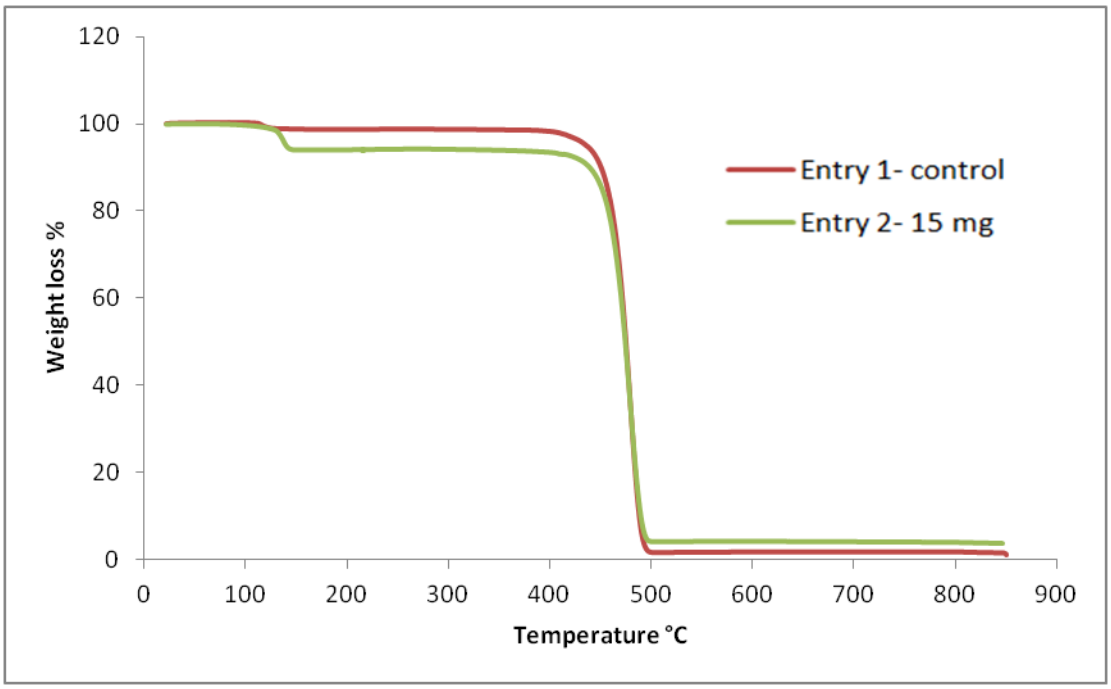
120
100
80
60
40
20
0
Weight loss %
0
100
200
300
400
500
600
700
800
900
Temperature °C
Entry 1- control
Entry 2- 15 mg

(a)

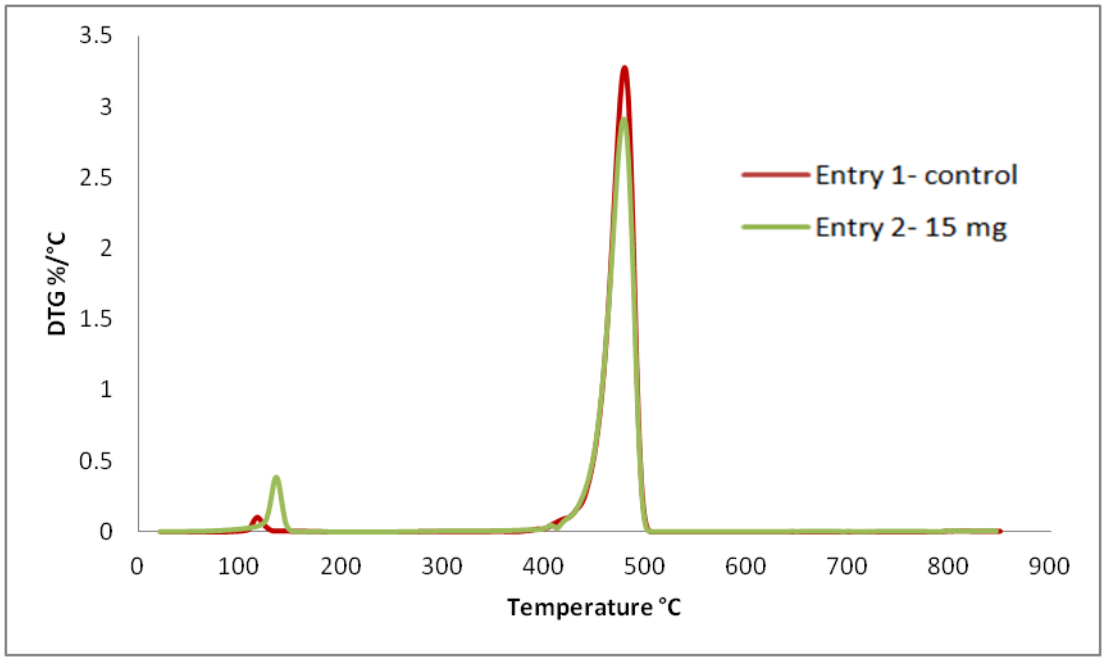

(b)

Figure 0-4: Temperature degradation profiles of a (50/50) molar ratio of (E/P) samples determined by thermal gravimetric analysis (TGA): (a) weight curves (b) derivative weight curves.

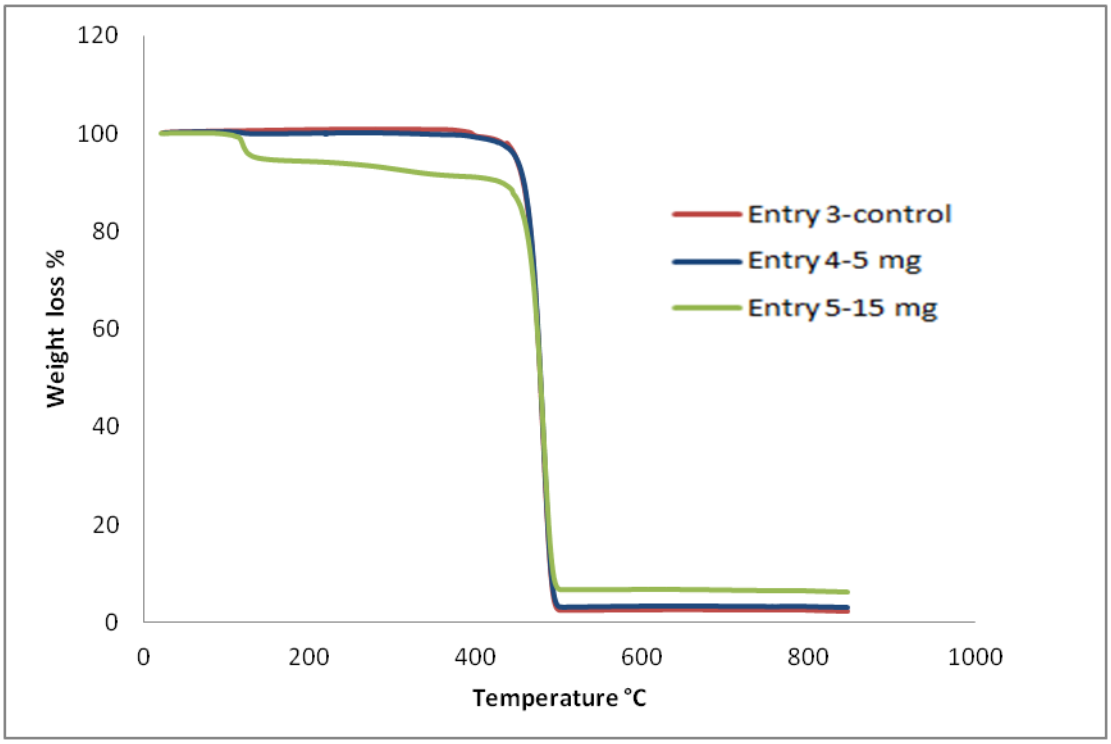
120
100
80
60
40
20
0
Weight loss %
0
200
400
600
800
1000
Temperature °C
Entry 3-control
Entry 4-5 mg
Entry 5-15 mg

(a)

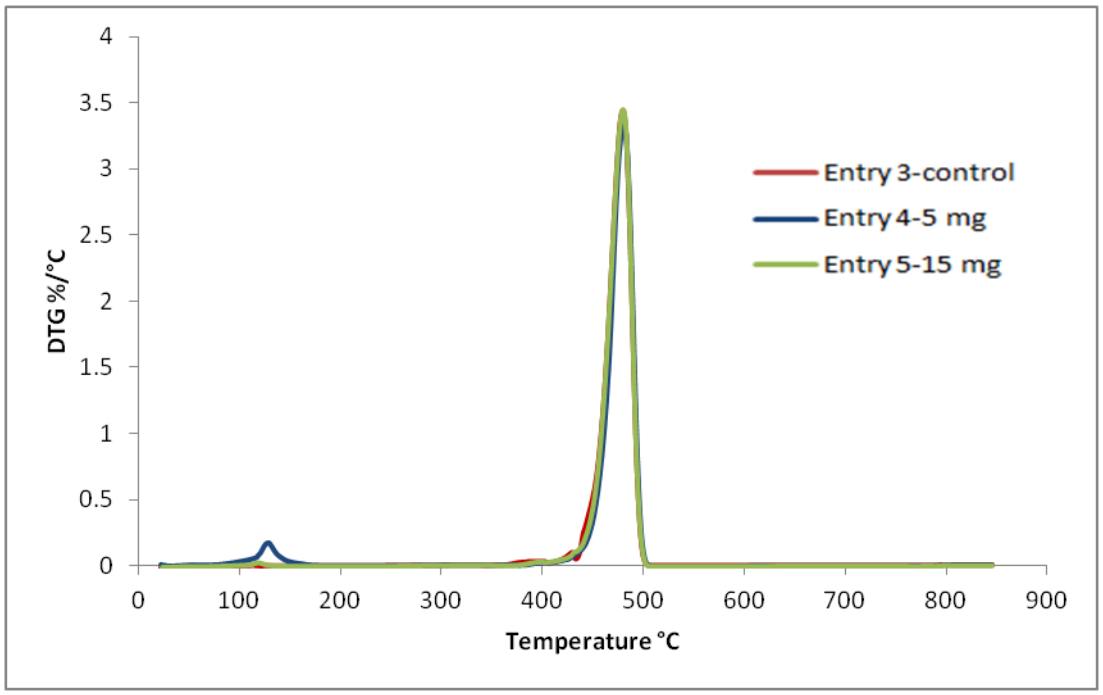

(b)

Figure 0-5: Temperature degradation profiles of a (60/40) molar ratio of (E/P) samples determined by thermal gravimetric analysis (TGA): (a) weight curves (b) derivative weight curves.

4.4.3 Crystallization kinetics model

The effect of nanofiller on the crystallization kinetics of homo polyethylene and ethylene /propylene copolymer was studied by using non isothermal Avrami-Erofeev

crystallization model by following the same procedure as reported by Atiqullah et al., by using cooling rate of 10°C/min [27].

The non isothermal Avrami-Erofeev crystallization rate equation is given by:

$$\frac{d\alpha(T)}{dT} = \frac{k_0}{\beta} \times exp\left[-\frac{E_a^A}{R}\left(\frac{1}{T} - \frac{1}{T_0}\right)\right] \times n(1-\alpha(T))[-ln(1-\alpha(T))]^{\frac{n-1}{n}} \quad (4\text{-}6)$$

Where:

$$f(\alpha(T)) = n(1-\alpha(T))[-ln(1-\alpha(T))]^{\frac{n-1}{n}} \quad (4\text{-}7)$$

$$k'(T) = k_0 \times exp\left[-\frac{E_a^A}{R}\left(\frac{1}{T} - \frac{1}{T_0}\right)\right] \quad (4\text{-}8)$$

$$E_a^A(\text{apparent crystallization energy}) = E_{grow} - E_{nucl} \quad (4\text{-}9)$$

$$k_0 = \left(\frac{K_s N_0}{V_0}\right)\frac{k_{grow,0}}{k_{nucl,0}} \quad (4\text{-}10)$$

$$k_{grow}(T) = k_{grow,0} \times exp\left[-\frac{E_{grow}}{R}\left(\frac{1}{T} - \frac{1}{T_0}\right)\right] \quad (4\text{-}11)$$

$$k_{nucl}(T) = k_{nucl,0} \times exp\left[-\frac{E_{nucl}}{R}\left(\frac{1}{T} - \frac{1}{T_0}\right)\right] \quad (4\text{-}12)$$

$$\alpha(T) = \frac{\alpha_w(T)}{\alpha_w(T) + {}^{\rho_c}/_{\rho_a}[1-\alpha_w(T)]} \quad (4\text{-}13)$$

E_{grow} and E_{nucl} are the corresponding activation energies and $f(\alpha(T))$ is Avrami-Erofeev non isothermal crystallization function. n is the dimension of the growing crystal. V_0 represents the initial volume of the molten polymer. N_0 represents the number of germ nuclei. K_s is the shape factor for the growing nuclei. $k_{grow,0}$ and $k_{nucl,0}$ represent the frequency factors for crystal growth and nucleation respectively. k_{grow} and k_{nucl} follow

the Arrhenius form [28, 29]. T_0 is the reference temperature. ρ_c and ρ_a are the densities of the crystalline and amorphous phases respectively. The values reported for polyethylene areρ_c = 1.004 g/mL and ρ_a = 0.853 g/mL [27].

$\alpha_w(T)$ can be found from the data of a constant cooling rate (second cycle) of non isothermal DSC experiment.

$$\alpha_w(T) = \frac{\Delta H(T)}{\Delta H_{total}} = \frac{\int_{T_0}^{T}\left(\frac{dH}{dT}\right)dT}{\int_{T_0}^{T_\infty}\left(\frac{dH}{dT}\right)dT} \quad (4\text{-}14)$$

Where$\Delta H(T)$ is the enthalpy corresponding to temperature T of crystallization. ΔH_{total} represents the maximum enthalpy obtained at the end of the non isothermal crystallization process. T_0 and T_∞ represent the initial and the final temperatures of crystallization, respectively.

4.4.4 Numerical solution of the crystallization kinetics

The non-linear model system was solved by using NonLinearModelFit of MATHEMATICA. The performance of the crystallization kinetics model was evaluated based on the coefficient of determination (R^2), 95% confidence interval, standard error and the variance. The kinetics model parameters are shown in Table 4-3 and 4-4.

4.4.4.1 Polyethylene nanocomposites

Figure 4-6 (a, b, c and d) compare the experimental relative crystallinity profiles (α) of the PE homopolymer with the model predicted as a function of temperature using

(0, 5, 10 and 15) mg of the TiO_2/Fe nanofiller. The values of Avrami-Erofeev (*n)* varied from 4.6 to 6.5 for polyethylene nanocomposites. As the amount of the TiO_2/Fe nanofiller increases,(*n*) values increases. The increase in *n* values indicates that the crystal growth becomes more complex and has complicated growth mechanism [30,31]. The highest value of *n* was noticed by using 15 mg of the TiO_2/Fe nanofiller (*n*=6.5) as shown in Entry 4,Table 4-3.The higher value of *n* can be attributed to the increase in the crystallinity and increase the filler amount. The crystallization frequency factor k_0 (s^{-1}) was changed slightly. The apparent activation energy E_a varied from 18 to 26.5 kJ/mol. The lower values of E_a indicate the simplicity of crystallization process. The variation in E_a values can be attributed to the variation in the structural defect of the polymer backbones [27].

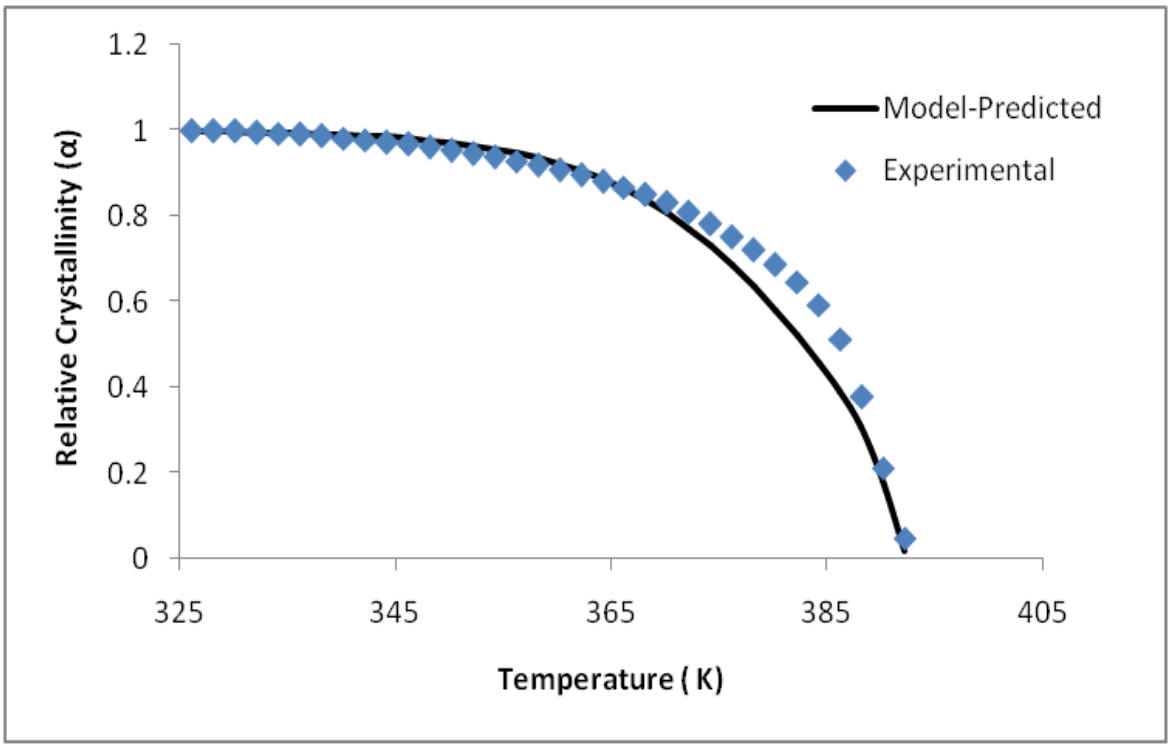
1.2
1
0.8
0.6
0.4
0.2
0
Relative Crystallinity (α)
325
345
365
385
405
Temperature (K)
Model-Predicted
Experimental

(a)

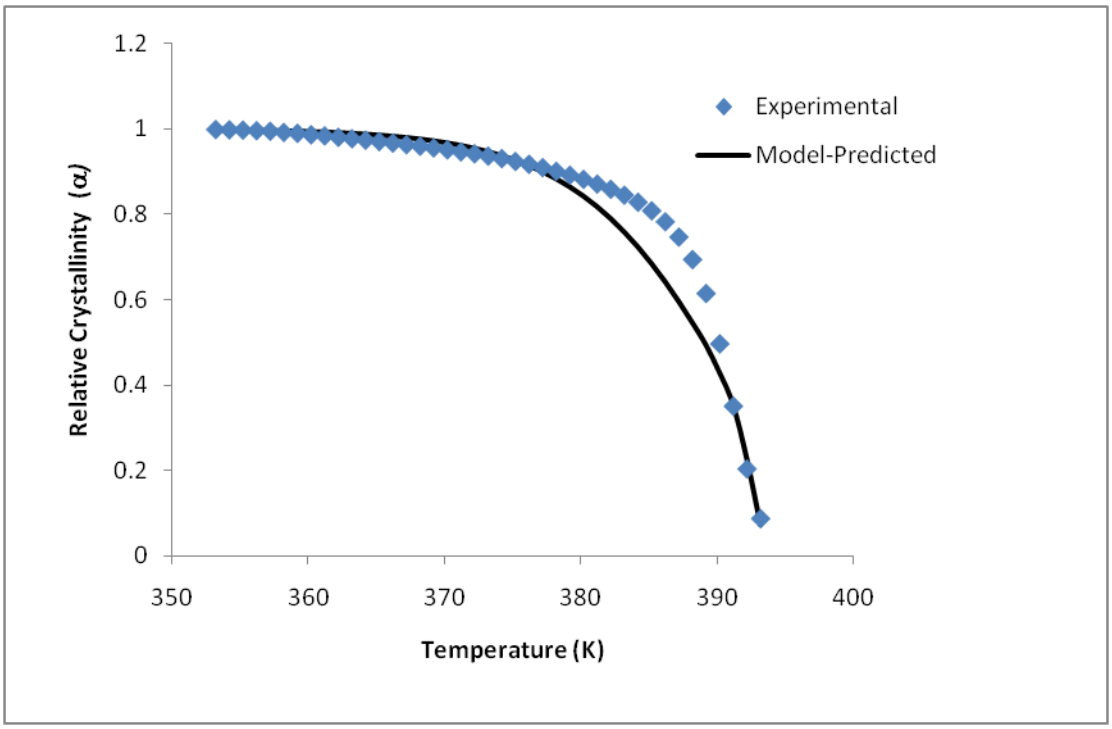
1.2
1
0.8
0.6
0.4
0.2
0
Relative Crystallinity (α)
350
360
370
380
390
400
Temperature (K)
Experimental
Model-Predicted

(b)

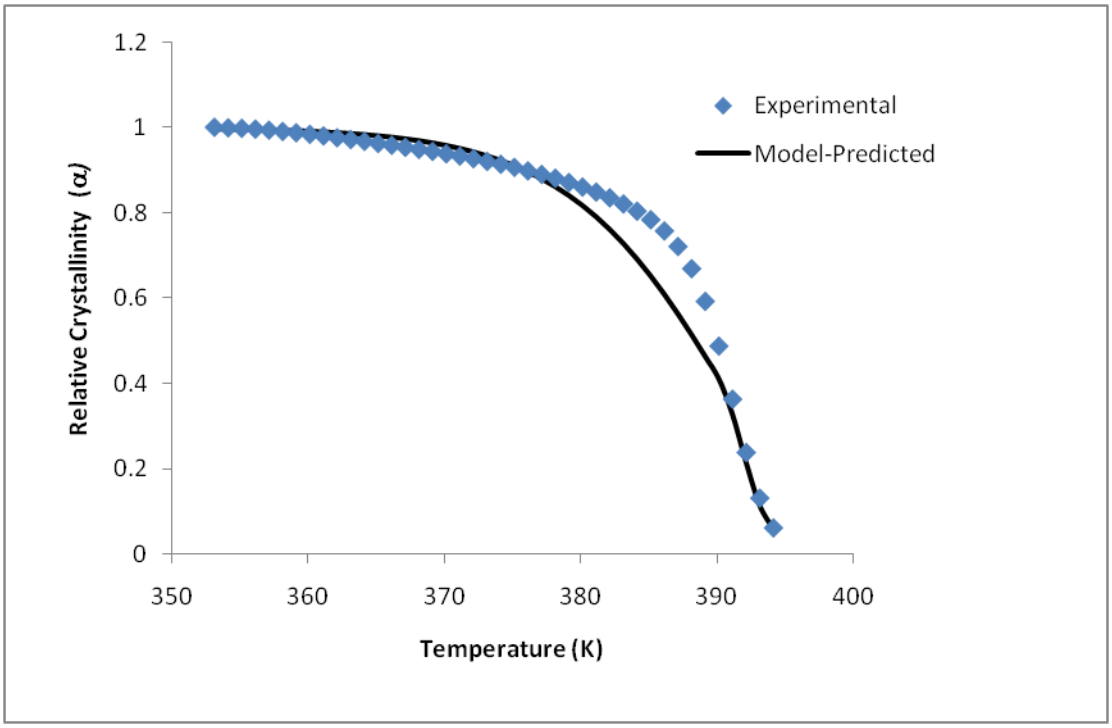
1.2
1
0.8
0.6
0.4
0.2
0
Relative Crystallinity (α)
350
360
370
380
390
400
Temperature (K)
Experimental
Model-Predicted

(c)

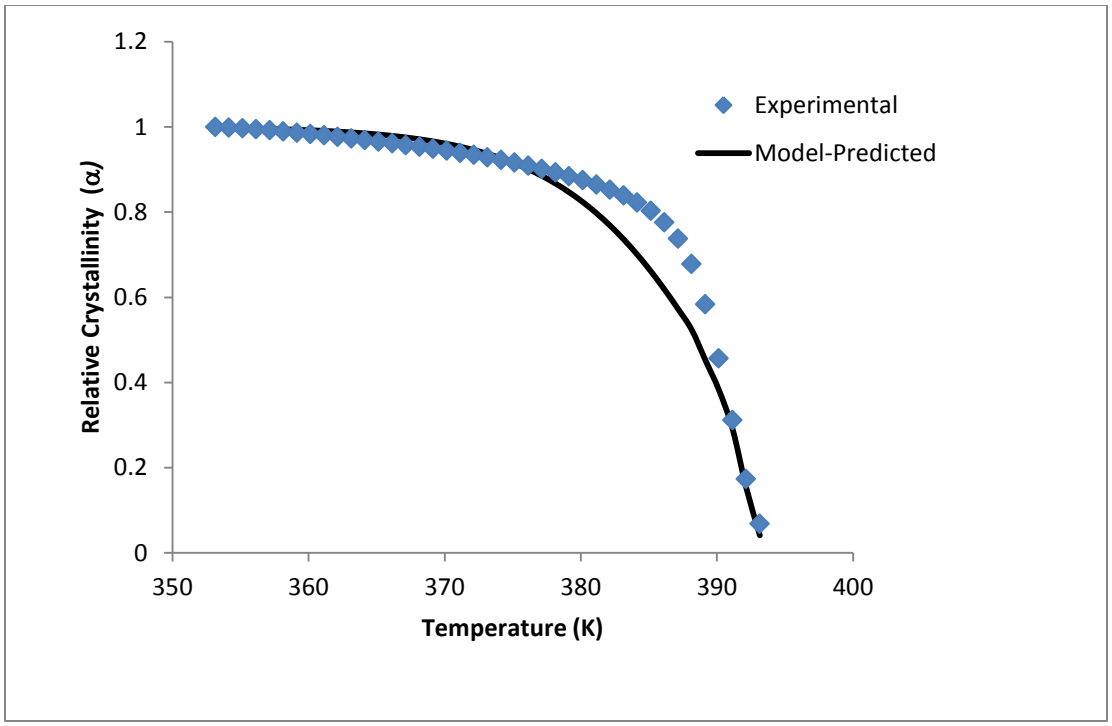

(d)

Figure 0-6: Comparison of model-predicted relative crystallinity with the experimental data as a function of DSC cooling temperature for PE homopolymer: (a) control (b) 5 mg TiO_2/Fe (c) 10 mg TiO_2/Fe (d) 15 mg TiO_2/Fe.

Table 0-3: Model-predicted non isothermal crystallization kinetics parameters of polyethylene nanocomposites.

Entry No.	Filler (mg)	n	E_a (kJ/mol)	k_0 (s^{-1})	R^2
1.	0	4.6	18.0	0.148	0.99
2.	5	6	26.5	0.159	0.99
3.	10	6.2	23.7	0.154	0.99
4.	15	6.5	22.6	0.151	0.99

4.4.4.2 Ethylene/Propylene Copolymer Nanocomposites

Figure 4-7 (a and b) and Figure 4-8 (a, b and c) show that the experimental relative crystallinity profiles (α) of the ethylene/ propylene copolymer with the model predicted as a function of temperature by using the TiO_2/Fe nanofiller at (50/50 and 60/40) molar feed ratios respectively. The values of Avrami-Erofeev (n) index varied from 4 to 4.5, 2.3 to 4.1 and 2.9 to 3.5 for (50/50 and 60/40) molar feed ratios of ethylene/propylene respectively as shown in Table 4-4. Avrami-Erofeev (n) index was decreased when the amount of the TiO_2/Fe nanofiller was increased as a result of decreasing in percentage of crystallinity due to the increase in polypropylene content [32]. Higher values of E_a indicate the complexity of the crystallization process.

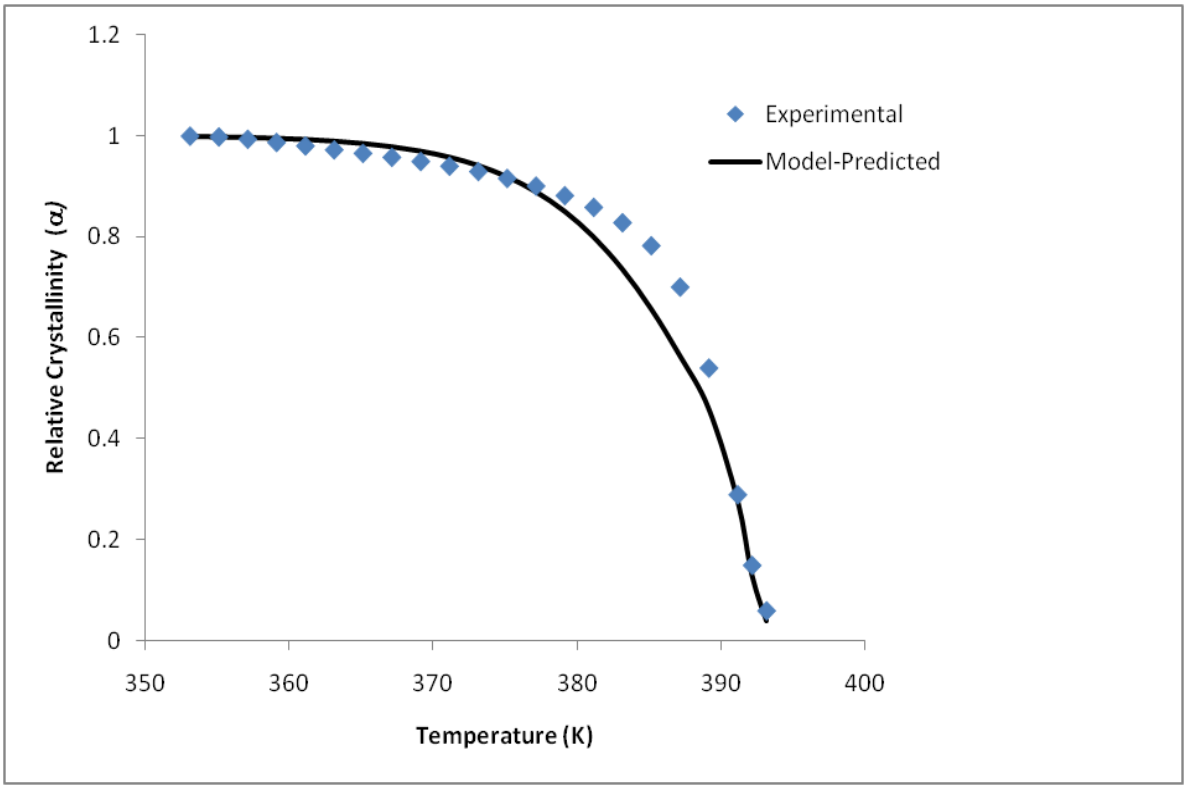
1.2
1
0.8
0.6
0.4
0.2
0
Relative Crystallinity (α)
350
360
370
380
390
400
Temperature (K)
Experimental
Model-Predicted

(a)

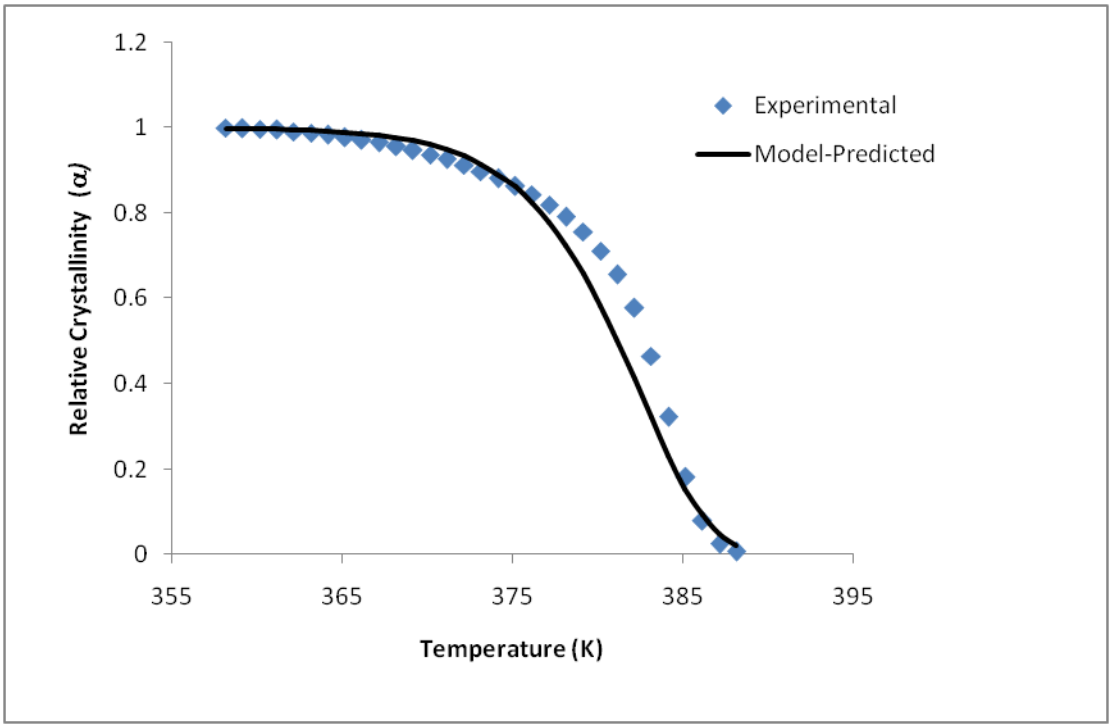

(b)

Figure 0-7: Model-predicted non isothermal crystallization kinetics parameters of ethylene/propylene copolymer nanocomposites (50/50) molar ratio of (E/P).

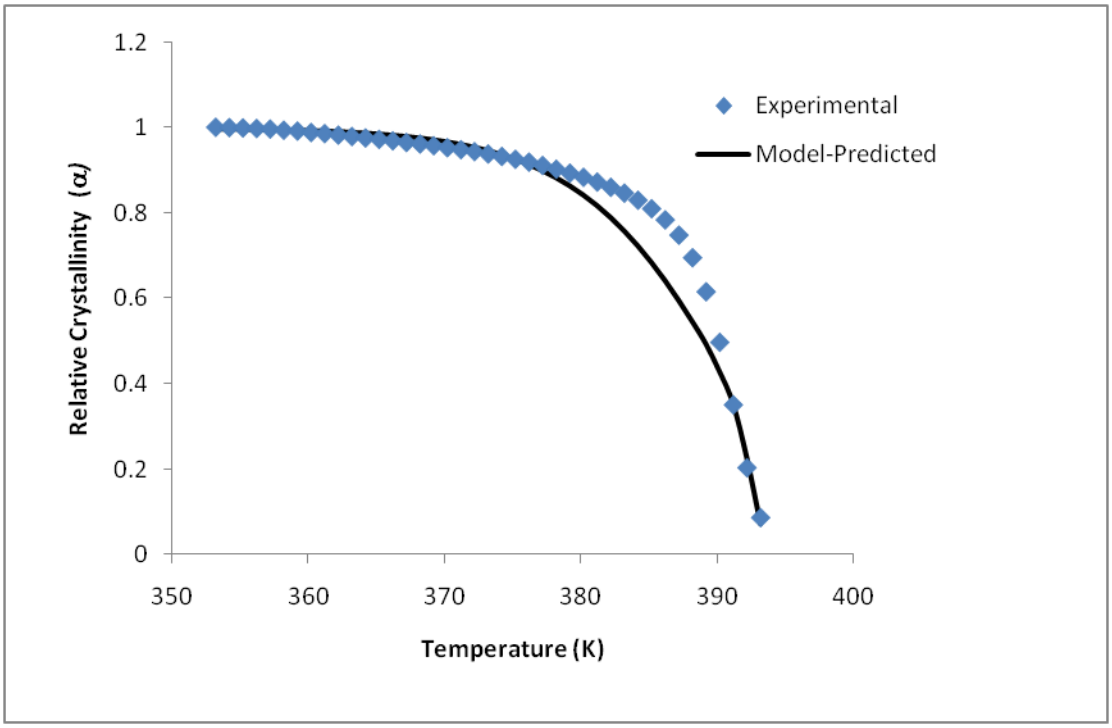
1.2
1
0.8
0.6
0.4
0.2
0
Relative Crystallinity (α)
350
360
370
380
390
400
Temperature (K)
Experimental
Model-Predicted

(a)

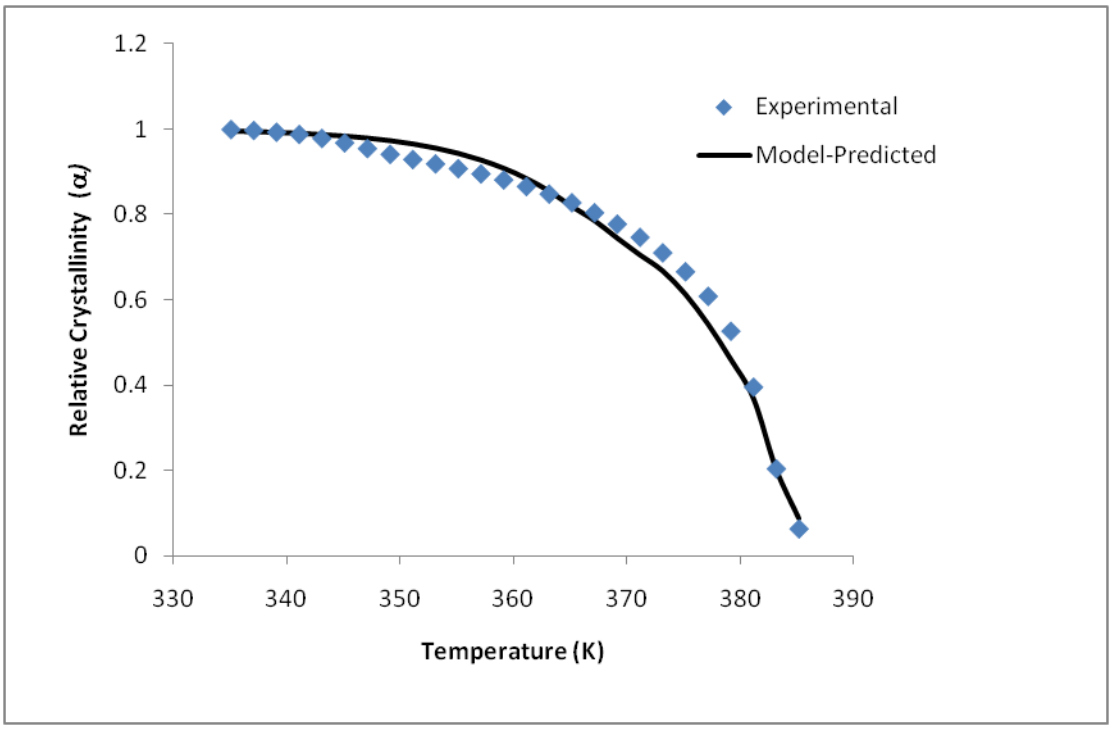
1.2
1
0.8
0.6
0.4
0.2
0
330
340
350
360
370
380
390
Relative Crystallinity (α)
Temperature (K)
Experimental
Model-Predicted

(b)

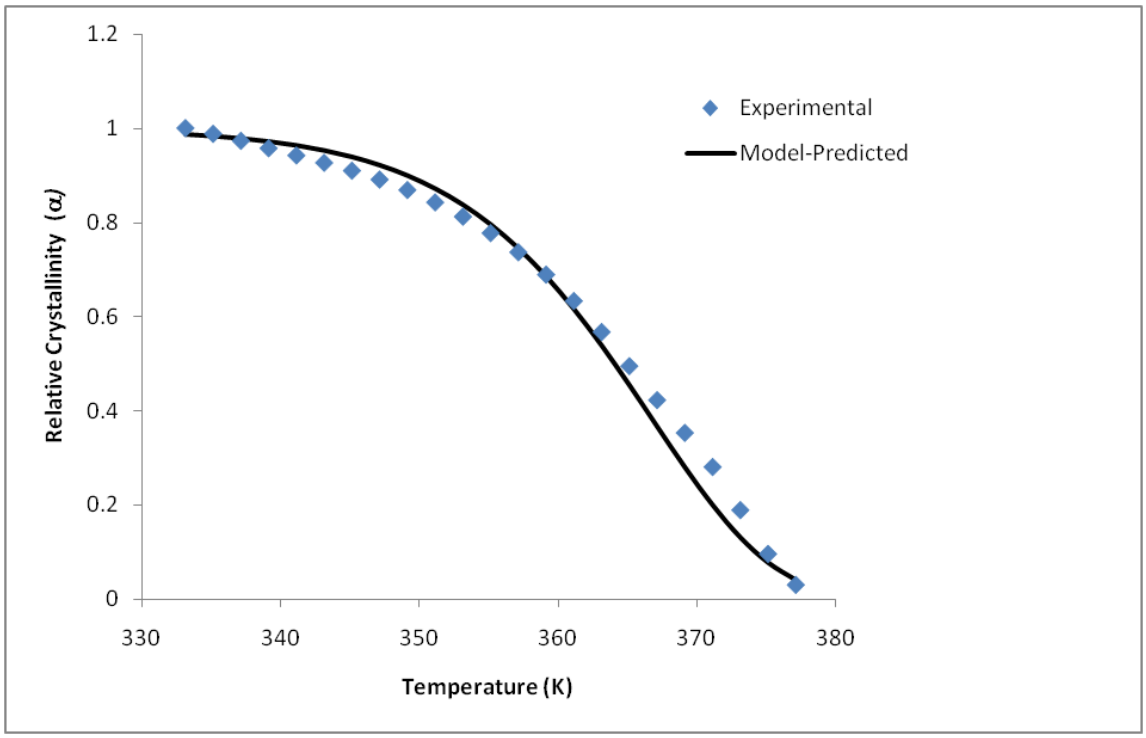

(c)

Figure 0-8: Model-predicted non isothermal crystallization kinetics parameters of ethylene/propylene copolymer nanocomposites (60/40) molar ratio of (E/P).

Table 0-4: Model-predicted non isothermal crystallization kinetics parameters of ethylene/propylene copolymer nanocomposites

Entry No.	E/P mol/mol	Filler (mg)	n	E_a (kJ/mol)	k_0 (s^{-1})	R^2
1.	50/50	0	4.5	36.7	0.178	0.99
2.	50/50	15	4	69.7	0.295	0.99
3.	60/40	0	3.5	56.0	0.355	0.99
4.	60/40	5	3.3	35.5	0.265	0.99
5.	60/40	15	2.9	40.6	0.458	0.99

Conclusions

Polyethylene and polyethylene/polypropylene nanocomposites were synthesized using vanadium (III) complex bearing salicylaldiminato ligands in the presence of TiO_2/Fe nanofillers. The molecular weight (M_w) was found to increase by adding TiO_2/Fe nanofillers in both polyethylene and polyethylene/polypropylene nanocomposites. The maximum catalyst activity was obtained by using 15 mg of the TiO_2/Fe nanofillers. The degradation temperature of polyethylene nanocomposites was increased by increasing the TiO_2/Fe nanofiller. However, the opposite trend was observed in polyethylene/polypropylene nanocomposites due to the increasing of the polypropylene

content. Crystallization analysis fractionation (Crystaf) and ^{13}C NMR showed that the polypropylene content was increased as the TiO_2/Fe nanofillers amount increased.

Acknowledgment

The authors wish to acknowledge the assistance of Deanship of Scientific Research, King Fahd University of Petroleum and Minerals for their support for providing adequate funds and infrastructure under Project no. IN101018.

References

1. Busico, V. and R. Cipullo, *Microstructure of polypropylene.* Progress in Polymer Science, 2001. **26**(3): p. 443-533.
2. Kaminsky, W., *New polymers by metallocene catalysis.* Macromolecular Chemistry and Physics, 1996. **197**(12): p. 3907-3945.
3. Jiang, T., et al., *Copolymerization of ethylene and propylene catalyzed by magnesium chloride supported vanadium/titanium bimetallic Ziegler-Natta catalysts.* Chinese Journal of Polymer Science, 2011. **29**(4): p. 475-482.
4. Bahuleyan, B.K., et al., *Ethylene oligomerization/polymerization over a series of iminopyridyl Ni(II) bimetallic catalysts modulated electronically and sterically.* Applied Catalysis A: General, 2008. **351**(1): p. 36-44.
5. Zhao, C., et al., *Mechanical, thermal and flammability properties of polyethylene/clay nanocomposites.* Polymer Degradation and Stability, 2005. **87**(1): p. 183-189.
6. Gopakumar, T.G., et al., *Influence of clay exfoliation on the physical properties of montmorillonite/polyethylene composites.* Polymer, 2002. **43**(20): p. 5483-5491.
7. Kuo, S.-W., et al., *Syntheses and characterizations of in situ blended metallocence polyethylene/clay nanocomposites.* Polymer, 2003. **44**(25): p. 7709-7719.
8. Rossi, G.B., et al., *Bottom-Up Synthesis of Polymer Nanocomposites and Molecular Composites: Ionic Exchange with PMMA Latex.* Nano Letters, 2002. **2**(4): p. 319-323.

9. Alexandre, M., et al., *Polyethylene-layered silicate nanocomposites prepared by the polymerization-filling technique: synthesis and mechanical properties.* Polymer, 2002. **43**(8): p. 2123-2132.

10. Mandal, T.K., M.S. Fleming, and D.R. Walt, *Preparation of Polymer Coated Gold Nanoparticles by Surface-Confined Living Radical Polymerization at Ambient Temperature.* Nano Letters, 2002. **2**(1): p. 3-7.

11. Abdul Kaleel, S.H., et al., *Effect of Mn doped-titania on the activity of metallocene catalyst by in situ ethylene polymerization.* Journal of Industrial and Engineering Chemistry, 2012. **18**(5): p. 1836-1840.

12. Nussbaumer, R.J., et al., *Polymer-TiO_2 Nanocomposites: A Route Towards Visually Transparent Broadband UV Filters and High Refractive Index Materials.* Macromolecular Materials and Engineering, 2003. **288**(1): p. 44-49.

13. Wang, Z., et al., *Dispersion Behavior of TiO_2 Nanoparticles in LLDPE/LDPE/TiO2 Nanocomposites.* Macromolecular Chemistry and Physics, 2005. **206**(2): p. 258-262.

14. Chen, X.D., et al., *Roles of anatase and rutile TiO_2 nanoparticles in photooxidation of polyurethane.* Polymer Testing, 2007. **26**(2): p. 202-208.

15. Owpradit, W. and B. Jongsomjit, *A comparative study on synthesis of LLDPE/TiO_2 nanocomposites using different TiO_2 by in situ polymerization with zirconocene/dMMAO catalyst.* Materials Chemistry and Physics, 2008. **112**(3): p. 954-961.

16. Chaichana, E., B. Jongsomjit, and P. Praserthdam, *Effect of nano-SiO_2 particle size on the formation of LLDPE/SiO_2 nanocomposite synthesized via the in situ*

polymerization with metallocene catalyst. Chemical Engineering Science, 2007. **62**(3): p. 899-905.

17. Li, K.-T., C.-L. Dai, and C.-W. Kuo, *Ethylene polymerization over a nano-sized silica supported Cp^2ZrCl_2/MAO catalyst.* Catalysis Communications, 2007. **8**(8): p. 1209-1213.

18. KUO, et al., *PEEK composites reinforced by nano-sized SiO_2 and Al_2O_3 particulates*. Vol. 90. 2005, Lausanne, SUISSE: Elsevier. 11.

19. Desharun, C., B. Jongsomjit, and P. Praserthdam, *Study of LLDPE/alumina nanocomposites synthesized by in situ polymerization with zirconocene/d-MMAO catalyst.* Catalysis Communications, 2008. **9**(4): p. 522-528.

20. Jongsomjit, B., et al., *Characteristics of LLDPE/ZrO 2 nanocomposite synthesized by in-situ polymerization using a zirconocene/MAO catalyst.* Iranian Polymer Journal (English Edition), 2006. **15**(5): p. 433-439.

21. Jongsomjit, B., J. Panpranot, and P. Praserthdam, *Effect of nanoscale SiO_2 and ZrO_2 as the fillers on the microstructure of LLDPE nanocomposites synthesized via in situ polymerization with zirconocene.* Materials Letters, 2007. **61**(6): p. 1376-1379.

22. Wu, J.-Q., et al., *Synthesis, Structural Characterization, and Ethylene Polymerization Behavior of the Vanadium(III) Complexes Bearing Salicylaldiminato Ligands.* Organometallics, 2008. **27**(15): p. 3840-3848.

23. Kumbhar, A. and G. Chumanov, *Synthesis of Iron(III)-Doped Titania Nanoparticles and its Application for Photodegradation of Sulforhodamine-B Pollutant.* Journal of Nanoparticle Research, 2005. **7**(4): p. 489-498.

24. Kožíšek, Z., et al., *Nucleation kinetics of polymer formation on nucleation agent.* Journal of Crystal Growth, 2005. **275**(1–2): p. e79-e83.

25. Cheng, H.N., *Carbon-13 NMR analysis of ethylene-propylene rubbers.* Macromolecules, 1984. **17**(10): p. 1950-1955.

26. Anantawaraskul, S., J. Soares, and P. Wood-Adams, *Fractionation of Semicrystalline Polymers by Crystallization Analysis Fractionationand Temperature Rising Elution Fractionation Polymer Analysis Polymer Theory*. 2005, Springer Berlin / Heidelberg. p. 686-686.

27. Atiqullah, M.; Hossain, M.; Kamal, M.; Al-Harthi, M. A.; Khan, M. J.; Hossaen, A.; Hussain, I. Crystallization kinetics of PE-b-isotacticPMMA diblock copolymer synthesized using $SiMe_2(Ind)_2ZrMe_2$ and MAO cocatalyst. *AIChE Journal*. **2013**, 59, 200-214.

28. Routray, K.; Deo, G. Kinetic parameter estimation for a multiresponse nonlinear reaction model . *AIChE Journal*. **2005**, 51, 1733-1746.

29. Hossain, M.M.; de Lasa , H.I. Reactivity and stability of Co-Ni/Al_2O_3 oxygen carrier in multicycle CLC. *AIChE Journal*, **2007**. 53, 1817-1829.

30. Al-Mulla, A.; Mathew, J.; Yeh, S.-K.; Gupta, R., Nonisothermal crystallization kinetics of PBT nanocomposites.*Composites Part A: Applied Science and Manufacturing*. **2008**, 39, 204-217.

31. Hao, W.; Yang, W.; Cai, H.; Huang, Y. Non-isothermal crystallization kinetics of polypropylene/silicon nitride nanocomposites. *Polymer Testing*. **2010**, 29, 527-533.

32. Fan, Z.-q.; Du, Z.-x.; Xu , J.-t. Crystallization kinetics of ethylene-propylene copolymers prepared by living coordination polymerization, *Chinese Journal of Polymer Science*. **2008**,26, 589-595.

Chapter 5

Polyethylene and Polyethylene/ Polypropylene Nanocomposites

Abstract

Bis(cyclopentadienyl) zirconium (IV) dichloride of empirical formula$C_{10}H_{10}Cl_2Zr$ is used as a catalyst. Doped titania with iron (TiO_2/Fe) nanofillers are employed to study the effect of nanofillers on the ethylene homopolymer and ethylene/ propylene copolymer properties. Using titanium dioxide doped with iron (TiO_2/Fe) is resulted in increasing the molecular weight (M_w) of polyethylene nanocomposites up to 80% compared to the neat polyethylene. The catalyst activity is increased by using TiO_2/Fe nanofiller for both ethylene polymerization and ethylene/ propylene copolymerization. Besides the investigation of the catalyst activity and the molecular weight (M_w) of the obtained polymer, molecular weight distribution, copolymer composition, crystallinity and thermal characteristics of polyethylene and polyethylene/polypropylene nanocomposites are studied. Non-isothermal crystallization kinetics of polyethylene and polyethylene/polypropylene nanocomposites is well fitted with Avrami-Erofeev model.

Keywords: ethylene/ propylene copolymer, nanocomposites, titania doped iron, Avrami-Erofeev model, non isothermal crystallization kinetics.

5.1 Introduction

The demand of polyolefins has been growing constantly and reached about120 million tons a year. Polyethylene (PE) and polypropylene (PP) are considered very popular as they are being used in a wide range of applications and its low cost. Their demand can be increased by copolymerizing to form new materials with new properties such as tensile strength, hardness, stiffness, melting point density, transparency and impact strength of the copolymer [1,2]. The copolymer of ethylene with propylene is a very important commercial product. The structure and copolymer composition depends on the catalyst characteristics, like homogeneity and stereospecificity. The studies showed that the physical properties of ethylene-propylene (EP) copolymers depend on the number of chemically inverted propylene units and the monomer sequence distribution [3,4].

Polyolefin nanocomposites have exceptional mechanical properties, flammability and gas barrier properties and thermal stability depending on the shape, loading, particle size, dispersion of the fillers and bonding [5, 6]. Polymer composites are produced by: solution mixing [7], melt compounding [8] and in situ polymerization [9]. In-situ polymerization is considered to be more talented compared to other methods as it gives a homogeneous dispersion of filler in the polymer matrix [10].

Different inorganic nanoparticles have been used such as titanium dioxide (TiO_2) [11-14], silicon dioxide (SiO_2) [15-18], aluminum trioxide (Al_2O_3) [19, 20] and zirconium dioxide (ZrO_2) [21,22] to improve the polymer properties. Polymer-based TiO_2 composites have been widely studied in the literature to develop mechanical and thermal properties of the polymer [23,24].

Ethylene/propylene copolymerization was carried out by using different catalysts such as Zeigler-Natta catalyst, post metallocene and metallocene catalysts. Recently, metallocene catalysts play a vital role in ethylene and ethylene copolymers due to their single center nature and synthesizing a wide range of new ligands structures that produce stereoregular polymers with a predetermined structure. The use of metallocene catalysts with titanium dioxide as nanofiller is an excellent combination to improve polymer properties. The studies showed that usage of impregnated nanofillers of TiO_2 increased the activity of the zirconocene catalyst up to four times [25,26].

In this paper, we used titanium dioxide nanofillers doped with iron (TiO_2/Fe) to investigate the effect of the TiO_2/Fe nanofiller on the ethylene homopolymer and ethylene/propylene copolymer properties in the presence of zirconocene complex and MAO as a cocatalyst.

5.2 Experimental Section

5.2.1 Materials

Ethylene, premixed ethylene and propylene gas mixtures were purchased from SIGAS with three different molar ratios (50:50, 60:40 and 40:60) of ethylene and propylene respectively. Titanium (IV) n-butoxide, iron (III) nitrate non hydrate $Fe(NO_3)_3{\cdot}9H_2O$, methanol and ethanol were purchased from Fisher Scientific. Bis(cyclopentadienyl) zirconium (IV) dichloride($C_{10}H_{10}Cl_2Zr$) was obtained from Sigma Aldrich. Solvents were purified by standard techniques. All manipulations were carried out under N_2 using standard Schlenk and glove box techniques.

5. 2.2 Synthesis of Undoped and Doped Titania Nanofillers

Undoped titania nanofillers were synthesized by a sol-gel process under constant sonication as following: 500 μL of titanium (IV) alkoxide precursor in ١٥ mL ethanol was hydrolyzed in the presence of 1 mL of water at room temperature to form white solution of hydrolyzed titania particles. For iron doped titania nanofillers, an inorganic precursor $Fe(NO_3)_3{\cdot}9H_2O$ (١% solution) was dissolved in 5 mL of ethanol solution and added to the hydrolyzed titania solution under constant sonication (500 rpm) for 30 minutes. After that, the precipitate was washed with ethanol many times to remove excess NO_3^-, Fe^{3+}. The precipitate was dried overnight at 100 ^{0}C and then heated for 5 hours to convert the amorphous titania into the crystalline anatase form. Finally, the product was ground into a fine powder [27]. The average particle size of produced nanofiller is 10 nm. The samples were denoted as TiO_2/Fe for titania doped iron.

5.2.3 Polymerization

Polymerization reaction was taken place in a 250 mL round-bottom flask provided with a magnetic stirrer. 6 mg of the catalyst and various amounts of the Fe/TiO_2 nanofiller (5, 10 and 15) mg were added to the flask and filled with 80 mL of toluene. Then, the flask was put in an oil bath at equilibrated temperature (30 °C) and nitrogen gas was removed by a vacuum pump. Then ethylene was supplied into the reactor. After 10 minutes of the saturation of ethylene in toluene, 5 mL of the cocatalyst (MAO) was charged into the flask and polymerization reaction was started. After 10 minutes, polymerization reaction was quenched by adding 250 mL of methanol containing HCl (5 vol. %). Finally, the polymer was put in an oven at 50 °C for 24 hours for drying. The

same procedure was followed for the ethylene/propylene copolymerization. The same procedure was followed for ethylene/propylene copolymerization.

5.3 Characterization

5.3.1 GPC Analysis

The molecular weight of polyethylene nanocomposites was determined by triple detection high temperature gel permeation chromatography (GPC) using 1, 2, 4-trichlorobenzene as a solvent. Twenty-five mg of the material was placed into a 40mL glass vial and accurately weighed and 10 mL of the solvent was added using a clean 10 mL glass pipette. The vial was capped with a Teflon coated cap and the samples were placed into the vortex auto sampler and left to dissolve for three hours at 160 °C while stirring gently.

5.3.2 DSC Analysis

Crystallinity of ethylene and ethylene/propylene copolymer nanocomposites (X_c%) and melting temperature (T_m) were measured by differential scanning calorimetry (DSC) from TA instruments Q1000. Cooling and heating cycles were done in a nitrogen environment at the rate of 10 °C min^{-1} from a temperature of 30 °C to 160 °C.

5.3.3 X-ray diffraction (XRD)

Crystallinity Measurements were carried out by using a LABX XRD-6000, Shimadzu Diffractometer operating at 40 kV, 40 mA. X-rays of 1.541 A° wavelength generated by Cu Kα source. The angle of diffraction, 2θ was varied from 2° to 70°.

5.3.4 NMR Analysis

^{13}C NMR was used to determine the composition of ethylene/propylene (E/P) copolymer by using a Bruker AVANCE III-600 NMR spectrometer and 1, 2, 4-trichlorobenzene as a solvent.

5.4 Results and Discussion

5.4.1 Polyethylene Nanocomposites

In this study, polyethylene (PE) nanocomposites were prepared by in-situ polymerization by using TiO_2/Fe nanofillers. The activity of the catalyst was increased in the presence of TiO_2/Fe nanofillers due to the increase in the chain propagation rate [26]. The activity was increased from 55.5 x 10^4 g PE/mol.Zr. h.bar (Entry 1, Table1) to 64.3 x 10^4 g PE/mol.Zr.h.bar (Entry 2, Table1) by adding 5 mg of TiO_2/Fe nanofiller. It was found that the maximum activity of the catalyst was achieved by using 10 mg of TiO_2/Fe nanofiller which equals 67.2 x 10^4 g PE/mol.Zr.h.bar (Entry 3, Table 5-1). However, the activity was decreased to ٤9.67 x 10^4 g PE/mol.Zr.h.bar when 15 mg of the nanofiller was used (Entry 4, Table 5-1) due to the steric hindrance arising from the nanoparticles and strong interaction might have been happened between the catalyst, nanofiller and the cocatalyst [15,26]. The activity was measured as a ratio of the amount of the produced polymer to the amount of the catalyst consumed per an hour at 1 bar. The experiments were repeated several times and these results are reproducible with an error less than 3%.

The molecular weight (M_w) was found to be increased when TiO_2/Fe nanofillers were added in the presence of zirconocene complex during polymerization. The optimum value for the nanofiller was 10 mg (Entry 3, Table 5-1) which is 8.4×10^4 ($g.mol^{-1}$). An

increase in the filler concentration to 15 mg resulted in decreasing in the molecular weight (M_w) to 6.3×10^4 ($g.mol^{-1}$) (Entry 4, Table 5-1) but it still showed a significant increase compared to the control (Entry 1, Table1).The increase in the molecular weight (M_w) could be contributed to the increase in the chain propagation rates.The polydispersity index (PDI) was increased by adding the TiO_2/Fe nanofiller and it was increased with increasing the amount of the TiO_2/Fe nanofiller as shown in Table 5-1 due to the increase of molecular weight (M_w). For the sake of reproducibility, the molecular weight (M_w) analysis was repeated three times for each entry and the average values were tabulated as shown in Table 5-1 with an error less than 4%.

The thermal characteristics of the polyethylene nanocomposites were measured by differential scanning calorimetry. The melting temperatures of polyethylene and polyethylene nanocomposites samples were measured by DSC from the second heating cycle and the average values for three experiments were selected with error less than 2%. The melting temperature (T_m) was increased in the presence of the nanofillers. The (T_m) was increased from 131 ^oC (Entry 1, Table 5-1) to 134^oC, 135 ^oC and 132 ^oC by using 5,10 and 15 mg (Entry 2,3 and 4, Table 5-1) respectively. This increase in melting temperature might be due to the increase in percentage of crystallinity and molecular weight (M_w). Percentage of crystallinity in polyethylene nanocomposites samples was determined and showed that the percentage of crystallinity in polyethylene nanocomposites was increased when the amount of the filler was increased as shown in Table 5-1, where the highest % crystallinity obtained by using 10 mg of TiO_2/Fe filler which is 71 (Entry 3, Table 5-1) comparing to the control which is 39 (Entry 1, Table 5-1) because the Fe/TiO_2 nanofillers could play as nucleating agents, which result in

decreasing energy barrier for formation of nuclei and increasing the nucleating sites. Then, small molecules will connect to each other to form polymer chains resulting in growing of the lamellar structure [28]. However, the crystallinity was decreased to 40 % by using 15 mg of TiO_2/Fe nanofiller (Entry 4, Table 5-1) which suggests that there is an optimum amount of the Fe/TiO_2 and beyond this amount, the Fe/TiO_2 nanofillers have a steric hindrance effect results in the decrease of the crystallinity [29]. The percentage of crystallinity was calculated by using the following expression:

$$\% \text{ of crystallinity } = \left(\Delta H_{fus} \,/\, \Delta H^{0}_{fus}\right) \text{X } 100 \qquad (5\text{-}1)$$

Where ΔH_{fus} is the enthalpy of fusion of the polyethylene nanocomposites, and ΔH^{0}_{fus} is the enthalpy of fusion of the 100% crystalline polyethylene. The percentage of crystallinity was also measured by using XRD and the results showed that the same effect of the nanofiller on the crystallinity. The difference between the percent of crystallinity calculated by using DSC and XRD is less than 10%. The crystallinity was measured via XRD by dividing the total area of crystalline peaks by the total area crystalline and amorphous peaks as shown in Figure 5-1. In this case, two crystalline regions were defined at approximately 21^{o} and 23^{o} in 2θ. Table 5-1 summarizes the results of the polymerization and polymer nanocomposites characteristics.

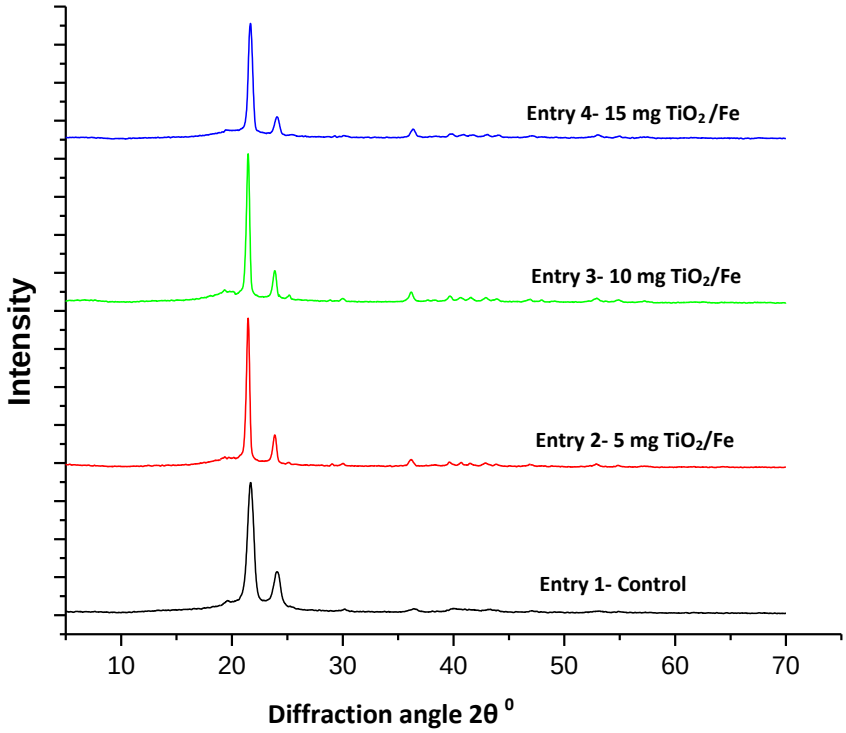

Figure 5-1: XRD patterns of polyethylene nanocomposites.

Table 5-1: Experimental conditions and properties of polyethylene prepared by in situ polymerization using zirconocene complex catalyst and an MAO cocatalyst system at 1.3 bar [a]

Entry No.	Filler (mg)	Activity [b] (× 10^{-4})	M_w [c] (× 10^{-4})	PDI [c] (Mw/ Mn)	T_m [d] (^oC)	X_c [e] (%)	X_c [f] (%)
1.	0	55.5	4.7	4	131	39	35
2.	5	64.3	5.9	4.1	134	52	50
3.	10	67.2	8.4	8.1	135	71	68
4.	15	49.67	6.3	4.1	132	40	36

[a] Polymerization conditions: toluene = 80 mL, Temp = 30 ^oC, Time = 10 min, catalyst amount = 6 mg, cocatalyst amount = 5 mL, filler is Fe (1%) doped TiO_2 ,[b] g PE/mol.Zr.h.bar, [c] determined by GPC , [d,e] determined by DSC, [f] determined by XRD.

5.4.2 Ethylene/propylene copolymer nanocomposites

Ethylene/propylene copolymer nanocomposites were prepared by in-situ polymerization in the presence of TiO_2/Fe nanofillers. The activity of the catalyst was increased when TiO_2/Fe nanofillers were added. It was found that using 10 mg of the TiO_2/Fe nanofiller gave the highest activity for molar ratios of E/P. For 60/40 molar ratios of E/P, the activity of the catalyst was increased from 49.7x 10^4 g (PE/PP)/mol.Zr.h.bar (Entry 1, Table 5-2) to 64.3 and 67.2x 10^4 g (PE/PP)/mol.Zr.h.bar using 5 and 10 mg of TiO_2/Fe nanofiller respectively (Entry 2 and 3, Table 5-2).The activity was reduced slightly to 55.5 x 10^4 g (PE/PP)/mol.Zr.h.bar by using 15 mg of the TiO_2/Fe nanofiller (Entry 4, Table 5-2). Same trend was observed in (50/50) molar ratios

of E/P, where the activity was increased from 32.2 g (PE/PP)/mol.Zr.h.bar (Entry 5, Table 5-2) up to 35.1 x 10^4 and 46.8x 10^4 g (PE/PP)/mol.Zr. h.bar by adding 5 and 10 mg of TiO_2/Fe nanofiller respectivily (Entry 6 and 7, Table 5-2). Then, it was reduced to 40.9 x 10^4 g (PE/PP)/mol.Zr.h.bar (Entry 8, Table 5-2) . For (40/60) molar ratios of E/P, the activity was increased from 29.2 x 10^4 g (PE/PP)/mol.Zr.h.bar (Entry 9, Table 5-2) to 55.5 x 10^4 g (PE/PP)/mol.Zr.h.bar (Entry 10, Table 5-2) by using 5 and then reduced to 41.5 and 36.4 x 10^4 g (PE/PP)/mol.Zr.h.bar by using 5 and 10 mg ofTiO_2/Fe nanofiller respectively (Entry 11 and 12, Table 5-2). However, the activity of the catalyst using TiO_2/Fe nanofiller was greater than control in all samples. The increase in the activity of the catalyst could be due to the increase in the chain propagation rate [26].

Polypropylene composition in ethylene/propylene copolymer was calculated as reported by Cheng [30] using ^{13}C NMR. It is important to recognize that, mole percent of polypropylene (PP %) was affected by adding TiO_2/Fe nanofiller in the presence of zirconocene complex. The polypropylene composition was increased with increasing of TiO_2/Fe nanofillers dosage. From ^{13}C NMR spectra of 60/40 molar ratio of ethylene/propylene, the polypropylene content was increased from 21% (Entry 1, Table 5-2) to 29, 33 and 38% (Entry 2,3 and 4, Table 5-2) by using 5, 10 and 15 mg of TiO_2/Fe nanofiller respectively. For 50/50 molar ratio of ethylene/propylene, the polypropylene composition was increased to 29, 31 and 35% by adding 5, 10 and 15 mg of TiO_2/Fe nanofiller respectively (Entry 6, 7 and 8, Table 5-2). The same effect of TiO_2/Fe nanofiller was observed for (40/60) molar ratio of ethylene/propylene samples. The Polypropylene composition was increased from 40% (Entry 9, Table 5-2) to 43, 46 and 53% by using 5, 10 and 15 mg of TiO_2/Fe respectively (Entry 10,11 and 12, Table 5-

2). It is worthwhile to mention that, these results are reproducible with an error less than 5%.

Percentage of crystallinity in polyethylene/polypropylene nanocomposites samples was determined by using DSC and XRD. The results showed that the percentage of crystallinity was decreased when the amount of the filler was increased as shown in Table 5-2, where the lowest % crystallinity obtained using 15 mg of the TiO_2/Fe filler compared to the control because of the increasing of the polypropylene percent when the amount of TiO_2/Fe filler increases. There are two crystalline regions were observed at approximately 21^o and 23^o in 2θ via XRD as shown in Figure 5-2. These peaks become shorter and broader when the crystallinity decreases as a result of increasing in polypropylene content [31].

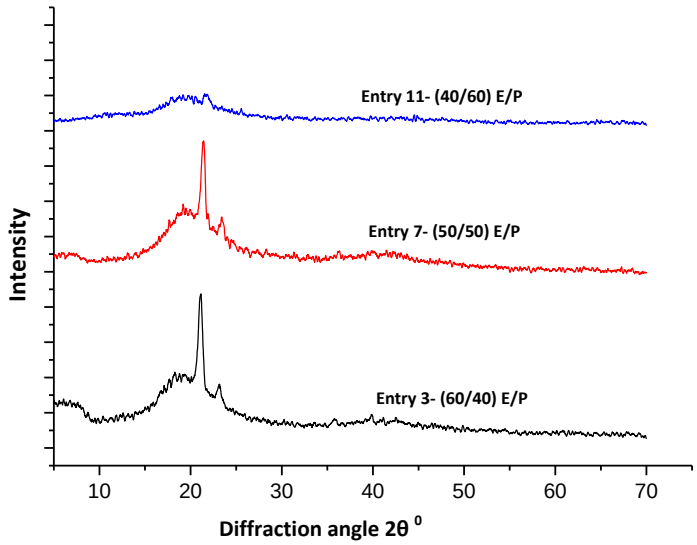

Figure 5-2: XRD patterns of ethylene- propylene copolymer nanocomposites using 10 mg of TiO_2/Fe.

The melting temperature (T_m) of polyethylene/polypropylene nanocomposites was reduced by adding the TiO_2/Fe nanofiller in all molar ratios of E/P as shown in Table 5-2. This decrease in melting temperature may be due to the decrease in percentage of crystallinity because of the increasing polypropylene content [31]. These values are the averages of three experiments for each entry as shown in Table 5-2.

Table 5-2: Experimental conditions and properties of polyethylene/polypropylene nanocomposites prepared by in situ copolymerization using a zirconocene complex catalyst and an MAO cocatalyst system at 1.3 bar.[a]

Entry No.	E/P mol/mol	Filler (mg)	Activity [b] (× 10^{-4})	PP [c] (%)	T_m [d] (^{O}C)	X_C [d] (%)	X_C [f] (%)
1.	60/40	0	49.7	21	101	8.5	7.6
2.	60/40	5	64.3	29	99	7	6.7
3.	60/40	10	67.2	31	98.1	4.5	4
4.	60/40	15	55.5	38	93	1.2	1.1
5.	50/50	0	32.2	25	95.8	5.4	4.8
6.	50/50	5	35.1	29	94.1	5.2	4.7
7.	50/50	10	46.8	33	92.3	2.48	2.2
8.	50/50	15	40.9	35	90.2	1.44	1.3
9.	40/60	0	29.2	40	82.3	1.13	1
10.	40/60	5	55.5	43	80.1	0.69	0.6
11.	40/60	10	41.5	46	76.7	0.61	0.55
12.	40/60	15	36.5	53	73.1	0.34	0.30

[a] Copolymerization conditions: Toluene = 80 mL, Temp = 30 ^{o}C, Time = 10 min, Catalyst amount = 6 mg, cocatalyst amount= 5 mL, filler is Fe (1%) doped TiO_2, [b] g(PE/PP)/mol Zr h bar, [c] determined by ^{13}C NMR, [d,e] determined by DSC, [f] determined by XRD.

5.5.3 Crystallization kinetics model

The effect of nanofiller on the crystallization kinetics of homo polyethylene and ethylene /propylene copolymer was investigated by using non isothermal Avrami-Erofeev crystallization model by following the same procedure as reported by Atiqullah et al., using cooling rate of 10°C/min [32].

The non isothermal Avrami-Erofeev crystallization rate equation is given by:

$$\frac{d\alpha(T)}{dT} = \frac{k_0}{\beta} \times exp\left[-\frac{E_a^A}{R}\left(\frac{1}{T} - \frac{1}{T_0}\right)\right] \times n(1-\alpha(T))[-ln(1-\alpha(T))]^{\frac{n-1}{n}} \quad (5\text{-}2)$$

Where:

$$f(\alpha(T)) = n(1-\alpha(T))[-ln(1-\alpha(T))]^{\frac{n-1}{n}} \quad (5\text{-}3)$$

$$k'(T) = k_0 \times exp\left[-\frac{E_a^A}{R}\left(\frac{1}{T} - \frac{1}{T_0}\right)\right] \quad (5\text{-}4)$$

$$E_a^A(\text{apparent crystallization energy}) = E_{grow} - E_{nucl} \quad (5\text{-}5)$$

$$k_0 = \left(\frac{K_s N_0}{V_0}\right)\frac{k_{grow,0}}{k_{nucl,0}} \quad (5\text{-}6)$$

$$k_{grow}(T) = k_{grow,0} \times exp\left[-\frac{E_{grow}}{R}\left(\frac{1}{T} - \frac{1}{T_0}\right)\right] \quad (5\text{-}7)$$

$$k_{nucl}(T) = k_{nucl,0} \times exp\left[-\frac{E_{nucl}}{R}\left(\frac{1}{T} - \frac{1}{T_0}\right)\right] \quad (5\text{-}8)$$

$$\alpha(T) = \frac{\alpha_w(T)}{\alpha_w(T) + {}^{\rho_c}/_{\rho_a}[1-\alpha_w(T)]} \quad (5\text{-}9)$$

E_{grow} and E_{nucl} are the corresponding activation energies and $f(\alpha(T))$ is Avrami-Erofeev non isothermal crystallization function. n is the dimension of the growing crystal.

V_0 represents the initial volume of the molten polymer. N_0 represents the number of germ nuclei. K_s is the shape factor for the growing nuclei.$k_{grow,0}$ and $k_{nucl,0}$ represent the frequency factors for crystal growth and nucleation respectively. k_{grow} and k_{nucl} follow the Arrhenius form [33, 34]. T_0 is the reference temperature. ρ_c and ρ_a are the densities of the crystalline and amorphous phases respectively. The values reported for polyethylene areρ_c = 1.004 g/mL and ρ_a = 0.853 g/mL [32].

$\alpha_w(T)$ can be found from the data of a constant cooling rate (second cycle) of non isothermal DSC experiment.

$$\alpha_w(T) = \frac{\Delta H(T)}{\Delta H_{total}} = \frac{\int_{T_0}^{T}\left(\frac{dH}{dT}\right)dT}{\int_{T_0}^{T_\infty}\left(\frac{dH}{dT}\right)dT} \tag{5-10}$$

Where$\Delta H(T)$ is the enthalpy corresponding to temperature T of crystallization. ΔH_{total} represents the maximum enthalpy obtained at the end of the non isothermal crystallization process. T_0 and T_∞ represent the initial and the final temperatures of crystallization, respectively.

5.4.4 Numerical solution of the crystallization kinetics

The non-linear model system was solved by using NonLinearModelFit of MATHEMATICA. The performance of the crystallization kinetics model was evaluated based on the coefficient of determination (R^2), 95% confidence interval, standard error and the variance. The kinetics model parameters are shown in Table 5-3 and 5-4.

5.4.4.1 Polyethylene nanocomposites

Figure 5-3 (a, b, c and d) compare the experimental relative crystallinity profiles (α) of the PE homopolymer with the model predicted as a function of temperature using (0, 5, 10 and 15) mg of the TiO_2/Fe nanofiller. The values of Avrami-Erofeev (*n)* varied from 4.6 to 6.5 for polyethylene nanocomposites. As the amount of the TiO_2/Fe nanofiller increases,(*n*) values increases. The increase in *n* values indicates that the crystal growth becomes more complex and has complicated growth mechanism [35,36]. The highest value of *n* was noticed by using 10 mg of the TiO_2/Fe nanofiller (*n*=6.5) as shown in Entry 3,Table 5-3.The high value of *n* can be attributed to the increase in the crystallinity and the molecular weight (M_w).The crystallization frequency factor k_0 (s^{-1}) was changed slightly. The apparent activation energy E_a varied from17.3 to 20.4 kJ/mol. Lower values of E_a indicate the simplicity of the crystallization process. The variation in E_a values can be attributed to the variation in the structural defect of the polymer backbones [32].

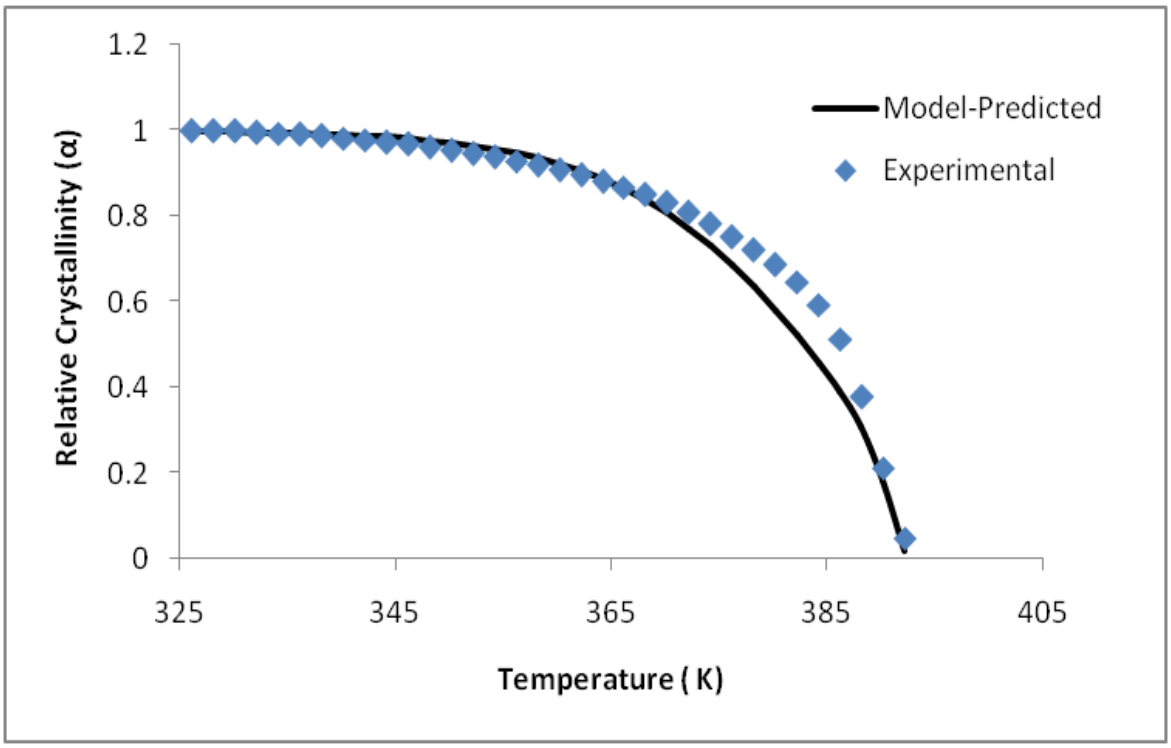
1.2
1
0.8
0.6
0.4
0.2
0
Relative Crystallinity (α)
325
345
365
385
405
Temperature (K)
Model-Predicted
Experimental

(a)

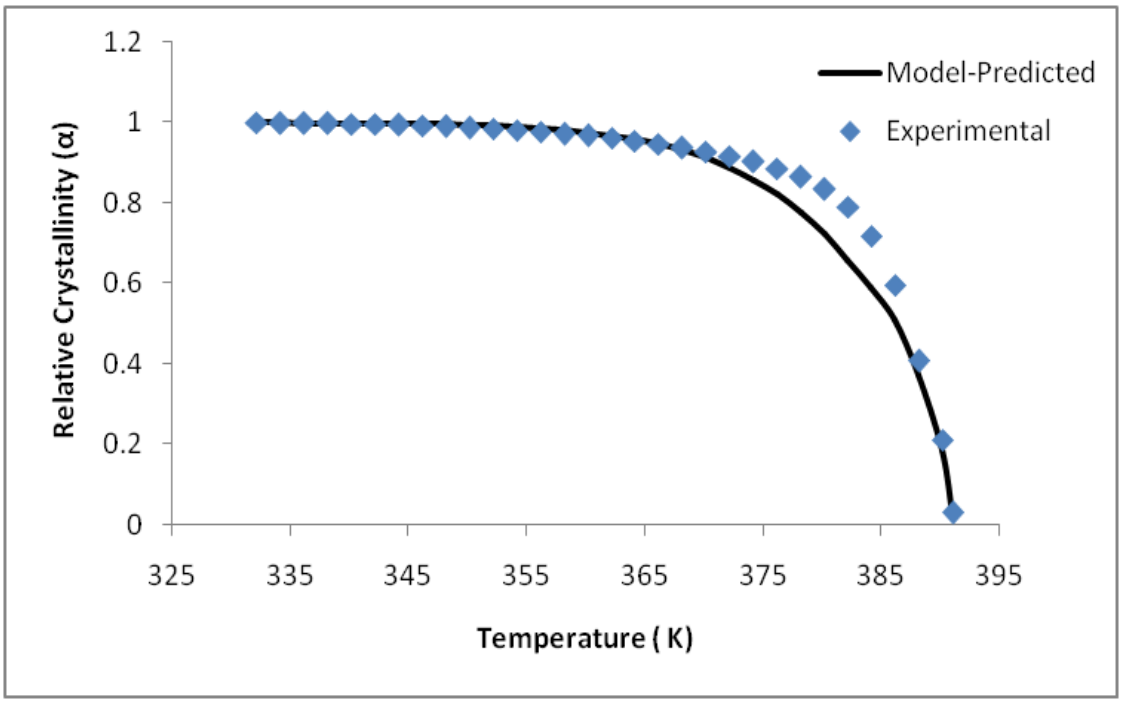
Relative Crystallinity (α)
1.2
1
0.8
0.6
0.4
0.2
0
325
335
345
355
365
375
385
395
Temperature (K)
Model-Predicted
Experimental

(b)

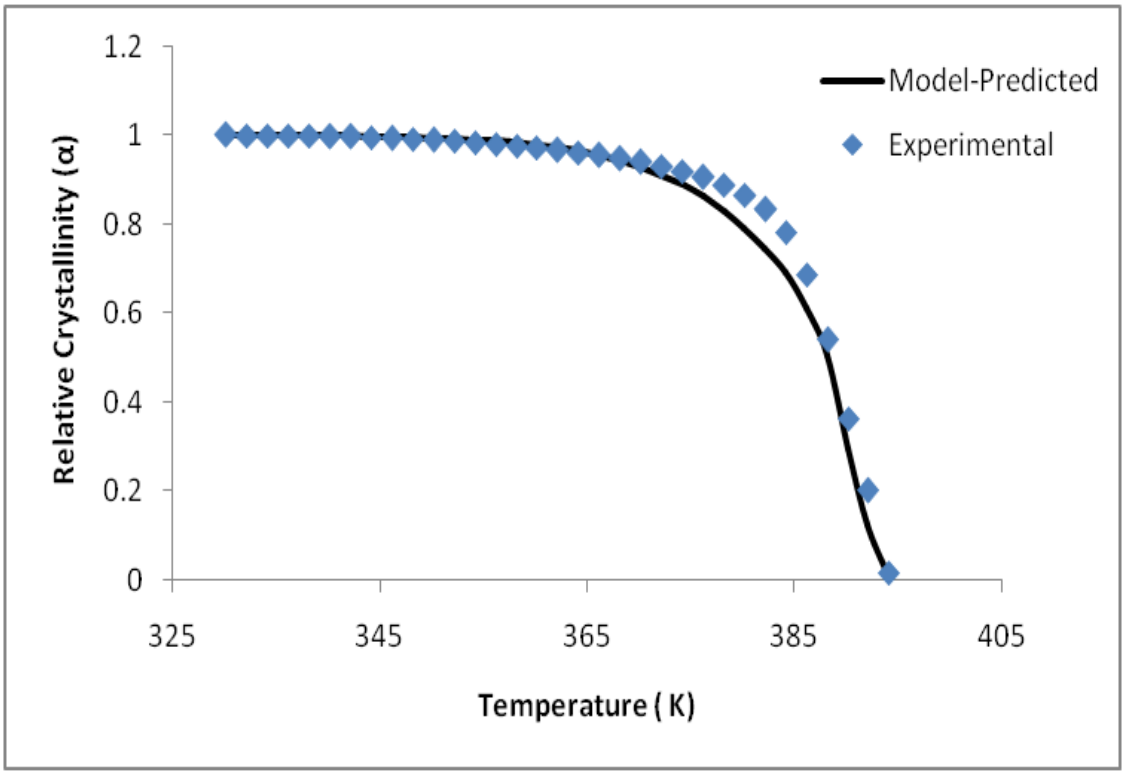
1.2
1
0.8
0.6
0.4
0.2
0
Relative Crystallinity (α)
325
345
365
385
405
Temperature (K)
Model-Predicted
Experimental

(c)

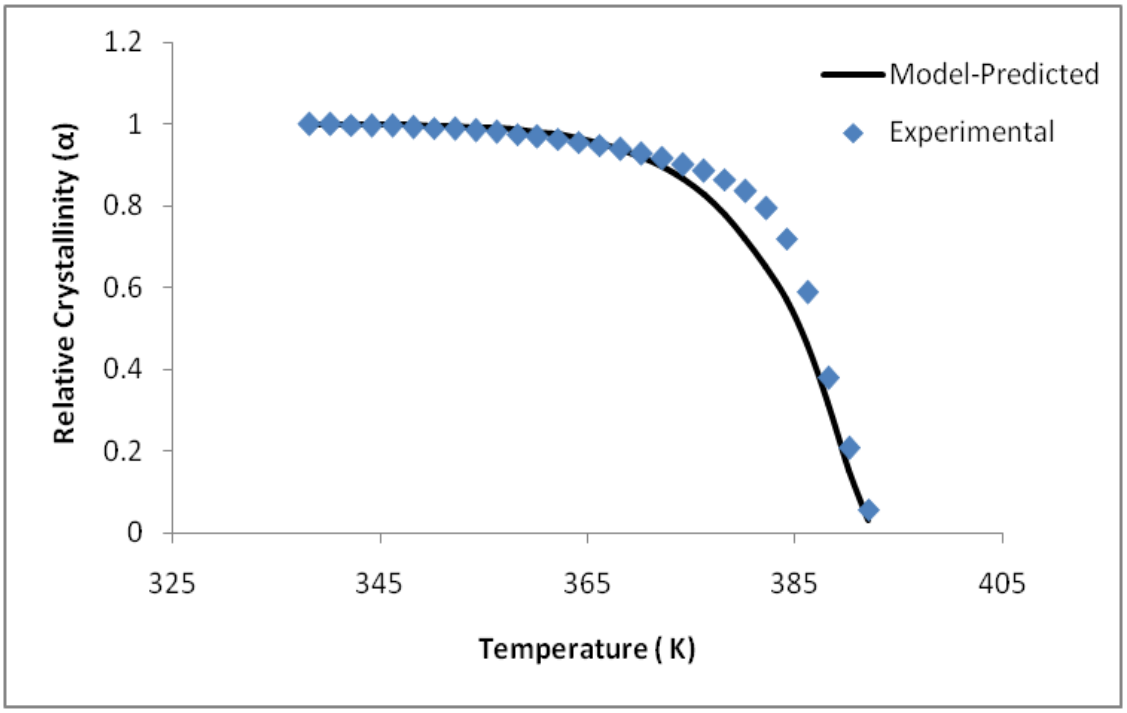

(d)

Figure 5-3: Comparison of model-predicted relative crystallinity with the experimental data as a function of DSC cooling temperature for PE homopolymer: (a) control (b) 5 mg TiO_2/Fe (c) 10 mg TiO_2/Fe (d) 15 mg TiO_2/Fe.

Table 5-3: Model-predicted non isothermal crystallization kinetics parameters of polyethylene nanocomposites.

Entry No.	Filler (mg)	n	E_a (kJ/mol)	k_0 (s^{-1})	R^2
1.	0	4.6	18.0	0.148	0.988
2.	5	5.25	20	0.136	0.989
3.	10	6.5	17.3	0.138	0.988
4.	15	6.2	20.4	0.152	0.986

5.4.4.2 Ethylene/Propylene Copolymer Nanocomposites

Figure 5-4(a, b and c) shows that the experimental relative crystallinity profiles (α) of the ethylene/ propylene copolymer with the model predicted as a function of temperature by using 10 mg of the TiO_2/Fe nanofiller at (60/40, 50/50 and 40/60) molar feed ratios respectively . The values of Avrami-Erofeev (n) index varied from 3 to 4.7, 2.3 to 4.1 and 2.7 to 3.7 for (60/40, 50/50 and 40/60) molar feed ratios of ethylene/propylene respectively as shown in Table 5-4. Avrami-Erofeev (n) index was decreased when the amount of the TiO_2/Fe nanofiller was increased as a result of decreasing in percentage of crystallinity due to the increase in polypropylene content [37]. The high values of E_a indicate the complexity of crystallization process.

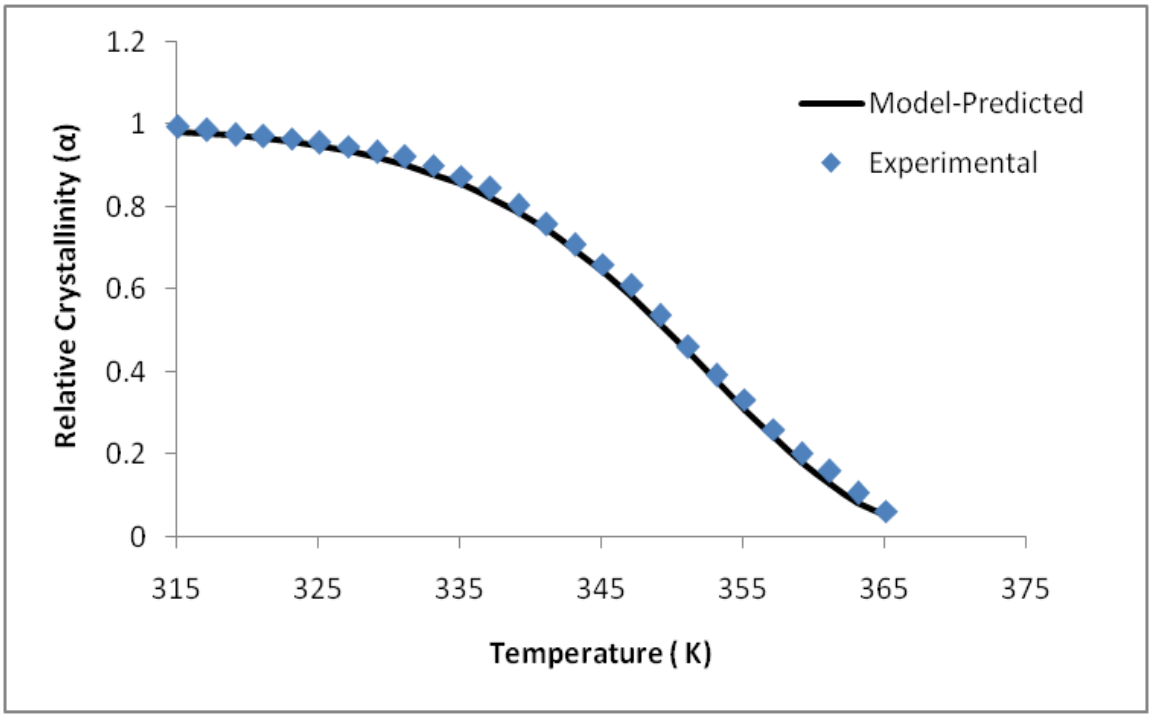
1.2
1
0.8
0.6
0.4
0.2
0
Relative Crystallinity (α)
315
325
335
345
355
365
375
Temperature (K)
Model-Predicted
Experimental

(a)

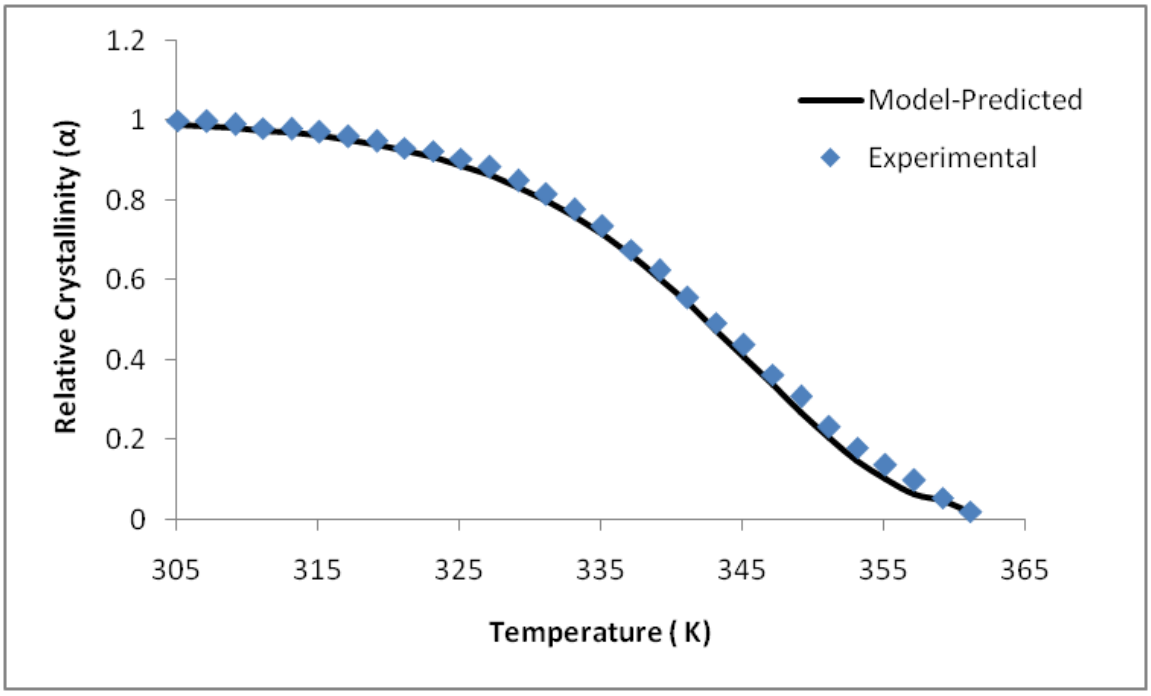
1.2
1
0.8
0.6
0.4
0.2
0
Relative Crystallinity (α)
305
315
325
335
345
355
365
Temperature (K)
Model-Predicted
Experimental

(b)

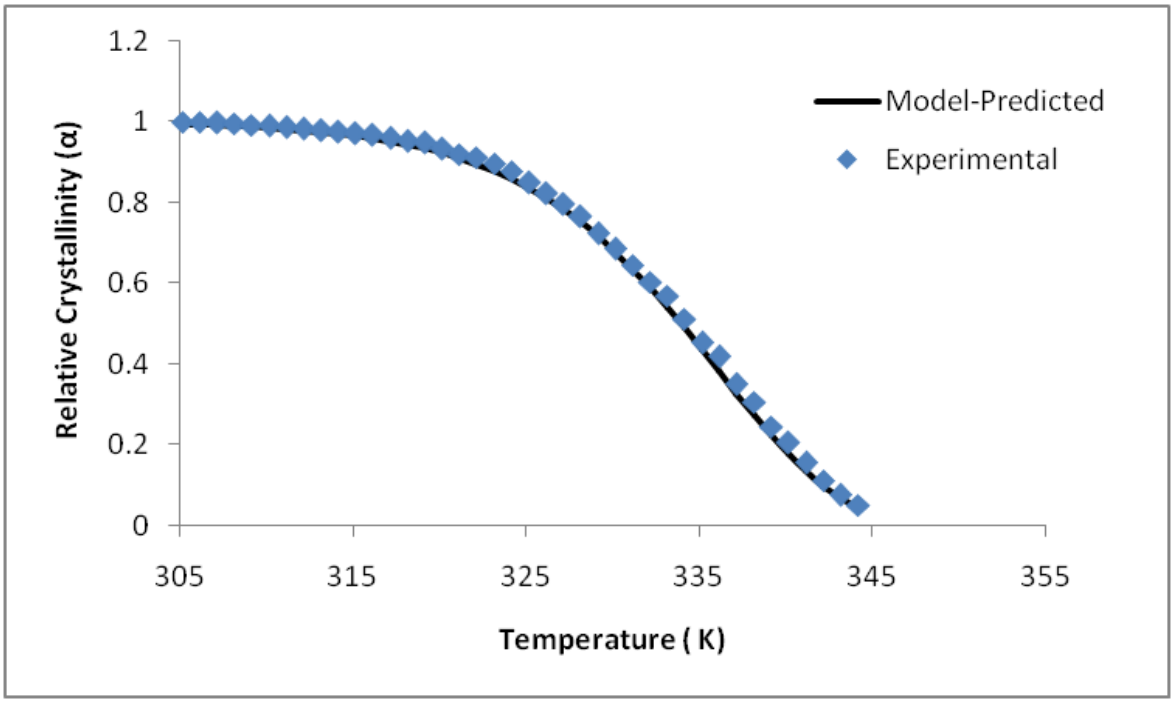

(c)

Figure 5-4: Model-predicted non isothermal crystallization kinetics parameters of polyethylene nanocomposites.

Table 5-4: Model-predicted non isothermal crystallization kinetics parameters of ethylene/propylene copolymer nanocomposites

Entry No.	E/P mol/mol	Filler (mg)	n	E_a (kJ/mol)	k_0 (s^{-1})	R^2
1.	60/40	0	4.7	20.9	0.445	0.987
2.	60/40	5	4.4	19.9	0.387	0.988
3.	60/40	10	3.8	19.8	0.389	0.989
4.	60/40	15	3	25.2	0.548	0.989
5.	50/50	0	4.1	17.5	0.305	0.988
6.	50/50	5	4	23.3	0.483	0.991
7.	50/50	10	3.4	24	0.407	0.990
8.	50/50	15	2.3	30.9	0.569	0.993
9.	40/60	0	3.7	37.4	1.529	0.993
10.	40/60	5	3.3	53.1	4.161	0.996
11.	40/60	10	3.1	39.8	1.739	0.995
12.	40/60	15	2.7	53.4	4.3	0.996

Conclusions

Polyethylene and ethylene/propylene copolymer nanocomposites were synthesized by using Bis(cyclopentadienyl) zirconium (IV) dichloride in the presence of TiO_2/Fe nanofiller. The molecular weight (M_w) was found to be increased by adding the TiO_2/Fe nanofiller in polyethylene nanocomposites. The maximum catalyst activity was achieved by using 10 mg of TiO_2/Fe nanofiller in all polyethylene and polyethylene/polypropylene nanocomposites. The melting temperature (T_m) and crystallinity of polyethylene nanocomposites were increased by using TiO_2/Fe nanofiller. However, the contrary trend was detected in polyethylene/polypropylene nano-composites due to the increase of the polypropylene content. ^{13}C NMR showed that the polypropylene content was increased when the TiO_2/Fe nanofiller amount increases. Non-isothermal crystallization kinetics of polyethylene and polyethylene/polypropylene nanocomposites were well fitted with Avrami-Erofeev model. The crystallization behavior of ethylene/propylene copolymers nanocompopsites was influenced by the comonomer distribution.

Acknowledgments

The authors wish to acknowledge the assistance of Deanship of Scientific Research, King Fahd University of Petroleum and Minerals for their support for providing adequate funds and infrastructure under Project no. IN101018.

References

1. Suárez, I.; Caballero, M.; Coto, B. Characterization of ethylene/propylene copolymers by means of a GPC-4D technique. *European Polymer Journal* **2011**, 47, 171-178.

2. Silva, F.; Lima, E.;Pinto, J.; McKenna, T. Synthesis of propylene/1-butene copolymers with Ziegler-Natta catalyst in gas-phase copolymerizations. *Macromolecular Chemistry and Physics* **2005**, 206, 2333-2341.

3. Busico, V.; Cipullo, R. Microstructure of polypropylene. *Progress in Polymer Science* **2001**, 26, 443-533.

4. Kaminsky, W. New polymers by metallocene catalysis. *Macromolecular Chemistry and Physics* **1996**, 197, 3907-3945.

5. Zhao, C.; Qin, H.;Gong, F.; Feng, M.; Zhang, S.; Yang, M. Mechanical, thermal and flammability properties of polyethylene/clay nanocomposites. *Polymer Degradation and Stability*. **2005**, 87, 183-189.

6. Wei, L.; Tang ,T.; Huang, B. Synthesis and characterization of polyethylene/clay–silica nanocomposites: A montmorillonite/silica-hybrid-supported catalyst and in situ polymerization. *Journal of Polymer Science Part A: Polymer Chemistry*. **2004**, 42, 941-949.

7. Rossi, G.B.; Beaucage, G.; Dang, D.; Vaia, R. Bottom-Up Synthesis of Polymer Nanocomposites and Molecular Composites: Ionic Exchange with PMMA Latex. *Nano Letters*. **2002**, 2, 319-323.

8. Verbeek, C.J.R. Effect of preparation variables on the mechanical properties of compression-moulded phlogopite/LLDPE composites. *Materials Letters*. **2002**, 56, 226-231.

9. Mandal, T.K.; Fleming, M.S.; Walt , D.R. Preparation of Polymer Coated Gold Nanoparticles by Surface-Confined Living Radical Polymerization at Ambient Temperature. *Nano Letters*. **2002**, 2, 3-7.

10. Sohail, O.B.; Sreekumar, P. A.; De, S. K.; Jabarullah Khan, M. H., Abbas Alshaiban, A. A.; Al-Harthi, M. A. Thermal Effect of Ceramic Nanofiller Aluminium Nitride on Polyethylene Properties. Journal of Nanomaterials. *Journal of Nanomaterials*. **2012**, 7.

11. Nussbaumer, R.J.; Caseri, W. R.;Smith, P.; Tervoort,T. Polymer-TiO_2 Nanocomposites: A Route Towards Visually Transparent Broadband UV Filters and High Refractive Index Materials. *Macromolecular Materials and Engineering*. **2003**, 288, 44-49.

12. Wang, Z., Li, G.; Xie, G.; Zhang, Z., Dispersion Behavior of TiO_2 Nanoparticles in LLDPE/LDPE/TiO2 Nanocomposites. *Macromolecular Chemistry and Physics*. **2005**, 206, 258-262.

13. Chen, X.D.; Wang, Z.; Liao, Z. F.; Mai, Y. L.; Zhang, M. Q. Roles of anatase and rutile TiO_2 nanoparticles in photooxidation of polyurethane. *Polymer Testing*. **2007**, 26, 202-208.

14. Owpradit, W.; Jongsomjit, B. A comparative study on synthesis of LLDPE/TiO_2 nanocomposites using different TiO_2 by in situ polymerization with zirconocene/dMMAO catalyst. *Materials Chemistry and Physics*. **2008**, 112, 954-961.

15. Jongsomjit, B.; Ekkrachan, C.; Praserthdam, P. LDPE/nano-silica composites synthesized via in situ polymerization of ethylene/1-hexene with MAO/metallocene catalyst. *Journal of Materials Science*. **2005**, 40, 2043-2045.

16. Kontou, E.; Niaounakis, M. Thermo-mechanical properties of LLDPE/SiO_2 nanocomposites. *Polymer*. **2006**, 47, 1267-1280.

17. Chaichana, E.; Jongsomjit, B.; Praserthdam, P. Effect of nano-SiO_2 particle size on the formation of LLDPE/SiO_2 nanocomposite synthesized via the in situ polymerization with metallocene catalyst. *Chemical Engineering Science*. **2007**, 62, 899-905.

18. Li, K.-T.; Dai, C.-L.; Kuo, C.-W. Ethylene polymerization over a nano-sized silica supported Cp^2ZrCl_2/MAO catalyst. *Catalysis Communications*. **2007**, 8, 1209-1213.

19. KUO, M. C.; TSAI, C. M.; HUANG, J. C.; CHEN, M. PEEK composites reinforced by nano-sized SiO_2 and Al_2O_3 particulates. *Materials Chemistry and Physics*. **2005,** 90, 185–195.

20. Desharun, C.; Jongsomjit, B.; Praserthdam, P. Study of LLDPE/alumina nanocomposites synthesized by in situ polymerization with zirconocene/d-MMAO catalyst. *Catalysis Communications*. **2008**, 9, 522-528.

21. Jongsomjit, B.; Panpranot, J.; Okada, M.; Shiono, T.; Praserthdam, P. Characteristics of LLDPE/ZrO_2 nanocomposite synthesized by in-situ polymerization using a zirconocene/MAO catalyst. *Iranian Polymer Journal*. **2006**, 15, 433-439.

22. Jongsomjit, B.; Panpranot, J.; Praserthdam, P. Effect of nanoscale SiO_2 and ZrO_2 as the fillers on the microstructure of LLDPE nanocomposites synthesized via in situ polymerization with zirconocene. *Materials Letters*. **2007**, 61, 1376-1379.

23. Wang, Z.; Wang, X.; Xie, G.; Li, G.; Zhang, Z. Preparation and characterization of polyethylene/TiO_2 nanocomposites. *Composite Interfaces*. **2006**, 13, 623-632.

24. Supaphol, P.; Thanomkiat, P.; Junkasem, J.; Dangtungee, R. Non-isothermal melt-crystallization and mechanical properties of titanium(IV) oxide nanoparticle-filled isotactic polypropylene. *Polymer Testing*. **2007**, 26, 20-37.

25. Owpradit, W., Mekasuwandumrong, O.; Panpranot, J.; Shotipruk, A.; Jongsomjit, B. Synthesis of LLDPE/TiO_2 nanocomposites by in situ polymerization with zirconocene/dMMAO catalyst: effect of [Al]/[Zr] ratios and TiO_2 phases. *Polymer Bulletin*. **2011**, 66, 479-490.

26. Abdul Kaleel, S.H., Kottukkal Bahuleyan, B.; De, S. K.; Jabarulla Khan, M.; Sougrat, R.; Al-Harthi, M. A. Effect of Mn doped-titania on the activity of

metallocene catalyst by in situ ethylene polymerization. *Journal of Industrial and Engineering Chemistry*. **2012**, 18, 1836-1840.

27. Kumbhar, A.; Chumanov, G. Synthesis of Iron(III)-Doped Titania Nanoparticles and its Application for Photodegradation of Sulforhodamine-B Pollutant. *Journal of Nanoparticle Research*. **2005**, 7, 489-498.

28. Kožíšek, Z.; Hikosaka, M.; Demo, P.; Sveshnikov, A. M. Nucleation kinetics of polymer formation on nucleation agent. *Journal of Crystal Growth*. **2005**, 275-83.

29. Liang, G.; Xu, J.; Xu, W.; Shen, X.; Zhang, H.; Yao, M. Effect of filler-polymer interactions on the crystalline morphology of PEO-based solid polymer electrolytes by Y_2O_3 nano-fillers. *Polymer Composites*. **2011**, 32, 511-518.

30. Cheng, H.N. c. Carbon-13 NMR analysis of ethylene-propylene rubbers. *Macromolecules*. **1984**, 17, 1950-1955.

31. Anantawaraskul, S.; Soares, J., Wood-Adams, P. Fractionation of Semicrystalline Polymers by Crystallization Analysis Fractionationand Temperature Rising Elution Fractionation. *Polymer Analysis Polymer Theory*. **2005**, 182, 1-54.

32. Atiqullah, M.; Hossain, M.; Kamal, M.; Al-Harthi, M. A.; Khan, M. J.; Hossaen, A.; Hussain, I. Crystallization kinetics of PE-b-isotacticPMMA diblock copolymer synthesized using $SiMe_2(Ind)_2ZrMe_2$ and MAO cocatalyst. *AIChE Journal*. **2013**, 59, 200-214.

33. Routray, K.; Deo, G. Kinetic parameter estimation for a multiresponse nonlinear reaction model . *AIChE Journal*. **2005**, 51, 1733-1746.

34. Hossain, M.M.; de Lasa , H.I. Reactivity and stability of Co-Ni/Al_2O_3 oxygen carrier in multicycle CLC. *AIChE Journal*, **2007**. 53, 1817-1829.

35. Al-Mulla, A.; Mathew, J.; Yeh, S.-K.; Gupta, R., Nonisothermal crystallization kinetics of PBT nanocomposites.*Composites Part A: Applied Science and Manufacturing*. **2008**, 39, 204-217.

36. Hao, W.; Yang, W.; Cai, H.; Huang, Y. Non-isothermal crystallization kinetics of polypropylene/silicon nitride nanocomposites. *Polymer Testing*. **2010**, 29, 527-533.

37. Fan, Z.-q.; Du, Z.-x.; Xu , J.-t. Crystallization kinetics of ethylene-propylene copolymers prepared by living coordination polymerization, *Chinese Journal of Polymer Science*. **2008**,26, 589-595.

Chapter 6

An Innovative method to Produce UHMWPE

ABSTRACT

A vanadium (III) complex catalyst bearing a salicylaldiminato ligand of the general formula [ArN=CH(2,4-$^{t}Bu_2C_6H_2O$)]$VCl_2(THF)_2$, where Ar = 2,6-$^{i}Pr_2C_6H_3$ is synthesized. Titanium dioxide doped with tungsten (TiO_2/W) nanofillers are used to study the effect of nanofillers on the polyethylene nanocomposites properties. Using titanium dioxide doped with tungsten (TiO_2/W) is resulted in increasing the molecular weight (M_w) of polyethylene nanocomposites up to five times compared to the neat polyethylene. The optimum dosage of the TiO_2/W nanofiller was 10 mg which molecular weight (M_w) was 1.2×10^{6} ($g.mol^{-1}$). The catalyst activity is increased up to 60 % by using the same amount of the TiO_2/W nanofiller. Besides investigation of the molecular weight (M_w) and catalyst activity, the crystallinity and thermal characteristics of polyethylene and polyethylene nanocomposites are studied. Non-isothermal crystallization kinetics of polyethylene and polyethylene nanocomposites are well fitted to Avrami-Erofeev model.

Keywords: polyethylene, nanocomposites, UHMWPE, titania doped tungsten, Avrami-Erofeev model, non isothermal crystallization kinetics.

6.1 Introduction

Ultra-high molecular weight polyethylene (UHMWPE) is an exceptional polymer with unique mechanical and physical properties such as chemical resistance, thermal stability, impact resistance, abrasion resistance and lubricity as a result of their supermolecular structure and the high molecular weight [1, 2]. Ultra-high molecular weight polyethylene (UHMWPE) can be used in medical as joint replacements and joint arthroplasty or in military as personal armor and vehicle armor and in various industry applications [3, 4]. Ultra-high molecular weight polyethylene is obtained by polymerization of ethylene at low pressure using Zeigler-Natta catalyst supported by fixing $TiCl_4$ or $VOCl_3$ onto amorphous SiO_2 [1, 5].

Polyolefin nanocomposites have exceptional mechanical properties, flammability and gas barrier properties and thermal stability depending on the shape, loading, particle size, dispersion of the fillers and bonding [6-16]. There are three important methods to make polymer composites: solution mixing [17], melt compounding [18-22] and in situ polymerization [23]. In-situ polymerization is considered the best method since it gives a uniform dispersion of nanofiller in the polymer matrix.

Different inorganic nanoparticles have been used such as titanium dioxide (TiO_2) [24-27], silicon dioxide (SiO_2) [28-31], aluminum trioxide (Al_2O_3) [32, 33] and zirconium dioxide (ZrO_2) [34, 35] to improve polymer properties. Polymer-based TiO_2 composites have been extensively studied in the literature to improve mechanical and thermal properties of the polymer [36-45]. UHMWPE was composited with fiber and powder carbon to improve the mechanical properties [46]. The use of metallocene catalyst with titanium dioxide doped with nanofillers resulted in improving polymer properties [47].

In this paper, we synthesized titania (TiO_2) nanofiller doped with tungsten to study the effect of the nanofiller on the polyethylene nanocomposites properties using in situ polymerization method. To our knowledge, this is the first time titanium dioxide doped with tungsten has been used as a nanofiller in ethylene polymerization using a vanadium complex with MADC as a cocatalyst. The molecular weight (M_w), activity of catalyst, thermal characteristics and crystallinity of polyethylene nanocomposites were investigated.

6.2 Experimental Methods

6.2.1 Materials

Ethylene gas was purchased from SIGAS. Titanium (IV) n-butoxide, tungsten (VI) oxide methanol and ethanol were purchased from Fisher Scientific. VCl_3 $(THF)_3$, tetrahydrofuran were obtained from Sigma Aldrich. Solvents were purified by standard techniques. All manipulations were carried out under N_2 using standard Schlenk and glove box techniques.

6.2.2 Catalyst Synthesis

Vanadium(III) complex bearing salicylaldiminato ligand, [RN=CH(2,4-$^{t}Bu_2C_6H_2O$)] $VCl_2(THF)_2$, where R = 2,6-$^{i}Pr_2C_6H_3$, was synthesized according to reported procedure [48].

6.2.3 Synthesis of undoped and doped Titania nanofillers

Undoped titania nanofillers were synthesized by a sol-gel process under constant sonication as following: 1 mL of titanium (IV) alkoxide precursor in 5 ml ethanol was

hydrolyzed in the presence of 1 ml of water at room temperature to form white solution of hydrolyzed titania particles. For titania nanofillers doped with tungsten, 1.2 g of tungsten (VI) oxide were dissolved in 25 ml of ethanol and then added to the hydrolyzed titania solution under constant sonication. The reaction mixture was sonicated for 30 minutes. After that, the precipitate was washed with ethanol many times to remove excess NO_3^-. The precipitate was dried overnight at 100 ^{0}C and then heated for 5 hours to get a crystalline anatase form. Finally, the product was ground into a fine powder. The samples were denoted as TiO_2/W for titania doped with tungsten [49]. The samples were denoted as TiO_2/W for titania doped with tungsten and the average particles size of produced nanofillers is 10 nm.

6.2.4 Polymerization

Polymerization reaction was taken place in a 250 mL round-bottom flask provided with a magnetic stirrer. 1.8 mg of the catalyst and various amounts of the TiO_2 /W nanofiller (5, 10 and 15) mg were added to the flask and filled with 80 mL of toluene. Then, the flask was put in an oil bath at equilibrated temperature (30 °C) and nitrogen gas was removed by a vacuum pump. Then ethylene was supplied into the reactor. After 10 minutes of the saturation of ethylene in toluene, 1 mL of the cocatalyst (MADC) was charged into the flask and polymerization reaction was started. After 10 minutes, polymerization reaction was quenched by adding 250 mL of methanol containing HCl (5 vol. %). Finally, the polymer was put in an oven at 50 °C for 24 hours for drying.

6.3 Characterization

6.3.1 GPC Analysis

Molecular weight of polyethylene nanocomposites was measured by Triple Detection High Temperature Gel Permeation Chromatography (GPC) by using 1, 2, 4-trichlorobenzene as a solvent. Twenty-five mg of the material was placed into a 40 mL glass vial and accurately weighed and 10 mL of the solvent was added using a clean 10 mL glass pipette. The vial was capped with a Teflon coated cap and the samples were placed into the Vortex Auto Sampler and left to dissolve for 3hrs at 160 °C while stirring gently.

6.3.2 DSC Analysis

Crystallinity and the melting temperature (T_m) of polyethylene/polyethylene nanocomposites (X_c %) were determined by differential scanning calorimetry (DSC) using TA instruments Q1000. Cooling and heating for both cycles were carried out in nitrogen environment using the rate of 10 °C min^{-1} and a temperature range from 30 °C to 160 °C.

6.3.3 X-ray diffraction (XRD)

Crystallinity Measurements were determined by using a LABX XRD-6000, Shimadzu Diffractometer running at 40 kV, 40 mA. X-rays of 1.541 A° wavelength generated by Cu Kα source. The angle of diffraction, 2θ was varied from 2 ° to 70 °.

6.3.4 CRYSTAF Analysis

Crystallization analysis fractionation (CRYSTAF) (Polymer Char, Spain) of polyethylene / polyethylene nanocomposites was achieved using an IR detector in 1, 2, 4-

trichlorobenzene in a stainless-steel stirred vessel of 50-mL volume and the crystallization rate was 0.2 °C/min.

6.3.5 Scanning Electron Microscopy (SEM)

Morphology of polyethylene / polyethylene nanocomposites was studied using scanning electron microscopy (SEM) using the polymer films prepared as following: First, aluminum substrates with 10 mm x 15 mm x 2 mm dimensions were heated up to 160 °C. Then, polyethylene / polyethylene nanocomposites powders were put inside the hot substrates and compressed using Carver 25-ton press by applying 4000 pounds load for 5 minutes. After that, the substrates were cooled to get uniform polymer films. Finally, the films were put in liquid nitrogen and quickly cracked.

6.4 Results and Discussion

6.4.1 Molecular weight

Molecular weight (M_w) was found to increase by adding TiO_2/W nanofiller with vanadium complex during polymerization. The optimum value for the nanofiller was 10 mg (Entry 3, Table 6-1) which molecular weight (M_w) was 1.2×10^6 ($g.mol^{-1}$). An increase in the nanofiller concentration 15 mg resulted in a decrease in the molecular weight (M_w) to 0.786×10^6 ($g.mol^{-1}$) (Entry 4, Table 6-1) when compared to the 10 mg of nanofiller concentration but still showed a significant increase compared to the control (Entry 1, Table 6-1). Polydispersity index (PDI) was decreased by adding TiO_2/W nanofiller and decreased with increasing the amount of the TiO_2/W nanofiller as shown in Table 6-1. This decrease in PDI improved the thermal properties of polyethylene

nanocomposites. It is worthy to mention that, these results are reproducible with an error of less than 3 %.

6.4.2 Catalyst activity

The activity of the catalyst was measured as a ratio of the amount of product (polyethylene or polyethylene nanocomposites) to amount of catalyst consumed per hour at 1 bar. The activity of the catalyst was increased when TiO_2/W nanofillers were added. It was found that the maximum activity of the catalyst was achieved using 10 mg of TiO_2/W nanofiller which equals 1798 kg PE/mol V h bar (Entry 3, Table 6-1) compared to the control (1135 kg PE/mol V h bar, Entry 1, Table 6-1). The increase in the activity of the catalyst could be due the increasing in the chain propagation rate [47]. The experiments were repeated several times and these results are reproducible with error less than 3%.

6.4.3 The thermal characteristics

The thermal characteristics of the polyethylene nanocomposites were determined by differential scanning calorimetry. The melting temperatures of polyethylene and polyethylene nanocomposites samples were determined by DSC from the second heating cycle. Polyethylene nanocomposites showed that the melting temperature (T_m) was slightly higher (Entry 2, 3 and 4, Table 6-1) than the control (Entry 1, Table 6-1) due to both increase in the M_w of polyethylene nanocomposites and the existence of the nanofiller.

The degradation temperature of polyethylene nanocomposites was raised when the TiO_2/We nanofillers were added to the polymerization reaction as shown in Figure 6-

1. The increase in degradation temperature is attributed to the increase in the high molecular weight (M_w) and filler content. About ٧ wt. % of the control polyethylene (Entry 1, Table 6-1) started to degrade at 117 °C and the rest at 404 °C. This early degradation may be due to the presence of a low molecular weight portion which is confirmed by the higher PDI of control polyethylene (PDI = 3.7, Entry 1, Table 6-1) compared to polyethylene nanocomposites (PDI = 2.5, 2.1 and 2.6, Table 6-1) (Entry 2, 3 and 5) respectively. This higher PDI of control polyethylene suggests that it has a low molecular weight segment in addition to the majority high molecular weight segment.

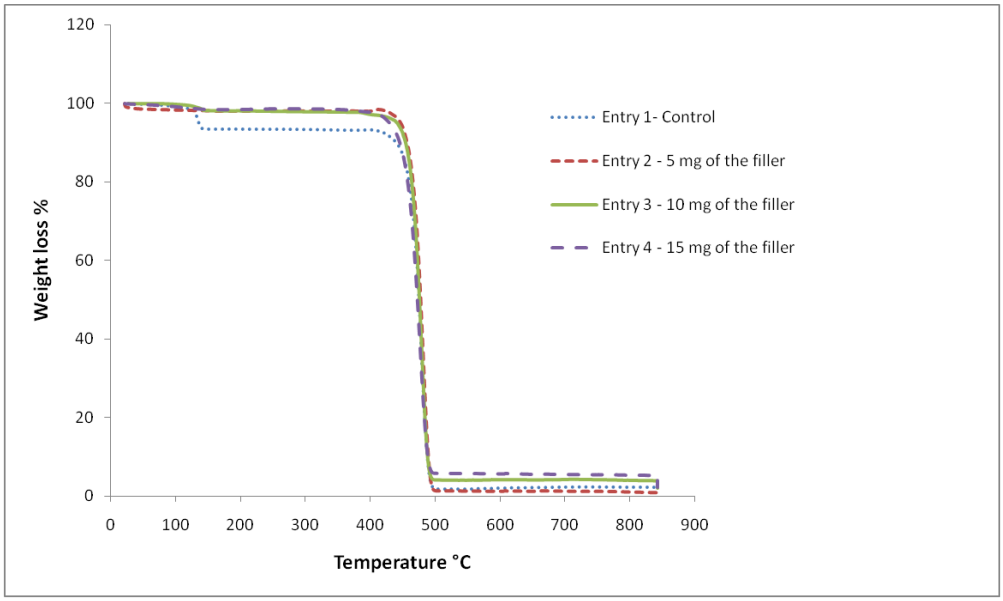

Figure 6-1: Temperature degradation of polyethylene and polyethylene nanocomposites determined by thermal gravimetric analysis (TGA).

Percentage of crystallinity in polyethylene nanocomposites samples was determined and the results showed that an insignificant change in the percentage of crystallinity in polyethylene nanocomposites in the presence of TiO_2/W nanofillers (Entry 2, Table 6-1) compared to the control (X_c = 50 %) (Entry 1, Table 6-1).

The percentage of crystallinity was also determined using XRD and the results showed the same result of the nanofiller on the crystallinity. The difference between the percent of crystallinity calculated using DSC and XRD is less than 6%. The crystallinity was calculated using XRD by dividing the total area of crystalline peaks by the total area crystalline and amorphous peaks. There are two crystalline regions were observed at approximately 21^o and 23^o in 2θ via XRD as shown in Figure 2.

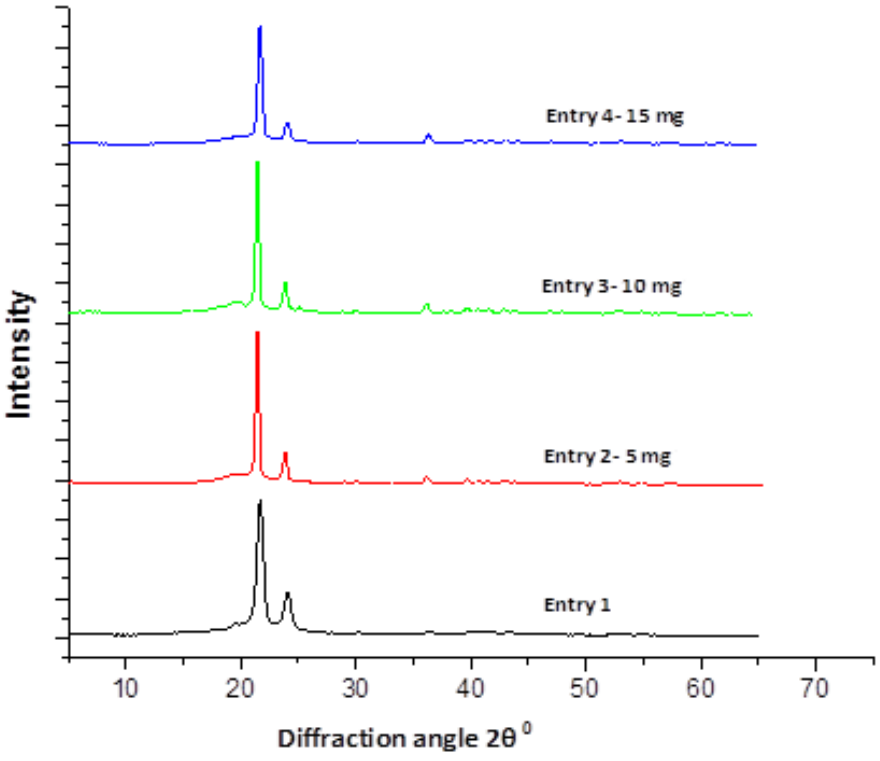

Figure 6-2: XRD patterns of polyethylene nanocomposites.

Table 6-1: Experimental conditions and properties of polyethylene prepared by in situ polymerization using vanadium complex catalyst and MADC co-catalyst system at 1.3 bar [a].

Entry No.	Filler (mg)	Activity [b]	M_w [c] (× 10^{-4})	PDI[c]	T_m [d] (^{O}C)	X_c [e] (%)	X_c [f] (%)
1.	0	1135	20	3.7	135	50	47
2.	5	1573	86	2.5	136	52	49
3.	10	1798	120	2.1	137	51	49
4.	15	1459	78.6	2.6	135.5	49	46

[a] Polymerization conditions: toluene = 80 mL, Temp = 30 °C, Time = 10 min, catalyst amount = 1.8 mg, cocatalyst amount = 1 mL, filler is W (1%) doped TiO_2, [b] kg PE/mol.V.h.bar, [c] determined by GPC , [d, e] determined by DSC, [f] determined by XRD.

6.4.4 CRYSTAF analysis

CRYSTAF analysis was carried out to study the effect of (TiO_2/W) nanofiller on CRYSTAF profiles. The results showed that CRYSTAF profiles of polyethylene / polyethylene nanocomposites become narrower with increasing molecular weight (M_w) as shown in Figure 6-3 (Entry 2,3 and 4) compared to control (Entry 1). The crystallization temperature was increased slightly from 83 °C to 86 °C when the molecular weight (M_w) increased as shown in Figure 6-3 (Entry 1 and 3). However, the crystallization temperatures showed an insignificant change for higher molecular weight (M_w) samples because the samples with higher molecular are not affected too much by long chains and they will start to crystallize at around the same temperature [50].

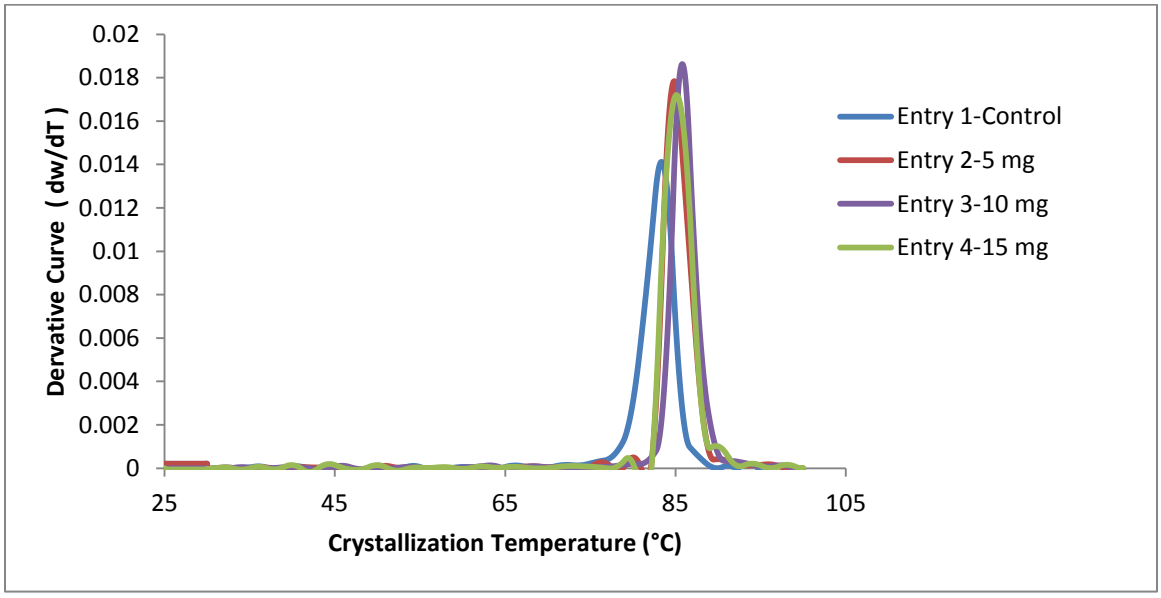

Figure 6-3: Differential crystallization analysis fractionation (Crystaf) profiles.

6.4.5 Scanning electron microscopy (SEM)

The morphology of polyethylene / polyethylene nanocomposites was studied by using scanning electron microscopy (SEM). Small swelling particles of (TiO_2/W) nanofiller were shown and they increased with increasing the amount of (TiO_2/W) nanofiller in polyethylene nanocomposites samples as shown in Figure 6-4.

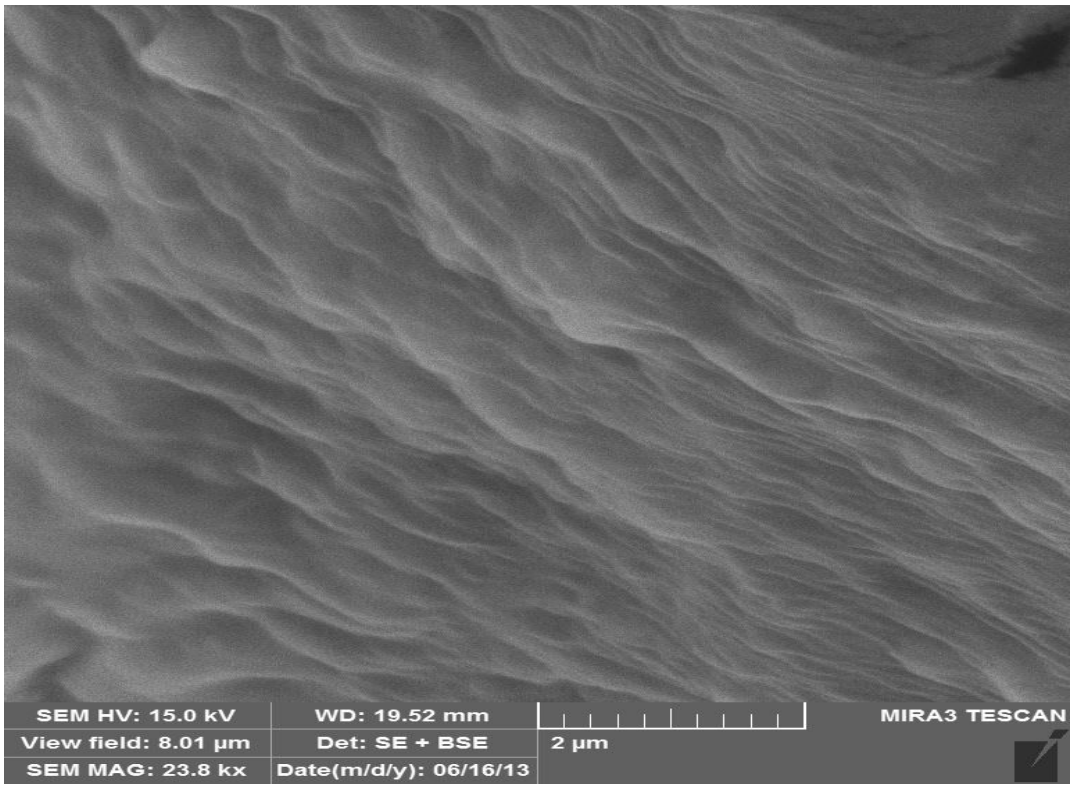

(a)

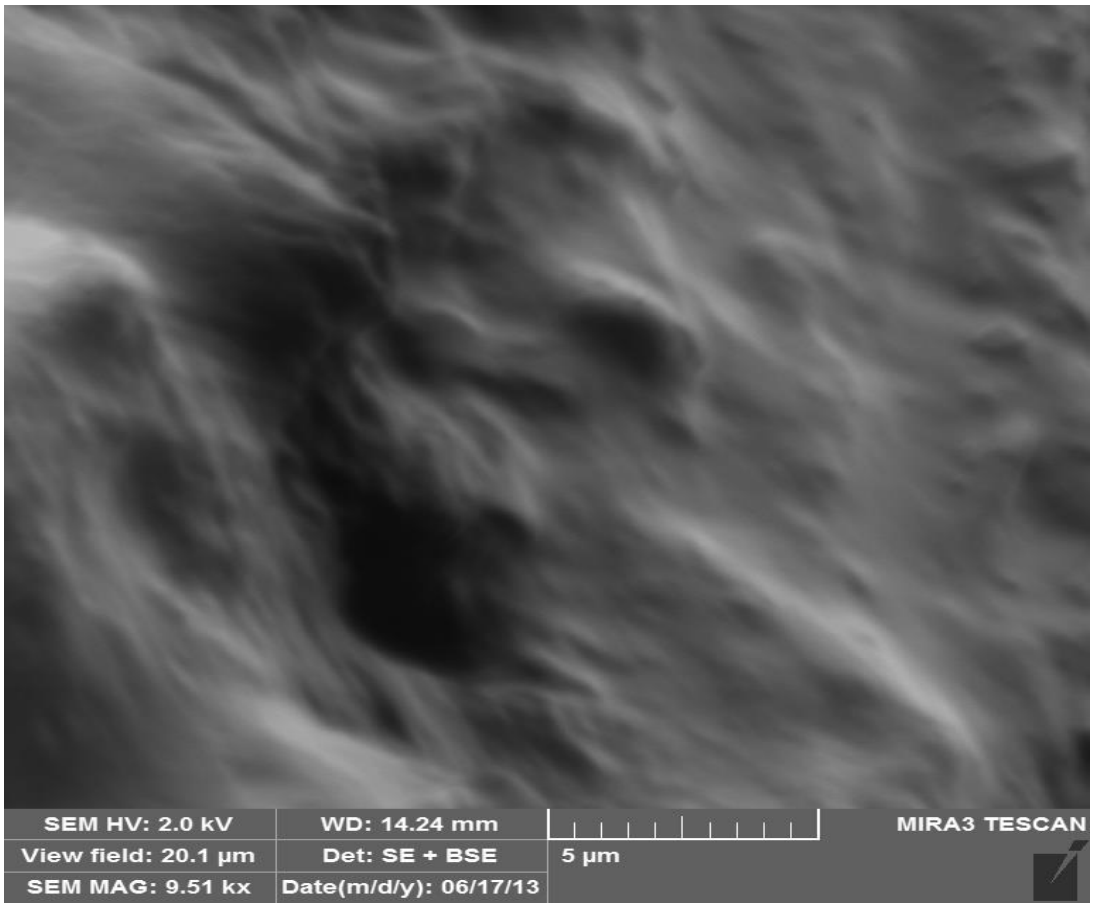
SEM HV: 2.0 kV
WD: 14.24 mm
MIRA3 TESCAN
View field: 20.1 µm
Det: SE + BSE
5 µm
SEM MAG: 9.51 kx
Date(m/d/y): 06/17/13

(b)

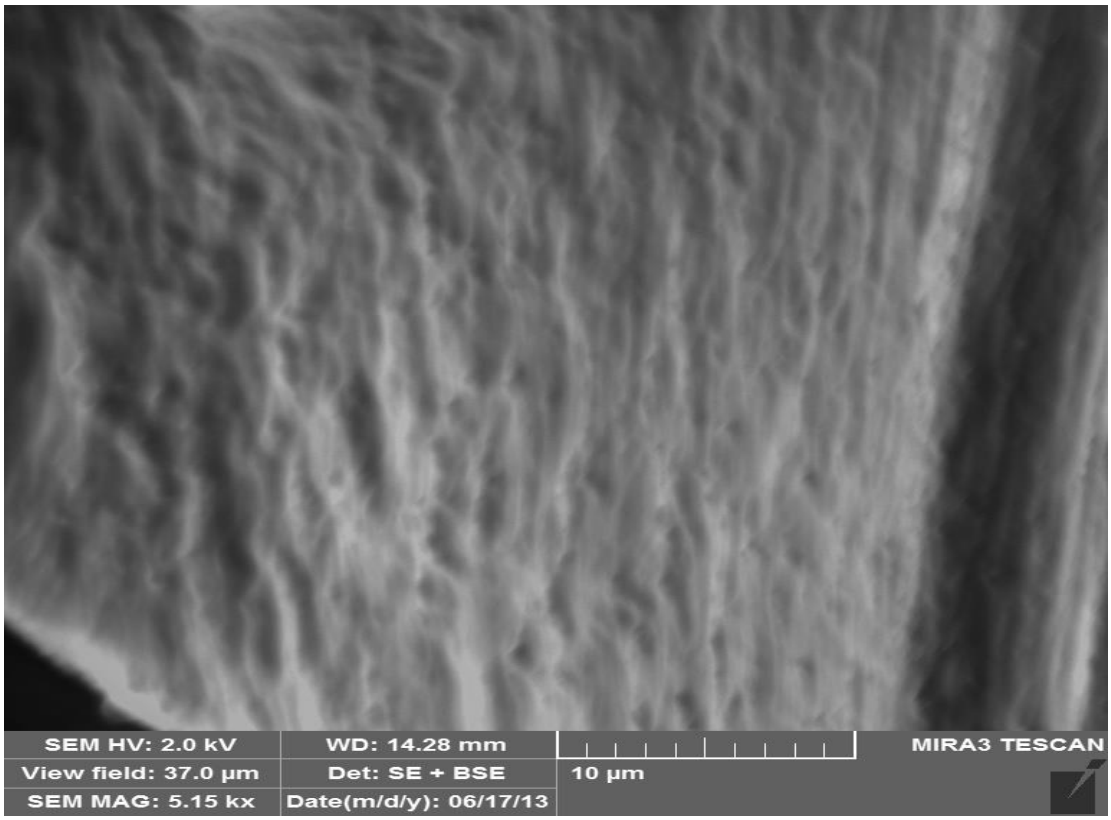
SEM HV: 2.0 kV
WD: 14.28 mm
MIRA3 TESCAN
View field: 37.0 µm
Det: SE + BSE
10 µm
SEM MAG: 5.15 kx
Date(m/d/y): 06/17/13

(c)

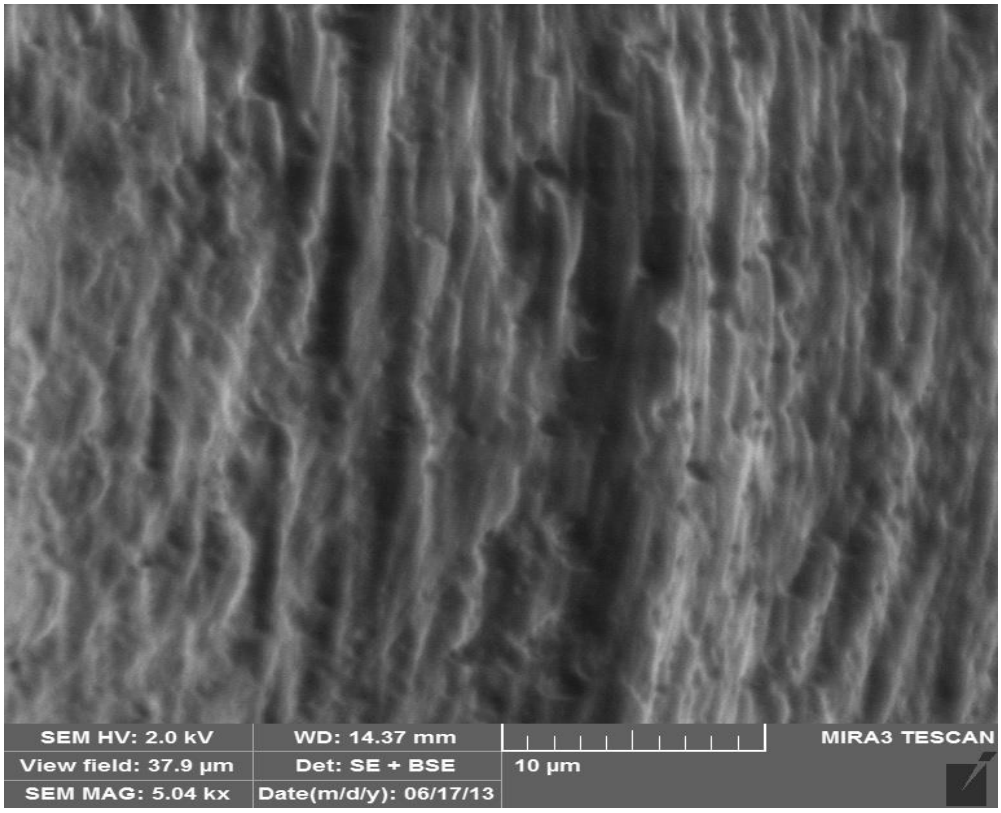

(d)

Figure 6-4: SEM Images of polyethylene nanocomposites: (a) control, (b) 5 mg TiO_2/W, (c) 10 mg TiO_2/W and (d) 15 mg TiO_2/W.

6.5 Crystallization Kinetic Model

The effect of nanofillers on the crystallization kinetics of polyethylene and polyethylene nanocomposites was studied using nonisothermal Avrami-Erofeev crystallization model as reported by Atiqullah et al., using cooling rate of 10°C/min [51]. The nonisothermal Avrami-Erofeev crystallization rate equation is given by:

$$\frac{d\alpha(T)}{dT} = \frac{k_0}{\beta} \times exp\left[-\frac{E_a^A}{R}\left(\frac{1}{T} - \frac{1}{T_0}\right)\right] \times n(1-\alpha(T))[-ln(1-\alpha(T))]^{\frac{n-1}{n}} \quad (6\text{-}1)$$

Where:

$$f(\alpha(T)) = n(1-\alpha(T))[-ln(1-\alpha(T))]^{\frac{n-1}{n}} \quad (6\text{-}2)$$

$$k'(T) = k_0 \times exp\left[-\frac{E_a^A}{R}\left(\frac{1}{T} - \frac{1}{T_0}\right)\right] \quad (6\text{-}3)$$

$$E_a^A(\text{apparent crystallization energy}) = E_{grow} - E_{nucl} \quad (6\text{-}4)$$

$$k_0 = \left(\frac{K_s N_0}{V_0}\right)\frac{k_{grow,0}}{k_{nucl,0}} \quad (6\text{-}5)$$

$$k_{grow}(T) = k_{grow,0} \times exp\left[-\frac{E_{grow}}{R}\left(\frac{1}{T} - \frac{1}{T_0}\right)\right] \quad (6\text{-}6)$$

$$k_{nucl}(T) = k_{nucl,0} \times exp\left[-\frac{E_{nucl}}{R}\left(\frac{1}{T} - \frac{1}{T_0}\right)\right] \quad (6\text{-}7)$$

$$\alpha(T) = \frac{\alpha_w(T)}{\alpha_w(T) + {}^{\rho_c}/_{\rho_a}[1-\alpha_w(T)]} \quad (6\text{-}8)$$

E_{grow} and E_{nucl} are the corresponding activation energies and $f(\alpha(T))$ is Avrami-Erofeev nonisothermal crystallization function. *n* is the dimension of the growing crystal.

V_0 represents the initial volume of the molten polymer. N_0 represents the number of germ nuclei. K_s is the shape factor for the growing nuclei. $k_{grow,0}$ and $k_{nucl,0}$ represent the frequency factors for crystal growth and nucleation respectively. $k_{grow}(T)$ and $k_{nucl}(T)$ follow the Arrhenius form [52, 53]. T_0 is the reference temperature. ρ_c and ρ_a are the densities of the crystalline and amorphous phases, respectively. The values reported for polyethylene are ρ_c = 1.004 g/mL and ρ_a = 0.853 g/mL [51].

$\alpha_w(T)$ can be found from the data of a constant cooling rate (second cycle) of nonisothermal DSC experiment.

$$\alpha_w(T) = \frac{\Delta H(T)}{\Delta H_{total}} = \frac{\int_{T_0}^{T}\left(\frac{dH}{dT}\right)dT}{\int_{T_0}^{T_\infty}\left(\frac{dH}{dT}\right)dT} \quad (10)$$

Where $\Delta H(T)$ is the enthalpy corresponding to temperature T of crystallization . ΔH_{total} represents the maximum enthalpy obtained at the end of the nonisothermal crystallization process. T_0 and T_∞ represent the initial and the final temperatures of crystallization, respectively.

6.5.1 Numerical solution of the crystallization kinetics

The non-linear model system was solved using NonLinearModelFit of MATHEMATICA. The performance of the crystallization kinetics model was evaluated based on coefficient of determination (R^2), 95% confidence interval, standard error and the variance. The kinetics model parameters are shown in Table 6-2. Figure 6-5 (a, b, c and d) shows a comparison between the experimental and model predicted of relative crystallinity profiles (α) of the polyethylene nanocomposites as a function of temperature using (0, 5, 10 and 15) mg of the TiO_2/W nanofillers.

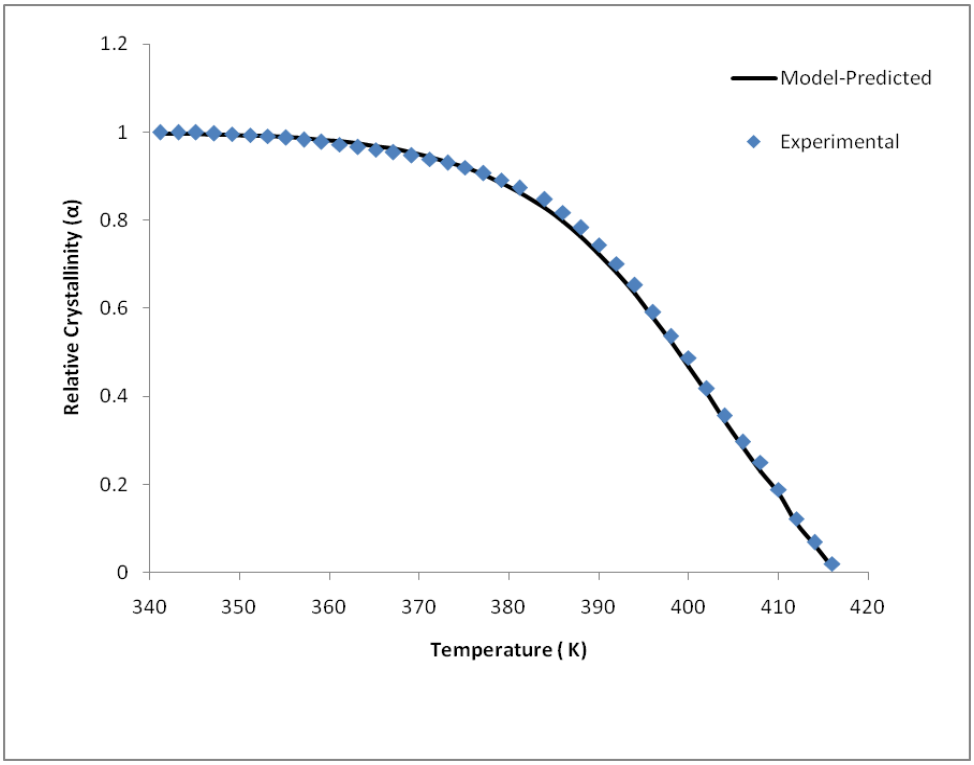
1.2
1
0.8
0.6
0.4
0.2
0
Relative Crystallinity (α)
340
350
360
370
380
390
400
410
420
Temperature (K)
Model-Predicted
Experimental

(a)

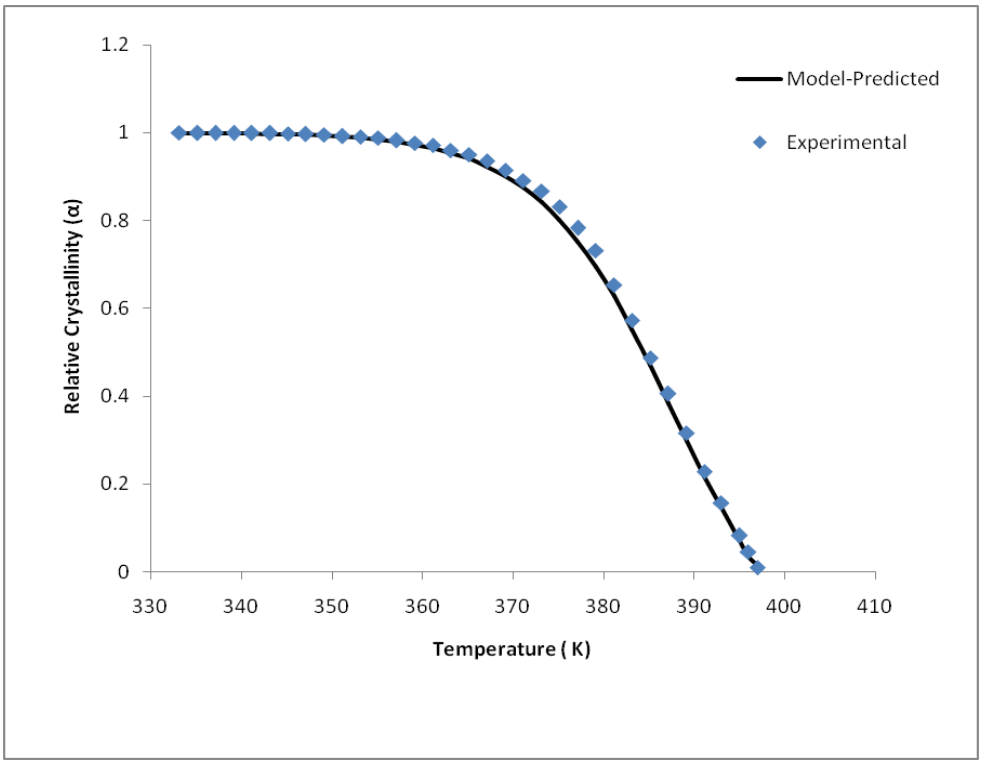
1.2
1
0.8
0.6
0.4
0.2
0
Relative Crystallinity (α)
330
340
350
360
370
380
390
400
410
Temperature (K)
Model-Predicted
Experimental

(b)

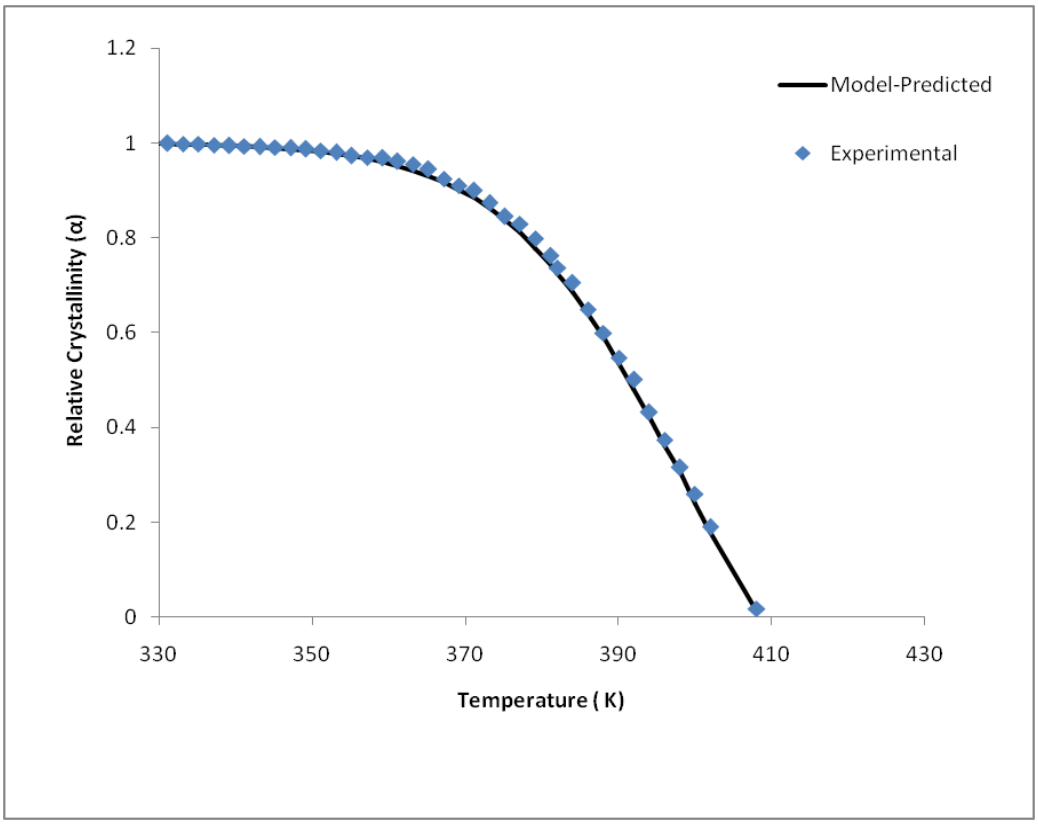
1.2
1
0.8
0.6
0.4
0.2
0
330
350
370
390
410
430
Relative Crystallinity (α)
Temperature (K)
Model-Predicted
Experimental

(c)

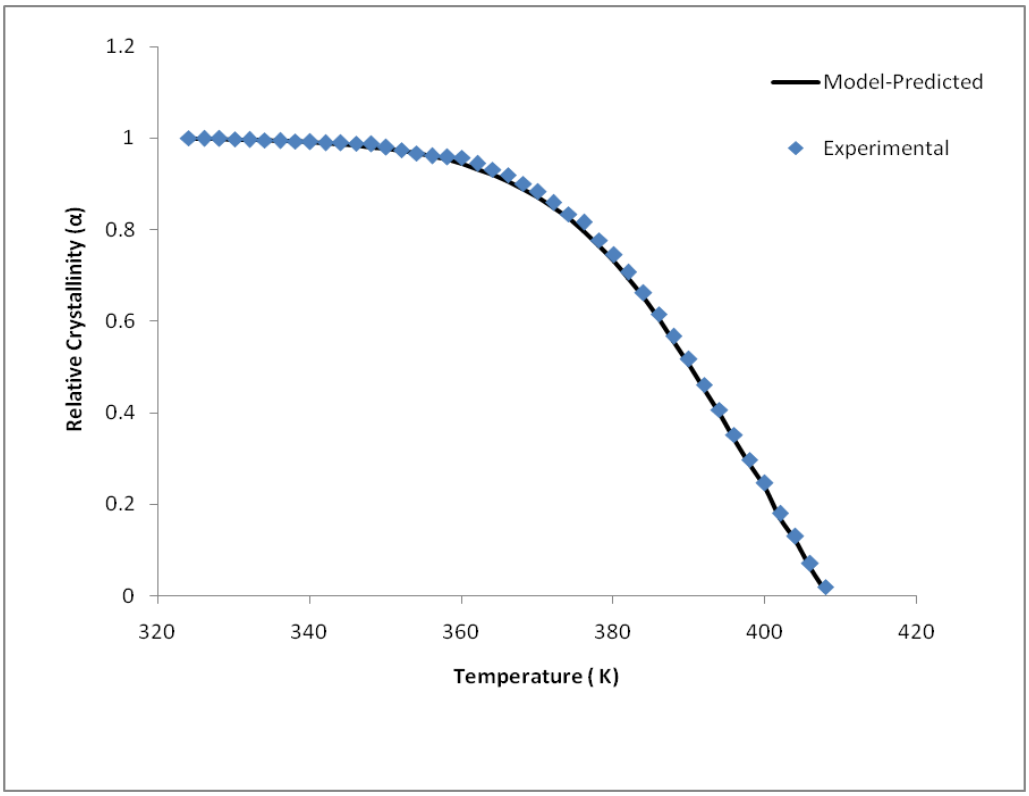

(d)

Figure 6-5: Comparison of model-predicted relative crystallinity with the experimental data as a function of DSC cooling temperature for PE: (a) control (b) 5 mg TiO_2/W (c) 10 mg TiO_2/W (d) 15 mg TiO_2/W.

The values of Avrami-Erofeev (*n)* varied from 2.1 to 3.9 for polyethylene nanocomposites. When the TiO_2/W nanofillers were added, (*n)* values were increased. The increasing in *n* values indicates that the crystal growth becomes more complex and has complicated growth mechanism [54, 55]. The highest value of *n* was noticed by using 15 mg of the TiO_2/W nanofiller (*n*=3.9) as shown in Table 6-2, Entry 4. This high value of *n* can be attributed to the increase in the crystallinity and the molecular weight (M_w). The crystallization frequency factor k_0 (s^{-1}) changed slightly. The apparent activation energy E_a varied from 19.1 to 46.8 kJ/mol. The low values of E_a indicate the simplicity of crystallization process. The variation in E_a values can be attributed to the variation in the structural defect of the polymer backbones [51].

Table 6-2: Model-predicted non-isothermal crystallization kinetics parameters of polyethylene nanocomposites

Entry No.	**Filler (mg)**	***n***	E_a **(kJ/mol)**	k_0 **(s^{-1})**	R^2
1.	0	2.1	46.8	0.112	0.991
2.	5	3.7	33.9	0.194	0.990
3.	10	3.8	24.5	0.135	0.991
4.	15	3.9	19.1	0.130	0.992

Conclusions

Polyethylene and polyethylene nanocomposites were produced using a vanadium (III) complex bearing salicylaldiminato ligands in the presence of TiO_2/W nanofiller. The molecular weight (M_w) and catalyst activity were found to increase by adding TiO_2/W nanofiller. The maximum molecular weight (M_w) and catalyst activity were achieved by using 10 and 15 mg of the TiO_2/W nanofillers respectively. Non-isothermal crystallization kinetics of polyethylene and polyethylene nanocomposites were well fitted with Avrami-Erofeev model.

Acknowledgment

The authors wish to acknowledge the assistance of Deanship of Scientific Research, King Fahd University of Petroleum and Minerals for their support for providing adequate funds and infrastructure under Project no. IN101018.

References

1. Velikova, M., European Polymer Journal, 2001. **37**(6): p. 1255-1262.
2. Li, S.B., Albert H, Journal Of Bone & Joint Surgery American Volume, 1994. **76**((7)): p. 1080-1090.
3. Kurtz, S.M., et al., Biomaterials, 1999. **20**(18): p. 1659-1688.
4. Simis, K.S., et al., Biomaterials, 2006. **27**(9): p. 1688-1694.
5. Minkova, L., M. Velikova, and D. Damyanov, European Polymer Journal, 1988. **24**(7): p. 661-665.
6. Jeon, H.G., et al., Polymer Bulletin, 1998. **41**(1): p. 107-113.
7. Zhao, C., et al., Polymer Degradation and Stability, 2005. **87**(1): p. 183-189.
8. Gopakumar, T.G., et al., Polymer, 2002. **43**(20): p. 5483-5491.
9. Zanetti, M., P. Bracco, and L. Costa, Polymer Degradation and Stability, 2004. **85**(1): p. 657-665.
10. Shin, S.-Y.A., et al., Polymer, 2003. **44**(18): p. 5317-5321.
11. Wang, J., et al., Macromolecular Rapid Communications, 2001. **22**(17): p. 1422-1426.
12. Alexandre, M., et al., Polymer, 2002. **43**(8): p. 2123-2132.
13. Yang, F., et al., Journal of Applied Polymer Science, 2003. **89**(13): p. 3680-3684.
14. Jin, Y.-H., et al., Macromolecular Rapid Communications, 2002. **23**(2): p. 135-140.
15. Wei, L., T. Tang, and B. Huang, Journal of Polymer Science Part A: Polymer Chemistry, 2004. **42**(4): p. 941-949.
16. Kuo, S.-W., et al., Polymer, 2003. **44**(25): p. 7709-7719.

17. Rossi, G.B., et al., Nano Letters, 2002. **2**(4): p. 319-323.

18. Verbeek, C.J.R., Materials Letters, 2002. **56**(3): p. 226-231.

19. Nawang, R., et al., Polymer Testing, 2001. **20**(2): p. 167-172.

20. Huang, Y.Q., Y.Q. Zhang, and Y.Q. Hua, Journal of Materials Science Letters, 2003. **22**(14): p. 997-998.

21. Verbeek, C.J.R., Materials Letters, 2002. **52**(6): p. 453-457.

22. Danjaji, I.D., et al., Polymer Testing, 2002. **21**(1): p. 75-81.

23. Mandal, T.K., M.S. Fleming, and D.R. Walt, Nano Letters, 2002. **2**(1): p. 3-7.

24. Nussbaumer, R.J., et al., Macromolecular Materials and Engineering, 2003. **288**(1): p. 44-49.

25. Wang, Z., et al., Macromolecular Chemistry and Physics, 2005. **206**(2): p. 258-262.

26. Chen, X.D., et al., Polymer Testing, 2007. **26**(2): p. 202-208.

27. Owpradit, W. and B. Jongsomjit, Materials Chemistry and Physics, 2008. **112**(3): p. 954-961.

28. Jongsomjit, B., E. Chaichana, and P. Praserthdam, Journal of Materials Science, 2005. **40**(8): p. 2043-2045.

29. Kontou, E. and M. Niaounakis, Polymer, 2006. **47**(4): p. 1267-1280.

30. Chaichana, E., B. Jongsomjit, and P. Praserthdam, Chemical Engineering Science, 2007. **62**(3): p. 899-905.

31. Li, K.-T., C.-L. Dai, and C.-W. Kuo, Catalysis Communications, 2007. **8**(8): p. 1209-1213.

32. KUO, et al., Vol. 90. 2005, Lausanne, SUISSE: Elsevier. 11.

33. Desharun, C., B. Jongsomjit, and P. Catalysis Communications, 2008. **9**(4): p. 522-528.

34. Jongsomjit, B., et al., Iranian Polymer Journal (English Edition), 2006. **15**(5): p. 433-439.

35. Jongsomjit, B., J. Panpranot, and P. Praserthdam, Materials Letters, 2007. **61**(6): p. 1376-1379.

36. Titelman, G.I., et al., Polymer Degradation and Stability, 2002. **77**(2): p. 345-352.

37. Turton, T.J. and J.R. White, Polymer Degradation and Stability, 2001. **74**(3): p. 559-568.

38. Wang, Z., et al., Composite Interfaces, 2006. **13**(7): p. 623-632.

39. Supaphol, P., et al., Polymer Testing, 2007. **26**(1): p. 20-37.

40. Schroeder, R., L.A. Majewski, and M. Grell, Advanced Materials, 2005. **17**(12): p. 1535-1539.

41. Parvatikar, N. and M.V.N. Ambika Prasad, Journal of Applied Polymer Science, 2006. **100**(2): p. 1403-1405.

42. Badheka, P., et al., Journal of Applied Polymer Science, 2006. **99**(5): p. 2815-2821.

43. Guo, N., et al., Journal of the American Chemical Society, 2007. **129**(4): p. 766-767.

44. Owpradit, W., et al., Polymer Bulletin, 2011. **66**(4): p. 479-490.

45. Nandi, D., et al., Materials Research Bulletin, 2012. **47**(8): p. 2095-2103.

46. Kurtz, S.M., *Chapter 17 - Composite UHMWPE Biomaterials and Fibers*, in *UHMWPE Biomaterials Handbook (Second Edition)*, M.K. Steven and P.D. Ph.D.A2 - Steven M. Kurtz, Editors. 2009, Academic Press: Boston. p. 249-258.

47. Abdul Kaleel, S.H., et al., Journal of Industrial and Engineering Chemistry, 2012. **18**(5): p. 1836-1840.

48. Wu, J.-Q., et al., *Synthesis*, Organometallics, 2008. **27**(15): p. 3840-3848.

49. Kumbhar, A. and G. Chumanov, Journal of Nanoparticle Research, 2005. **7**(4): p. 489-498.

50. Soares, J.B.P. and S. Anantawaraskul, Journal of Polymer Science Part B: Polymer Physics, 2005. **43**(13): p. 1557-1570.

51. Atiqullah, M., et al., AIChE Journal, 2013. **59**(1): p. 200-214.

52. Routray, K. and G. Deo, AIChE Journal, 2005. **51**(6): p. 1733-1746.

53. Hossain, M.M. and H.I. de Lasa, AIChE Journal, 2007. **53**(7): p. 1817-1829.

54. Al-Mulla, A., et al., Composites Part A: Applied Science and Manufacturing, 2008. **39**(2): p. 204-217.

55. Hao, W., et al., Polymer Testing, 2010. **29**(4): p. 527-533.

Chapter 7

New Method to produce polyolefins adhesive

Abstract

For the first time, pressure sensitive adhesives (PSAs) were produced by copolymerization of ethylene and propylene copolymerization using a special catalyst with methyl aluminoxane (MAO) as a cocatalyst. Three different molar feed ratios (50:50, 60:40 and 40:60) of ethylene/propylene (E/P) respectively, were used to investigate the adhesion properties of producing copolymer and the results showed the molar feed ratio (50:50) of (E/P) resulted in producing the highest adhesion properties. Besides investigation of the adhesion properties, molecular weight (M_w), copolymer composition, crystallinity and thermal characteristics of ethylene/propylene adhesive copolymers were studied.

Keywords: ethylene/propylene copolymer, pressure sensitive adhesives , adhesive.

7.1 Introduction

The copolymers of ethylene with higher olefins are vital commercial products. The structure and copolymer composition are supposed to depend on the catalyst characteristics, like homogeneity and stereospecificity. The studies found that the physical properties of ethylene-propylene (EP) copolymers are strongly dependent upon on the number of chemically inverted propylene units and the monomer sequence distribution [1,2].

Ethylene/propylene copolymerization has been carried out by using different catalysts such Zeigler-Natta catalyst, postmetallocene and metallocene catalysts, FI catalysts [3-6].

Recently, diimine nickel and palladium catalysts were found to be promising systems for the homo polymerization and copolymerization of ethylene producing highly branched , high molecular weight, amorphous or linear semi-crystalline materials due to chain-walking mechanism [7-11]. Decreasing polymerization temperature or pressure resulted in a decrease in the degree of branching and increasing the crystallinity and melting temperature of polymer [12].

A huge increase in activity was obtained when diethylaluminum chloride (DEAC) and 1,3-dichloro-1,3-diisobutyldialuminoxane (DCDAO) was used for ethylene and propylene polymerizations in the presence of Ni(II) -diimine complexes compared to polymethylaluminoxane (MAO) [13].

Zahed et al., used a-Diimine nickel dibromide complexes of dibromo[N,N'-bis(2,6-diisopropylphenyl)- 2,3-butanediimine] nickel(II) and dibromo[N,N'-

(phenanthrene-9,10-diylidene)bis(2,6-diisopropylaniline)] nickel(II) to copolymerize ethylene and propylene and found polymers had similar properties with ethylene-propylene copolymer and copolymer with more rubber-like behavior [14, 15].

Adhesives are substances could be either natural or synthetic existing in liquid or semi-liquid that bonds or adhere objects together. Several mechanisms of adhesion have been proposed like mechanical interlocking [16], electronic theory [17], theory of boundary layers and interphases[18], diffusion theory [19] and chemical bonding theory [20, 21]. Adhesives are classified due to method of adhesion into different types such as drying adhesives, contact adhesives, hot adhesives and pressure sensitive adhesives [22, 23]. There are many types of polymeric adhesives: natural rubber [24], polysulfide [25], polyurethane [25], polyvinyl acetate [26, 27], ethylene-vinyl acetates [28], unsaturated polyester [29] and epoxy [30, 31].

Adhesives are used in wood industry, electronic industry, drug delivery, dentistry and automotive industry [23].

Pressure sensitive adhesives PSAs (self adhesives) are adhesives that are able to form bonds on surfaces by applying light pressure. No heat, solvent or water required to stimulate the adhesive. They are classified to three major products: solvent based, water based and hot melt [23].

In this study, we have used special catalyst (CAT1) to produce ethylene/ propylene copolymer adhesives using MAO as a cocatalyst. The molecular weight (M_w), copolymer composition, crystallinity and thermal characteristics of polyethylene/polypropylene adhesives were investigated

7.2 Experimental Methods

7.2.1 Materials

Premixed ethylene and propylene gas mixtures were purchased from SIGAS with three different molar ratios (50:50 , 60:40 and 40:60) of ethylene and propylene respectively. All materials were purchased from Sigma Aldrich and used without additional purification. All manipulations were carried out under N_2 using standard Schlenk and glove box techniques.

7.2.2 Copolymerization

Ethylene/propylene copolymerization was carried out in a 250 mL round-bottom flask equipped with a magnetic stirrer. A 7.1 mg of the catalyst was added to the flask and the reactor was filled with 80 mL of toluene. Then, the flask was immersed in oil bath and when reactor temperature was equilibrated with bath oil temperature (30 ^{o}C), nitrogen gas was removed using pump vacuum. Then ethylene/propylene was fed into the reactor .After 10 minutes of saturation of ethylene/propylene in toluene, 3 ml of the cocatalyst (MAO) was introduced into the reactor and then copolymerization was started. Copolymerization reaction was quenched by adding 250 ml of methanol containing HCl (5 vol. %). Finally, the copolymer was washed with an excess amount of methanol and put inside an oven at 50 ^{o}C for 24 hours for drying.

7.3 Characterization

7.3.1 DSC Analysis

Melting temperature (T_m) and transition temperature (T_g) of ethylene/propylene adhesive copolymers was measured by differential scanning calorimetry (DSC) from TA instruments Q1000.

7.3.2 CRYSTAF analysis

Crystallization analysis fractionation (CRYSTAF) (Polymer Char, Spain) of adhesive copolymers was performed using an IR detector in 1, 2, 4-trichlorobenzene in a stainless-steel stirred vessels of 50-ml volume and the crystallization rate was 0.2°C/min.

7.3.3 NMR analysis

^{13}C NMR was used to determine the composition of ethylene/propylene (E/P) adhesive copolymer using Bruker AVANCE III-600 and 1, 2, 4-trichlorobenzene as a solvent.

7.3.4 GPC Analysis

Molecular weight and intrinsic viscosity (IV) of polyethylene/polypropylene adhesive were determined by Triple Detection High Temperature Gel Permeation Chromatography (TDHT-GPC) using 1, 2, 4-trichlorobenzene as a solvent. 25mg of the material was placed into a 40ml glass vial and accurately weighed and 10ml of the solvent was added using a clean 10ml glass pipette. The vial was capped with a Teflon coated cap and the samples were placed into the Vortex Auto Sampler and left to dissolve for 3hrs at 160°C while stirring gently.

7.3.5 Adhesive lap joint shear strength test

First, Two specimens, each 70 x 20 mm are bonded together with adhesive by applying adhesive over 20 mm x 20 mm of each aluminum substrate. Then, the specimens were compressed slightly using Carver 25-ton press by applying 1000 pounds load for 5 minutes to get uniform adhesive coverage. Finally, the test specimens were placed in the grips of a universal testing machine and pulled at 5 mm/min using LFPlus universal testing model.

7.4 Results and Discussion

The ethylene/propylene adhesive copolymers were prepared by in-situ polymerization in the presence of CAT1.

Mole percent of polypropylene (mol % PP) in ethylene/propylene adhesive copolymer was calculated as published by Cheng [32] using ^{13}C NMR as shown in Figure 7-1,2 and 3. Mole percent of polypropylene was calculated by using the following formulas:

$$mol\ \%\ of\ PP = \frac{2t}{s+t} = \frac{2p}{s+p} \qquad (7\text{-}1)$$

Where:

$$s = \sum_{ij} S_{ij} \qquad (7\text{-}2)$$

$$t = \sum_{ij} T_{ij} \qquad (7\text{-}3)$$

$$p = \sum_{ij} P_{ij} \qquad (7\text{-}4)$$

S, T, and P refer respectively to secondary (methylene), tertiary (methine), and primary (methyl) carbons. More details are available in the previous reference [32].

From ^{13}C NMR spectra, polypropylene percent was 42, 55 and 88 for 60:40, 50:50 and 40:60 of feed molar ratios of ethylene/propylene respectively (Table 7-1, Entry 1, 2 and 3) as shown in Figures 1, 2 and 3. Table 7-1 summarizes the results of the copolymerization characteristics:

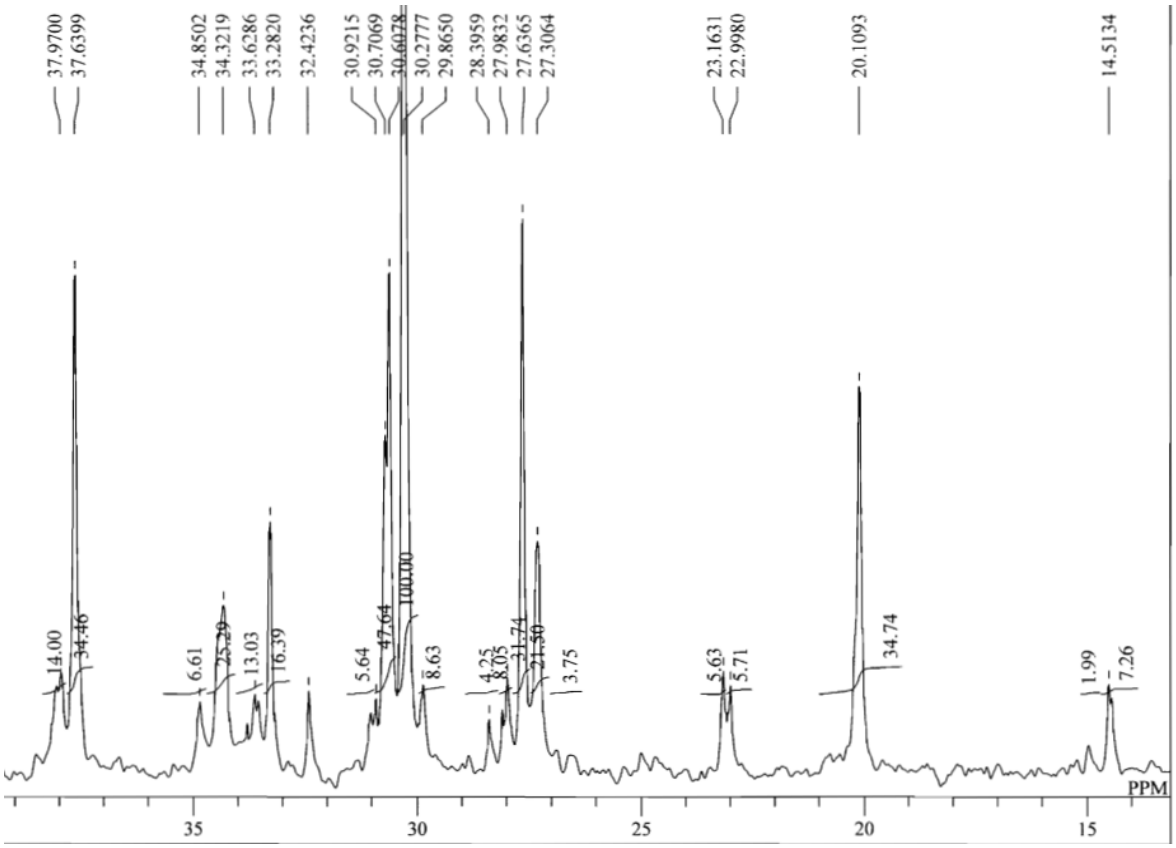

Figure 7-1: 13C NMR spectra of 60:40 feed molar ratio of (E/P) adhesive copolymer.

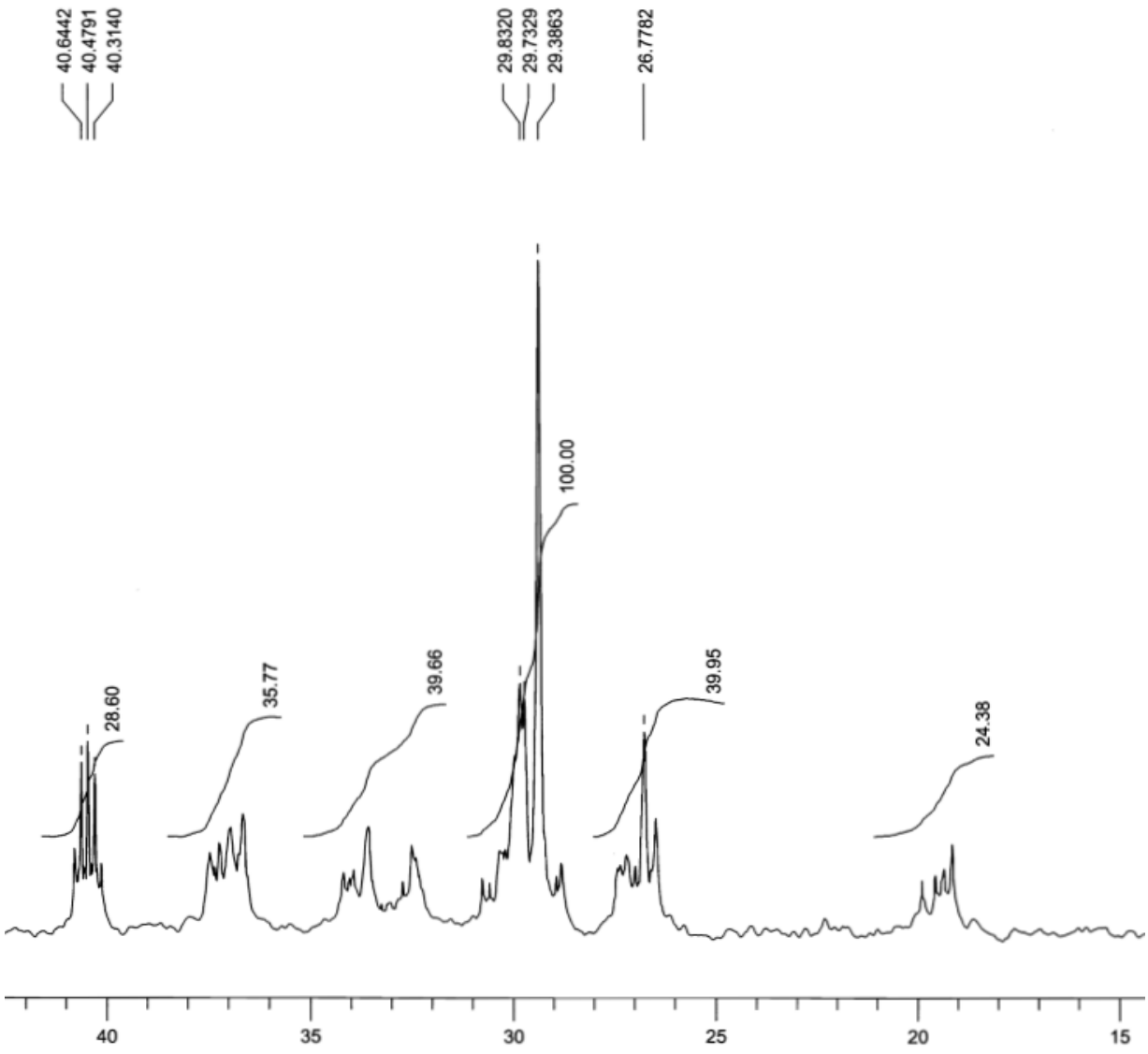

Figure 7-2: 13C NMR spectra of 50:50 feed molar ratio of (E/P) adhesive copolymer.

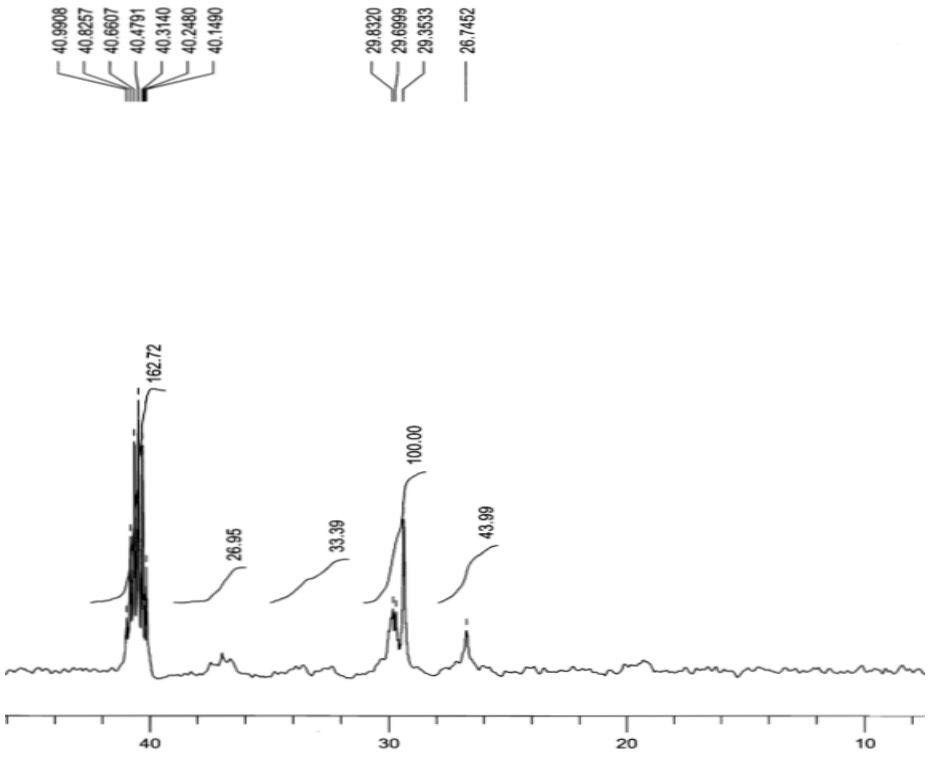

Figure 7-3: 13C NMR spectra of 40:60 feed molar ratio of (E/P) adhesive copolymer.

Table 7-1: Experimental conditions and properties of ethylene/propylene adhesive copolymers prepared by in situ copolymerization using CAT1catalyst and an MAO co-catalyst system at 1.3 bar.[a]

Entry No.	E/P mol/mol	mol % PP [b]	Tg[c] °C
1.	60:40	٤٢	- 65.56
٢.	50:50	٥٥	- 64.45
٣.	40:60	٨٨	- 63.85

[a] Copolymerization conditions: Toluene = 80 mL, Temp = 30°C, Time = 10 mins, Catalyst amount = 7.1 mg, cocatalyst amount= 3 ml, [b] Determined by ^{13}C NMR, [c] Determined by DSC.

Glass transition temperature (T_g) of ethylene/propylene adhesive copolymers was measured using DSC within different temperature ranges, from 30 °C to 160 °C, -30 °C to 60 °C but neither T_g nor T_m were observed .Finally, the cooling range was extended to -80 °C and the glass transition temperatures were observed as shown in Figure 7-4 . No melting temperature (T_m) was observed for all samples.

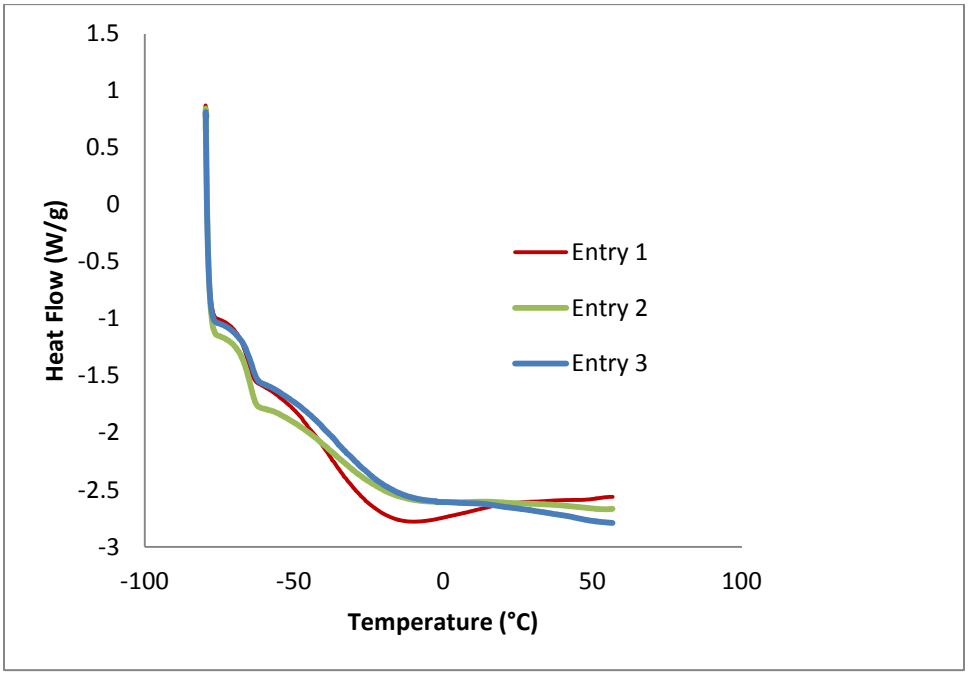

Figure 7-4: DSC profile of ethylene/propylene adhesive copolymers.

Crystallization analysis fractionation (Crystaf) was used to confirm the results obtained by ^{13}C NMR and DSC. Crystaf results showed that, ethylene/ propylene adhesive copolymers had amorphous structures as shown in Figure 7-5. Therefore, no melting temperatures (T_m) were noticed as shown in Figure 7-4 [33].

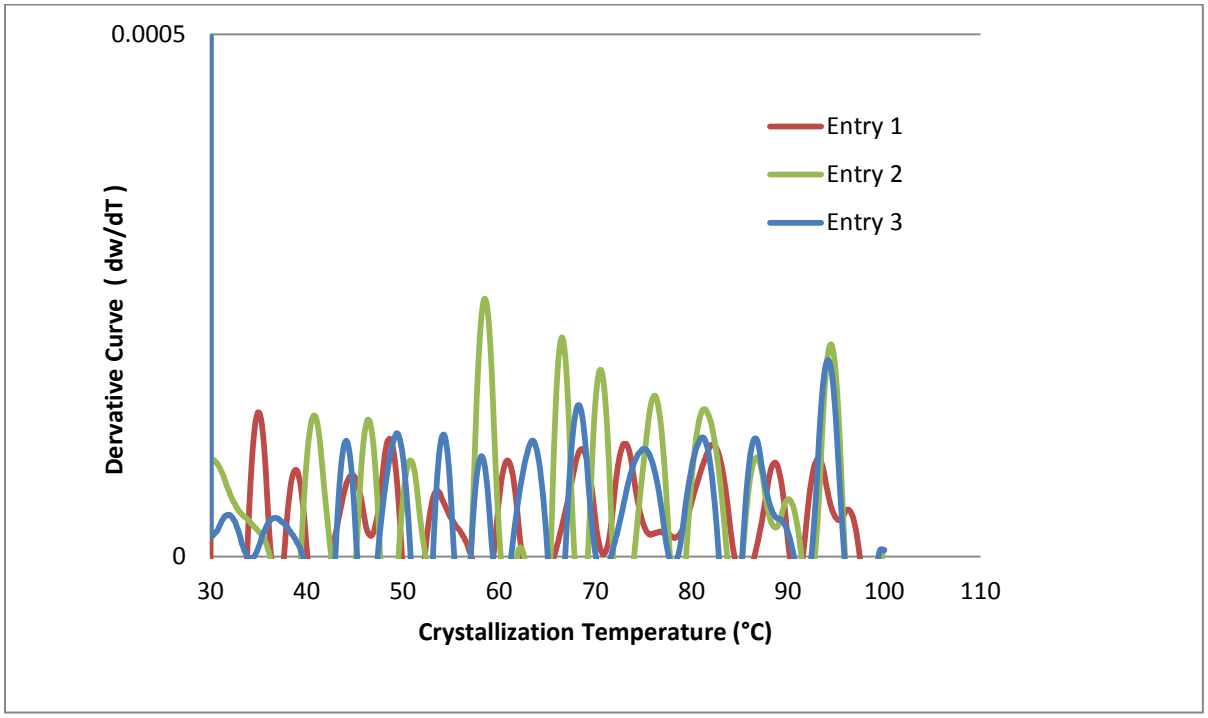

Figure 7-5: Differential crystallization analysis fractionation (Crystaf) profiles of ethylene/propylene adhesive copolymer.

From GPC results, low molecular weight of ethylene/propylene adhesive copolymer was obtained for all feed molar ratio of (E/P) (Table 7-2). Weight average molecular weight (M_w) was found to increase slightly with increase propylene feed ratio. Polydispersity index (PDI), which is the ratio of weight average molecular weight (M_w) to the number average molecular weight (M_n), was decreased by increasing the feed molar ratio of (E/P) (Table 7-2).

Table 7-2: GPC analysis of ethylene/propylene adhesive copolymers prepared by in situ copolymerization using CAT1 catalyst and an MAO co-catalyst system at 1.3 bar.[a]

Entry No.	E/P mol/mol	Mw (Daltons)	PDI
1.	60:40	24,917	2.4510
٢.	50:50	27,821	1.8390
٣.	40:60	33,314	1.7590

[a] Copolymerization conditions: Solvent toluene = 80 mL, Temp = 30 ^{o}C, Time = 10 mins, Catalyst amount = 7.1 mg, cocatalyst amount= 3 ml.

Adhesive lap joint shear strength test was performed to prove the adhesive characteristics of ethylene /propylene adhesive copolymer as shown in Figure 7-6 and 7. The results showed that there is an optimum molecular gives the maximum cohesive and adhesive strength. The shear strength was increased with increase the molecular weight up to 27,821 Daltons and then decreased. The maximum load was increased from 8.8 N (Table 7-2, Entry 1) to 11.2 N (Table 7-2, Entry 2) and then decreased to 6.4 N (Table 7-2, Entry 3). The weak adhesive strength of highest molecular weight can be contributed from the weak wettability [24]. The type of failure was cohesive.

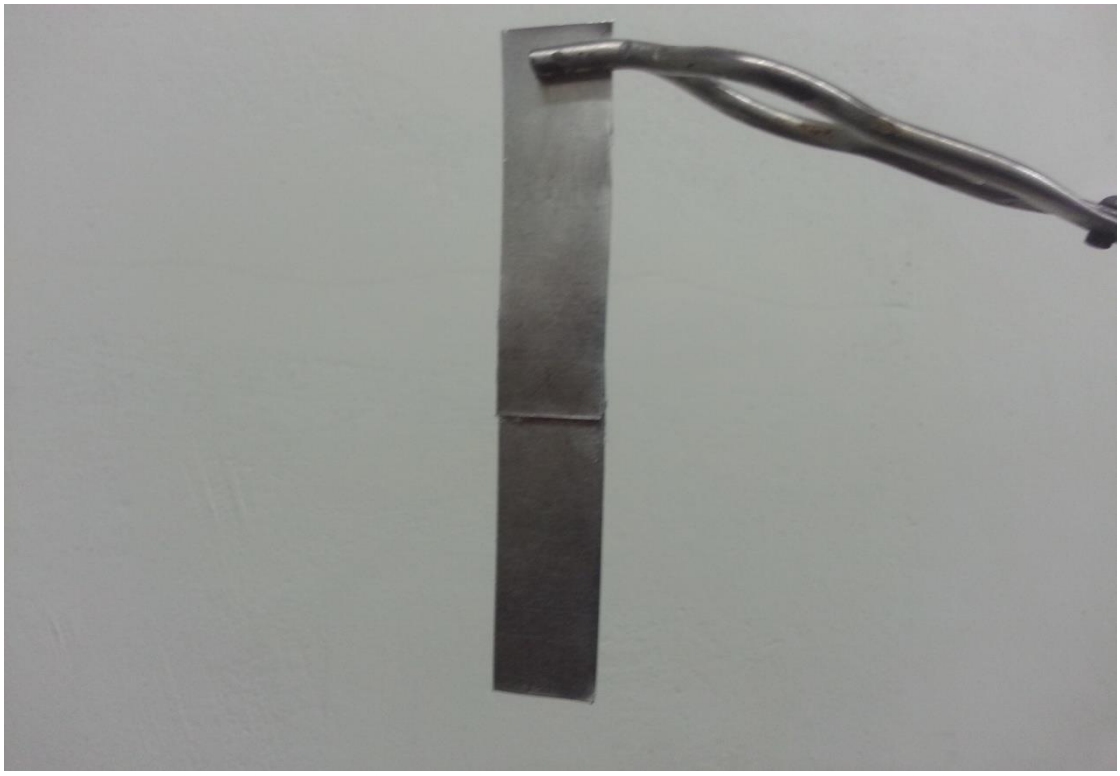

Figure 7-6: A photo of aluminum substrates joined using ethylene /propylene adhesive copolymer.

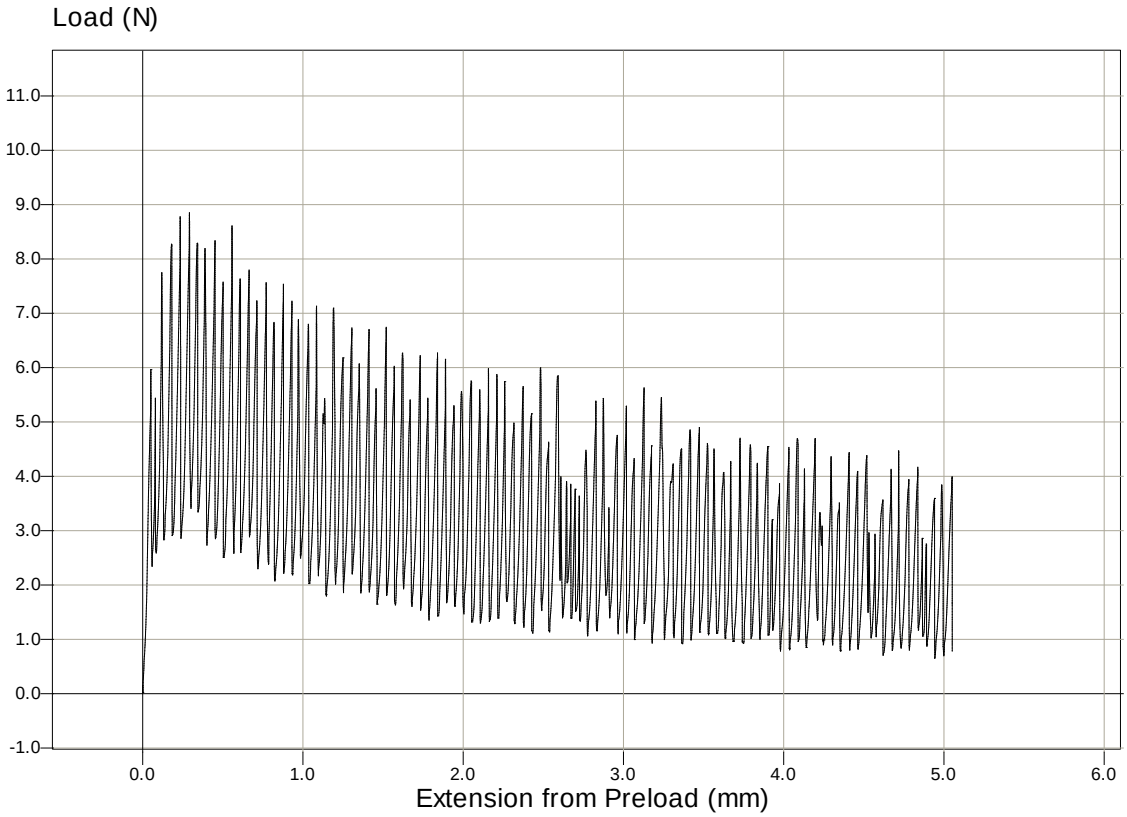
Load (N)
11.0
10.0
9.0
8.0
7.0
6.0
5.0
4.0
3.0
2.0
1.0
0.0
-1.0
0.0
1.0
2.0
3.0
4.0
5.0
6.0
Extension from Preload (mm)

(a)

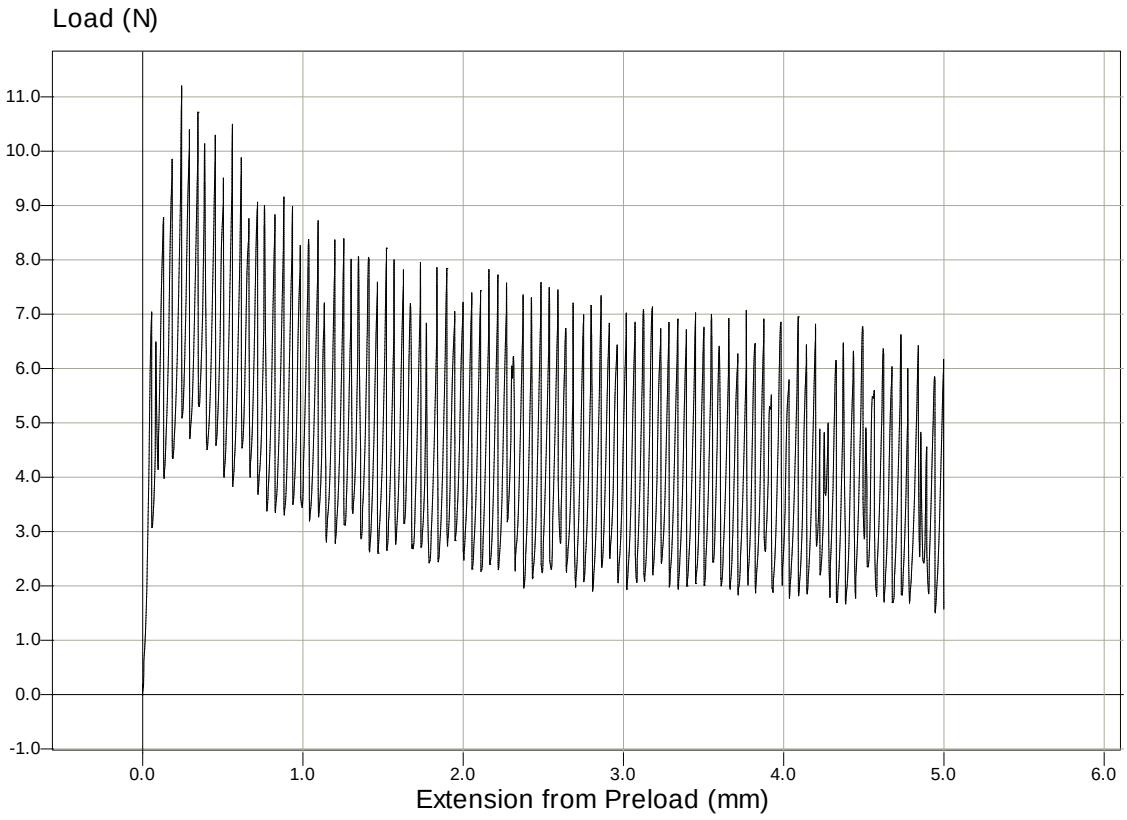
Load (N)
11.0
10.0
9.0
8.0
7.0
6.0
5.0
4.0
3.0
2.0
1.0
0.0
-1.0
0.0
1.0
2.0
3.0
4.0
5.0
6.0
Extension from Preload (mm)

(b)

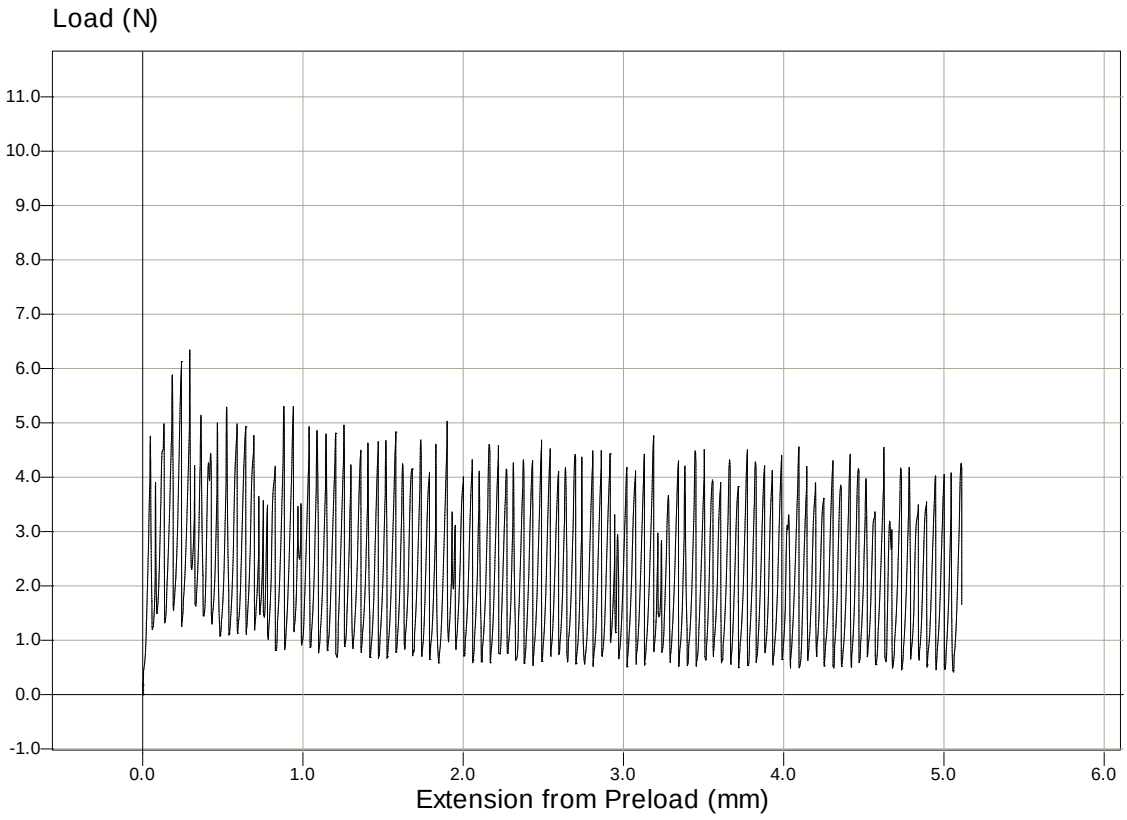

(c)

Figure 7-7: Adhesive lap joint shear strength test of (a) 60:40 E/P (b) (50:50) E/P (c) 40:60 E/P.

Conclusions

A special catalyst was synthesized and used to produce polyethylene/polypropylene pressure sensitive adhesives by copolymerization of ethylene and propylene in the presence of MAO as a cocatalyst. The produced pressure sensitive adhesives are totally amorphous and no melting temperatures were observed. The molecular weight M_w was found to increase when the molar feed ratio of ethylene/propylene increased. Maximum adhesive characteristics were achieved by using the molar feed ratio (50:50) of ethylene/propylene.

References

1. Busico, V. and R. Cipullo, Progress in Polymer Science, 2001. **26**(3): p. 443-533.
2. Kaminsky, W., Macromolecular Chemistry and Physics, 1996. **197**(12): p. 3907-3945.
3. Jiang, T., et al., Chinese Journal of Polymer Science, 2011. **29**(4): p. 475-482.
4. Dias, M.L., D.E.B. Lopes, and A.V. Grafov, Journal of Molecular Catalysis A: Chemical, 2002. **185**(1–2): p. 57-64.
5. Stephens, C.H., et al., Journal of Applied Polymer Science, 2006. **100**(2): p. 1651-1658.
6. Matsui, S. and T. Fujita, Catalysis Today, 2001. **66**(1): p. 63-73.
7. Johnson, L.K., C.M. Killian, and M. Brookhart, Journal of the American Chemical Society, 1995. **117**(23): p. 6414-6415.
8. Brookhart, M., et al., American Chemical Society, Polymer Preprints, Division of Polymer Chemistry, 1996. **37**(1): p. 254-255.
9. Killian, C.M., et al., Journal of the American Chemical Society, 1996. **118**(46): p. 11664-11665.
10. Laine, T.V., et al., Macromolecular Rapid Communications, 1999. **20**(9): p. 487-491.
11. Li, L., M. Jeon, and S.Y. Kim, Journal of Molecular Catalysis A: Chemical, 2009. **303**(1–2): p. 110-116.
12. AlObaidi, F., Z. Ye, and S. Zhu, Polymer, 2004. **45**(20): p. 6823-6829.
13. Maldanis, R.J., et al., Journal of Organometallic Chemistry, 2002. **645**(1–2): p. 158-167.

14. Pourtaghi-Zahed, H. and G.H. Zohuri, Polymer Bulletin, 2013.

15. Pourtaghi-Zahed, H. and G. Zohuri, Journal of Polymer Research, 2012. **19**(11): p. 1-8.

16. Gent, A.N. and J. Schultz, The Journal of Adhesion, 1972. **3**(4): p. 281-294.

17. B.V., D., Research 8, 1955. **70**.

18. Gaylord, N.G. and H. Dannenberg, *J. J. BIKERMAN. Academic Press, New York, 1961*. Journal of Polymer Science, 1962. **62**(173): p. S21-S21.

19. Voyutskii, S.S., *Autohesion and Adhesion of High Polymers*. 1963, New York: wiley-interscience.

20. Ahagon, A. and A.N. Gent, Journal of Polymer Science: Polymer Physics Edition, 1975. **13**(7): p. 1285-1300.

21. Brown, H.R., Macromolecules, 1991. **24**(10): p. 2752-2756.

22. Phillipe Cognard, V., *Handbook of Adhesives and Sealants*. Vol. 2. 2006: Hardbound.

23. Mittal, K.L.a.P., A., *Handbook of Adhesive Technology, Revised and Expanded*. 2d ed. 2003, New York: Marcel Dekker.

24. Khan, I. and B.T. Poh, Materials & Design, 2011. **32**(5): p. 2513-2519.

25. Barber, J.W., et al., Polymer Testing, 1990. **9**(5): p. 291-313.

26. Rodwell, D.F.G., International Journal of Adhesion and Adhesives, 1990. **10**(1): p. 43-48.

27. Kaboorani, A. and B. Riedl, Composites Part A: Applied Science and Manufacturing, 2011. **42**(8): p. 1031-1039.

28. Park, Y.-J. and H.-J. Kim, International Journal of Adhesion and Adhesives, 2003. **23**(5): p. 383-392.

29. Huber, H.F. and H. Müller, International Journal of Radiation Applications and Instrumentation. Part C. Radiation Physics and Chemistry, 1989. **33**(5): p. 443-450.

30. Do, H.-S., J.-H. Park, and H.-J. Kim, European Polymer Journal, 2008. **44**(11): p. 3871-3882.

31. Park, Y.-J., et al., International Journal of Adhesion and Adhesives, 2009. **29**(7): p. 710-717.

32. Cheng, H.N., Macromolecules, 1984. **17**(10): p. 1950-1955.

33. Anantawaraskul, S., J. Soares, and P. Wood-Adams, *Polymer Analysis Polymer Theory*. 2005, Springer Berlin / Heidelberg. p. 686-686.

RECOMMENDATIONS

The following research topics are proposed for future work:

1. Synthesizing different catalysts.
2. Studying the polymerization activity of newly synthesized catalysts by various co catalysts like TMA and other alkyl aluminium halides.
3. Homo and copolymerization studies will be carried out by varying parameters like pressure and concentration of monomers.
4. Synthesizing polyolefin nanocomposites by the addition new nanofillers.
5. Investigation of mechanism, kinetics of polymerization of produced polymers in the presence of the nanofillers.
6. Investigation of the mechanical properties of the produced polymers.
7. Study more about the properties of the produced polyolefins adhesives.

VITAE

Name: Omer Yahya Bakather

Nationality: Yemeni

Date of Birth: 1st of Septemper, 1976

Email: omar9990@yahoo.com

Address: Yemen

ACADEMIC QUALIFICATION

- PhD in Chemical Engineering (21 April, 2014), King Fahd University of Petroleum and Minerals, Dhahran, Saudi Arabia.

Thesis Title: Copolymerization of ethylene and propylene in the presence of nanofillers.

- M. Sc. in Chemical Engineering, King Fahd University of Petroleum and Minerals, Dhahran, Saudi Arabia, 2009.

Thesis Title: Removal of Lead and Chromium from Water Using Modified and Nonmodified Carbon Nanotubes.

- B. Sc. Chemical Engineering, Hadhramout University, Al-Mukalla, Yemen, 2001.

Graduation Project: LPG Plant Design.

Field of Specialization

- Nanotechnology, Nanomaterials, Nanocomposites.
- Environmental Remediation.
- Optimization.
- Polymer synthesis, Characterization, Modeling.

Research Work

- **Refereed Journals (ISI Journals)**

1. Muataz Ali Atieh, **Omer Yehya Bakather**, et al., "Effect of Carboxylic Functional Group Functionalized on Carbon Nanotubes Surface on the Removal of Lead from Water," Bioinorganic Chemistry and Applications, vol. 2010, Article ID 603978, 9 pages, 2010. doi:10.1155/2010/603978.
2. Muataz Ali Atieh, **Omer Yahya Bakather**, Bassam S. Tawabini, et al., "Removal of Chromium (III) from Water by Using Modified and Nonmodified Carbon Nanotubes," Journal of Nanomaterials, vol. 2010, Article ID 232378, 9 pages, 2010. doi:10.1155/2010/232378.